VIRULENCE GENE REGULATION IN *BORDETELLA*

Eliza Mason

A dissertation submitted to the faculty of the University of
North Carolina at Chapel Hill in partial fulfillment of the requirements for
the degree of Doctor of Philosophy in The Department of Microbiology and Immunology

Chapel Hill
2013

Approved by:

Anthony R. Richardson

Miriam S. Braunstein

Tom Kawula

Rita Tamayo

Peggy A. Cotter

ABSTRACT

Eliza Mason: Virulence gene regulation in *Bordetella*
(Under the direction of Peggy A. Cotter)

Bordetella species cause respiratory infections in mammals. Their master regulatory system BvgAS controls expression of at least three distinct phenotypic phases in response to environmental cues. The Bvg^+ phase is necessary and sufficient for respiratory infection while the Bvg^- phase is required for survival *ex vivo*. We developed a plasmid, pGFLIP, that encodes a sensitive Flp recombinase-based fluorescent reporter system able to document gene activation both *in vitro* and *in vivo*. Using pGFLIP, we demonstrated that *cyaA*, considered to be a "late" Bvg^+ phase gene, is activated substantially earlier in *B. bronchiseptica* compared to *B. pertussis* following a switch from Bvg^- to Bvg^+ phase conditions. We show that the altered activation of *cyaA* is not due to differences in the *cyaA* promoter or in the *bvgAS* alleles of *B. bronchiseptica* compared to *B. pertussis*, but appears to be species-specific. Finally, we used pGFLIP to show that *flaA* remains repressed during infection, confirming that wild-type *B. bronchiseptica* do not modulate to the Bvg^- phase *in vivo*. Additionally, we obtained large colony variants (LCVs) from the lungs of mice infected with *B. bronchiseptica* strain RBX9, which contains an in-frame deletion mutation in *fhaB*, encoding filamentous hemagglutinin. RBX9 also yielded LCVs when switched from Bvg^- phase conditions to Bvg^+ phase conditions *in vitro*. We determined that LCVs are composed of both Bvg^+ and Bvg^- phase bacteria and that they result from defective *bvgAS* positive autoregulation. The LCV phenotype was linked to the presence of a divergent promoter 5′

to *bvgAS*, suggesting a previously undescribed mechanism of transcriptional interference that, in this case, leads to feedback-based multistability (FBM). Our results also indicate that a small proportion of RBX9 bacteria modulates to the Bvg$^-$ phase *in vivo*. In addition to providing insight into transcriptional interference and FBM, our data provide an example of an in-frame deletion mutation exerting a ‘polar’ effect on nearby genes.

ACKNOWLEDGEMENTS

I want to thank present and past members of Team Bordetella of the Cotter Lab for helpful discussion and inspiration for the beloved wonky project. I also want to thank Cris Campos, Matt Byrd, Jeff Melvin, Erich Scheller, and Mike Henderson for being great friends and colleagues. I want to thank my mother, father, sister, and Nathan for encouragement and support. Lastly, I couldn't have done it without my advisor, Peggy, who taught me how to speak and write professionally.

TABLE OF CONTENTS

LIST OF TABLES

LIST OF FIGURES

LIST OF ABBREVIATIONS AND SYMBOLS

ACT – adenylate cyclase toxin

BG – Bordet Gengou

c.f.u – colony forming units

FBM – feedback-based multistability

FHA – filamentous hemagglutinin

Flp, *flp*- flip recombinase

FRT – Flp recombinase target

GFP, *gfp* – green fluorescent protein

HA – hemagglutinin

LCV – large colony variant

MCS – multiple cloning site

p.i. – post inoculation

PCR – polymerase chain reaction

Ptx – Pertussis toxin

RIVET – Recombination-Based *In Vivo* Expression Technology

SS – Stainer-Scholte

TPS – Two Partner Secretion

Δ - in-frame deletion of

CHAPTER 1: Introduction

The goal of this dissertation was to explore *Bordetella* virulence gene regulation. Throughout this process we developed new and sensitive tools to detect gene activation as well as characterized an interesting colony morphotype. These projects were intimately related to understanding the *Bordetella* master regulatory system, BvgAS. However, the insight these projects have provided should be widely relevant to understanding other Gram-negative pathogens and bacterial transcription processes in general.

The *Bordetella* genus currently comprises nine species of Gram-negative bacteria, several of which are human-and animal-adapted pathogens. The so-called classical *Bordetella* species have been well-characterized and include extracellular respiratory pathogens *B. pertussis*, *B. parapertussis*$_{Hu}$, and *B. bronchiseptica* (1–3). The obligate human pathogens *B. pertussis* and *B. parapertussis*$_{Hu}$ cause the disease whooping cough, an acute respiratory illness that has a high mortality rate in infants (4, 5). *B. bronchiseptica* naturally infects a wide-range of mammals, including canines, livestock, and occasionally humans and generally causes a more chronic, asymptomatic infection (6, 7). Outside of the host, *B. bronchiseptica* is thought to inhabit environmental reservoirs, although none so far have been identified (6). The bird pathogen *B. avium* infects poultry and causes rhinotracheitis and coryza (2, 8). Only one species, *B. petrii*, has been isolated from the environment (9, 10). The remaining *Bordetella* species were discovered from various human clinical isolates, although their pathogenic potential remains unclear (9).

Historically, *B. pertussis* was a serious public health threat. Before vaccines were developed, whooping cough was a leading cause of infant death worldwide, causing almost 200,000 cases per year in the United States alone (http://www.cdc.gov/pertussis/surv-reporting/cases-by-year.html). Initially, a whole-cell vaccine (which consisted of killed *B. pertussis* organisms) was developed, and as a result, cases of whooping cough dramatically decreased (11). Although the whole cell vaccine was extremely successful in providing protection against infection, reports of severe neurological side effects cast doubt upon its safety (12). About two decades ago, a less reactogenic acellular vaccine, consisting of a cocktail of purified *B. pertussis* virulence factors, was deployed. This acellular vaccine was purported to be much safer, but just as effective, as the whole cell vaccine. These acellular vaccines are now the international standard for pertussis vaccination (13). Interestingly, however, the incidence of pertussis has gradually increased since the introduction of the acellular vaccine (14). In addition, the US has recently experienced several outbreaks, including one in California and an epidemic in Washington State (15, 16). Despite continuing efforts, the bordetellae continue to present problems not only for humans, but for domesticated animals as well, imparting significant economic losses (17). These trends demonstrate the importance of the continual investigation of *Bordetella* and provide an impetus for improving current vaccines.

Several *Bordetella* genomes have been fully sequenced and annotated, revealing their evolutionary relationships. Sequence data confirmed that *B. pertussis, B. parapertussis,* and *B. bronchiseptica* are extremely closely related, despite their diverse hosts (18). Additionally, phylogenetic analyses revealed that *B. pertussis* and *B. parapertussis* have recently (~3 m.y.a.) evolved from a *B. bronchiseptica*-like ancestor (19). Therefore, these species are

often regarded as subspecies and together encompass the *B. bronchiseptica* cluster. Research in the *Bordetella* field has been primarily focused on these pathogens.

Interesting clues about the evolution of *Bordetella* virulence have emerged from subsequent genome-wide studies. For example, all *Bordetella* are proposed to have evolved from a primitive *B. petrii*-like ancestor (hypothesized to be non-pathogenic) (9, 10). Coincidently, *B. petrii* and *B. bronchiseptica* (the evolutionarily ancestral species) have the largest genomes, containing over five mega-bases (Mb) and more than five thousand genes (10, 18). These large genomes likely encode a versatile repertoire of proteins that enable survival in diverse environments. In contrast, *B. pertussis*, and to a lesser extent, *B. parapertussis*$_{Hu}$, have considerably smaller genomes (~4 Mbp and 4.8 Mbp, respectively) and encode significantly fewer proteins. Remarkably, this massive loss of genetic information resulted in increased disease severity and narrowed host specificity. In many cases, virulence emerged with the acquisition of new genes, such as in *Salmonella* and *Vibrio* spp. (20). For *B. pertussis*, reductive evolution was strongly influenced by substantial genomic rearrangements, invasion of mobile elements, and rampant recombination (18). These events led to an increase in the frequency of pseudogenes and large genomic deletions, somehow allowing this organism to specialize in the human host. Despite the dramatic differences in genome size, the presence and regulation of virulence genes is highly conserved among the *Bordetella*.

The regulation of all known virulence factor genes in *Bordetella* has been attributed to a single two-component regulatory system, BvgAS, where BvgS is a sensor kinase and BvgA is a response regulator transcription factor (Figure 1) (21–24). Bacteria deficient for BvgAS are completely innocuous and cannot establish an infection (25). Homologues of

bvgAS have been found in all *Bordetella* species (9), supporting the hypothesis that BvgAS represents an ancestral system that was not initially dedicated to virulence. In the *B. bronchiseptica* cluster, BvgAS and its contribution to pathogenesis have been well characterized. BvgAS is a global regulator that controls hundreds of genes and at least three distinct phenotypic phases, including the Bvg^+, Bvg^i, and Bvg^- phases, in response to environmental signals (23). By investigating of the evolution of BvgAS and its regulon, we hope to understand differences in host specificity and disease severity between these species.

Although specific genes that determine the host ranges of these pathogens have not been found, a few species-specific patterns of regulation have been identified. While it is true that, among the *B. bronchiseptica* cluster, BvgAS and most of the virulence factors have remained conserved (i.e., the virulence factors filamentous hemaglutinnin , adenylate cyclase toxin, pertactin, and BipA share over 90% amino acid sequence identity), a number of mutations have confered altered patterns of regulation. For example, several genes that are not BvgAS-regulated in *B. bronchiseptica* have evolved to come under control of BvgAS in *B. pertussis*, and vice versa. One of the most characterized and highly expressed set of toxin genes in *B. pertussis*, *ptxA-E* (encoding the AB_5-type pertussis toxin), is not under BvgAS control in *B. bronchiseptica* (26). The Type III secretion system, which secretes only one known highly-cytopathic effector, BteA, is encoded by genes positively regulated by BvgA, but whose products are only secreted in *B. bronchiseptica* (27). Another gene that has remained conserved but is differentially expressed in *B. bronchiseptica* and *B. pertussis* is *batB,* which encodes an autotransporter involved in binding antibodies during *B. bronchiseptica* infection (28). Together, these genes have been maintained in *Bordetella*, yet have been reprogrammed to become active under different conditions. Although little is

understood about why the regulation has changed, it is likely that these changes represent examples of adaptation to species-specific niches.

In addition, although the BvgAS- (or *v*irulence) *a*ctivated *g*enes (*vags*) are generally conserved among *Bordetella* species, the BvgAS- (*v*irulence) *r*epressed *g*enes (*vrgs*) are quite diverse (1). Gene inactivation events in *B. pertussis* eliminated several *vrg* loci present in *B. bronchiseptica*, including those required for motility and chemotaxis, (which apparently became unnecessary in the human host) (18, 29). However, *B. pertussis* also expresses unique *vrgs* that encode outer membrane proteins of unknown function (30). In *B. bronchiseptica*, data suggest that the Bvg^- and Bvg^i phases increase fitness in nutrient-limiting conditions (i.e., *ex vivo*); however, the role of these phases in *B. pertussis* remains unclear (31, 32).

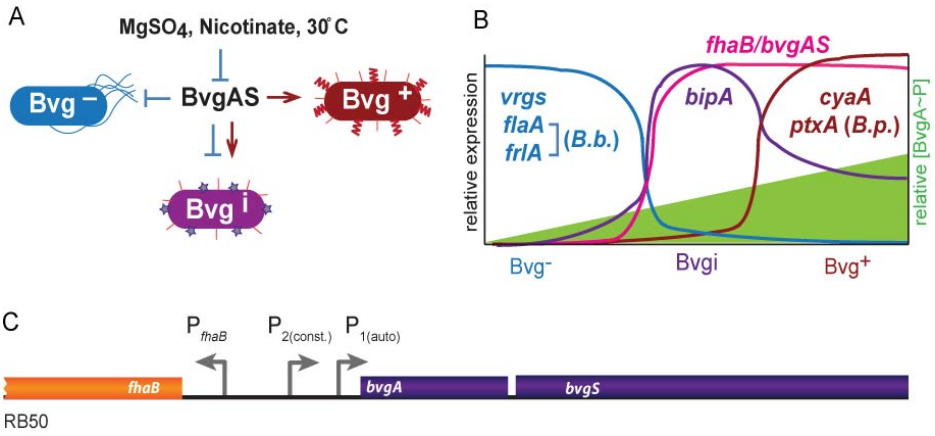

Figure 1. BvgAS controls least four classes of gene expression and three phenotypic phases in response to environmental stimuli; A, BvgAS controls the Bvg, Bvg^i, and Bvg^+ phases and is repressed by chemical modulators or low temperatures; B, The three phenotypic phases are defined by unique patterns of gene expression and rely on the intracellular concentration of BvgA~phosphate (BvgA~P); C, The chromosomal organization of the *fhaB* and *bvgAS* loci, including promoters that drive each gene (see text for details).

The Bvg^+, Bvg^i, and Bvg^- phenotypic phases were first described by Leslie and Gardner in the 1930s and 1940s and then further characterized by Lacey in 1960 (33, 34).

Since then, much has been learned about BvgAS and the regulation of these phases. *Bordetella* can freely transition between each state given the appropriate environmental signals that activate or inactivate BvgAS. Although the natural signals that BvgAS responds to are unknown, several laboratory conditions have been identified that manipulate its activity (Figure 1A). Growth on Bordet-Gengou (BG) blood agar plates or in Stainer-Scholte (SS) medium at 37˚C confers the Bvg^+ phase phenotype, in which BvgAS is abundant and highly active (35). With the addition of millimolar concentrations of nicotinic acid or magnesium sulfate to the growth media, or growth at lower temperature (30˚C), BvgAS activity is inhibited and bacteria convert to the Bvg^- phase (this transition is subsequently referred to as BvgAS *modulation*) (23). Addition of an intermediate concentration of chemical modulators induces the Bvg^i phase (23, 32).

Each phenotypic state can easily be distinguished by the physical characteristics exhibited during colony growth. For example, in the Bvg^+ phase, bacteria form colonies that are small, domed, and hemolytic on BG blood agar (34). In contrast, bacteria in the Bvg^- phase form colonies that are large, flat, and non-hemolytic when grown on BG blood agar + 50 mM $MgSO_4$ (34). Likewise, bacteria in the Bvg^i phase exhibit features intermediate to the Bvg^+ and Bvg^- phases, both in terms of colony size and hemolysis (32).

Each BvgAS-regulated phenotype is determined by unique patterns of gene expression. After several years of research, many details of transcriptional regulation have emerged. So far, four classes of BvgAS-regulated genes have been characterized, based on the location and affinity of BvgA binding sites at their promoter regions (Figure 1B) (23, 36–39). Because each phenotypic state can be induced both by steady-state environments as well as in a temporal manner upon change in environment, gene classes are also categorized based

on when they are expressed maximally. Class 1 (late Bvg^+ phase) genes include *cyaA* and *ptxA* (both Class 1 in *B. pertussis* only) (40). These genes are activated relatively late under Bvg^+ phase conditions and have multiple low affinity BvgA binding sites within their promoters (40). Cooperative binding of BvgA at low affinity sites permits activation only after a certain concentration of BvgA is achieved. In contrast, Class 2 (early Bvg^+ genes), including *fhaB* and *bvgAS* itself, have several high affinity BvgA binding sites in their promoters and are thus activated immediately upon the Bvg^+ phase transition (23). There is only one characterized Class 3 (Bvg^i phase) gene, *bipA*. Interestingly, this gene contains both high affinity BvgA binding sites, located upstream from its transcription start site, and low affinity BvgA binding sites, located downstream from its translational start site (41). When BvgA levels increase during the transition to Bvg^+ phase, *bipA* is immediately transcribed due to the high affinity binding sites. However, once BvgA levels reach a certain threshold, *bipA* is repressed due to the physical inhibition of RNA polymerase (RNAP) by BvgA~P bound at the low affinity sites (41). Lastly, Class 4 (Bvg^- phase) genes are *vrgs* such as *flaA* and *frlAB* (in *B. bronchiseptica* only); these genes are repressed (directly or indirectly) by BvgA (23). Despite the large amount of work that has been done to characterize each gene class, only a few genes have been actually classified. Additionally, the majority of *vrgs* remain grossly under-investigated, primarily because no role during infection has been established.

Like all two-component systems, BvgAS relies on a phosphorelay to convey signal activation. Upon sensing activating signals (Bvg^+ phase environments) in the periplasm, BvgS autophosphorylates and delivers this phosphate group forward through three subdomains (the transmitter, receiver, and histidine phosphotransfer-domain) and finally to

an aspartate residue in BvgA (21). When BvgA is converted into BvgA~P, it dimerizes and gains high affinity for specific DNA sequences (42). BvgA~P then activates or represses transcription by binding to promoter regions (37). Because *bvgAS* is positively autoregulated, the total concentration of BvgAS as well as BvgA~P gradually increases to a maximum when bacteria sense sustained Bvg^+ phase signals (43, 44). These observations have culminated in the hypothesis that the phenotypic phase of each bacterium is determined by the intracellular concentration of BvgA~P; in the Bvg^- phase, the concentration of BvgA~P is minimal, in the Bvg^i phase, the concentration of BvgA~P is intermediary, and in the Bvg^+ phase, BvgA~P is maximal. This hypothesis has been strongly supported by recent experiments that determined BvgA and BvgA~P levels within bacterial cultures under modulating and non-modulating conditions (45).

All evidence thus far supports the following series of events during the transition between phases. In the Bvg^- phase (where BvgAS-activating signals are absent – or BvgAS-inactivating signals are present), there is a low basal concentration of BvgA (and little to no BvgA~P), leading to activation of Bvg^- phase genes in the absence of BvgA~P-mediated repression. When switched to Bvg^+ phase conditions, the basal amount of BvgA is phosphorylated, leading to the activation of early Bvg^+ phase genes (including, importantly, *bvgAS* itself) and Bvg^i phase genes, which require a relatively low concentration of BvgA~P, as well as repression of the Bvg^- phase genes. Due to positive autoregulation, levels of BvgA increase with a concomitant increase in BvgA~P until the cellular concentration reaches that required to activate the late Bvg^+ phase genes. Cells remain in the Bvg^+ phase until BvgAS receives a repressive signal. Transition back to the Bvg^- phase requires that BvgA~P levels decrease to the minimum level and probably occurs through phosphatase activity of BvgS on

BvgA~P as well as through natural hydrolysis of the phosphoryl group from BvgA~P. In this manner, BvgAS precisely controls the physiological state of each cell.

Critical to the transition to the Bvg^+ phase, positive autoregulation of *bvgAS* was discovered around 1990 and later characterized by Williams et al. in 2007 (25, 43, 44, 46). In the *B. bronchiseptica* cluster, *bvgAS* lies adjacent to *fhaB* and is transcribed divergently (Figure 1C). The 426bp region between these genes contains at least three promoters: two that drive *bvgAS* and one that drives *fhaB* (25). Because both of these genes respond to BvgAS, there are also multiple BvgA binding sites associated with these promoters; therefore, it is likely that this entire region is completely occupied under Bvg^+ phase conditions due to cooperative binding of BvgA~P (47). The two promoters that regulate *bvgAS* are called P_2 (which is constitutively active at low levels) and P_1 (which is activated by BvgA~P) and control the transcription of *bvgAS* under modulating and non-modulating conditions, respectively (25). Therefore, under Bvg^- phase conditions, P_2 is active and responsible for the low, basal concentration of BvgA within the cell. Upon transition to the Bvg^+ phase, the basal level of BvgA is converted to BvgA~P, which is sufficient to activate transcription at P_1, as well as at other early and intermediate Bvg^+ phase promoters, including P_{fhaB} (23). Enhanced and sustained transcription at P_1 increases the concentration of BvgA such that, eventually (as BvgA is quickly converted to BvgA~P), the late Bvg^+ phase genes such as *ptxA* and *cyaA* (*B. pertussis* only) are transcribed (23, 40). Interestingly, Williams et al. demonstrated that by replacing the entire *bvgAS* promoter region with a constitutively high or constitutively low promoter (and thus removing autoregulation), the maintenance of and transition between phases could be altered (44). Because a constitutive promoter dictates a constant and specific level of BvgA (which is still converted into BvgA~P upon sensing

activating conditions), both the high and low constitutive mutants could achieve the Bvg$^-$ phase state (where BvgA~P is minimal), but the amount of time required to transition and the ability to transition to the Bvg$^+$ phase was altered (44). Notably, when *bvgAS* transcription was driven by the constitutively low active promoter, bacteria could transition to only the Bvg^i phase when exposed to Bvg$^+$ phase conditions, providing strong evidence that the Bvg^i phase is induced by relatively low levels of BvgA~P while much higher levels are required to induce the Bvg$^+$ phase.

Data obtained thus far indicate that the Bvg$^+$ phase is necessary and sufficient to cause respiratory infection, the Bvg$^-$ phase facilitates *ex vivo* survival (*B. bronchisetpica* only), and modulation to the Bvg^i or Bvg$^-$ phase does not occur during infection (31, 48–52). For example, Bvg$^+$ phase-locked bacteria behave identically to wild-type bacteria in colonization, persistence, and contribution to lung pathology (31, 48, 49, 52). In contrast, Bvg$^-$ phase-locked bacteria are rapidly cleared from the host, and Bvg^i phase-locked bacteria have severe defects in colonization and persistence (31, 48–52). Additionally, *flaA* is not expressed at a detectable level when mice are infected with the *B. bronchiseptica* wild-type strain RB50 (40) and the ectopic production of flagella in the Bvg$^+$ phase is actually detrimental to infection (48). Although the natural signals that affect BvgAS activity and the biological relevance of modulation remain unknown, all data suggest that wild-type *Bordetella* do not modulate to the Bvg$^-$ phase within the mammalian host.

The murine lung inflammation model has been popular for studying *Bordetella* pathogenesis (50, 53–57). This model has been used to characterize the roles of several virulence factors in *B. bronchiseptica* and *B. pertussis*. At least for *B. pertussis*, however, the mouse model is quite limited: mice are not natural hosts of *B. pertussis*, they do not mimic

human disease progression when infected, and “infection” requires enormous numbers of bacteria to be delivered directly to the lungs. Recently, a baboon model of *B. pertussis* infection has been developed (58). Preliminary studies appear very promising; infected baboons demonstrate both human-like symptoms and disease transmission (59–61). Several studies are underway to increase our understanding of *Bordetella* pathogenesis and vaccine efficacy using this model.

Studies using *B. bronchiseptica* and natural animal hosts have been particularly useful in characterizing specific virulence factors. Because *B. bronchiseptica* naturally infects a wide range of mammals, several natural host animal models are available, including mice, rabbits, rats, and swine. Additionally, *B. bronchiseptica* rarely infects humans, grows faster under laboratory conditions, and is more genetically tractable than *B. pertussis*. The fact that many virulence factors are interchangeable within the *B. bronchiseptica* cluster also allows the study of their function regardless of species (53, 62, 63).

Filamentous hemagglutinin (FHA) is regarded as one of the most important virulence factors of *Bordetella* and is a primary component of the acellular vaccine (1, 13, 64). FHA is a prototypical member of the Two-Partner Secretion (TPS) pathway (a subcategory of Type V Secretion), is both cell-associated and secreted, and was first characterized as an adhesin (64–66). In addition to mediating adherence to host cells, FHA mediates immunosuppression during infection, and acts in concert with other virulence factors to subvert host innate immunity (63, 67).

FHA function is directly dependent on its proper secretion, folding, and presentation on the cell surface (66, 68). This is accomplished efficiently through the TPS pathway, which is widespread in Gram-negative bacteria and is often associated with virulence (69–71). In

general, all TPS systems contain at least two components: a large TpsA exoprotein, and a TpsB β-barrel pore protein responsible for translocating the TpsA protein through the outer membrane (70). Once translated, TpsA proteins are directed through the inner membrane by the general secretory system Sec (70). The TpsA protein is then exported from the periplasm to the surface through the TpsB pore, although the energy source for this secretion step is unknown. Several conserved domains exist within TpsA proteins, all of which FHA possesses (Figure 2A) (71). For example, many TpsA proteins (and autotransporters) contain a signal pepide with an N-terminal extension. This signal peptide extension has been proposed to direct later steps in protein biogenesis and translocation, although these phenotypes are often subtle (72–74). Additionally, a TPS domain, which is found C-terminal to the signal peptide, is responsible for interacting with and recognizing sequences in the TpsB pore (70). TpsA proteins also frequently contain a structurally conserved β-helical shaft which can consist of loosely conserved repeats (75, 76) Lastly, a functional domain is often found at the distal terminus, providing adhesive or cytopathic functions.

FHA is an unusually large protein; it is initially translated as a ~370kD "preproprotein" which is then cleaved by the signal peptidase, and is additionally processed to several "mature" ~240kD forms by the surface-associated protease SphB1 and an as of yet unidentified periplasmic protease during secretion (Figure 2B) (66). FHA's unwieldy size is complemented by its extended conformation; it has a long stalk-like β-helical domain that terminates in the globular Mature C-terminal Domain (MCD). This protein is almost 50nm long in its secreted form (77) and it is hypothesized that this length is required to span across the extracellular region so that the functional domain, the MCD (66), can interact with host cells.

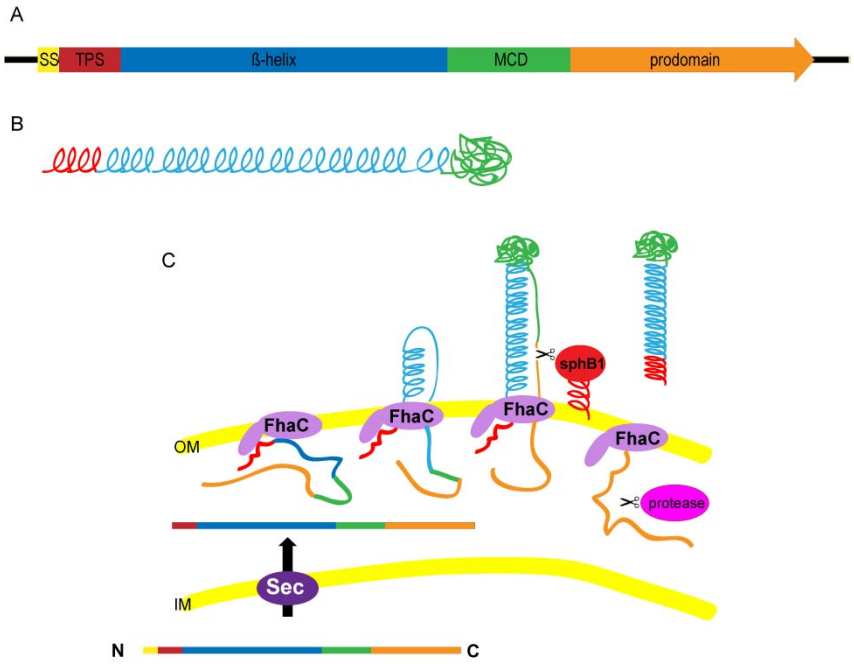

Figure 2. A, Schematic of the *fhaB* gene and its product, FhaB, including the domains Signal Sequence (SS) (yellow), Two-Partner Secretion domain (TPS) (red), β-helical shaft (blue), Mature C-Terminal Domain (MCD) (green), and prodomain (orange); B, schematic of the mature FHA tertiary structure; C, Simplified model of FhaB secretion, see text for details.

Secretion of FHA is an extremely convoluted process of which the details are still emerging. The *fhaB* gene encodes a 71 aa extended signal peptide (78), a feature that is conserved throughout the *B. bronchiseptica* complex. However, deletion of the extension has no observable effect on maturation or function of FHA (unpublished data). Once the signal peptide is cleaved in the periplasm, the extended "proprotein," called FhaB, must find its cognate TpsB protein, FhaC, which forms a β-barrel channel in the outer membrane. FhaC recognizes the conserved TPS domain in the N-terminus of FhaB via periplasmic POTRA domains and secretion to the surface commences (Figure 2) (79–81). Because many TPS exoproteins contain β-helical structure, it is hypothesized that the folding of these domains provides the energy for secretion through the outer membrane. Evidence suggests that FhaB travels through FhaC in an extended hairpin structure, with the β-helical domain folding

foremost while the N-and C-termini remain in the periplasm (Figure 2C) (66, 76, 82). Eventually, the MCD is secreted and folds, FhaB is cleaved by several proteases (SphB1 and an unidentified protease), and the FHA molecule is released (Figure 2C) (65). The order and details of these last events remain unknown.

The last third of FhaB contains the prodomain, a large region of the protein that is cleaved off prior to release. Although not much is known about the function of the prodomain or the mechanism by which it acts, it is required for the proper folding of FHA and remains intracellular during the entire secretion process (66, 68). Bacteria lacking the prodomain-encoding sequences of *fhaB* still secrete FHA in high quantities, but the MCD is rendered non-functional (68). Experiments have also shown that specific deletion mutations of conserved prodomain regions can inhibit release of FhaB (68). The prodomain has been hypothesized to function as a chaperone as well as a tether during secretion, but direct evidence for either of these functions is lacking.

FHA function has been characterized using both *in vitro* and *in vivo* models in attempts to understand its role during infection. FHA was first recognized as a *B. pertussis* colonization factor that could illicit a protective antibody response (83, 84). Soon after, experiments showed that FHA could mediate adherence to a wide range of ciliated and nonciliated cell lines *in vitro*, and was henceforth considered an adhesin (85, 86). In support of those studies, experiments using *B. bronchiseptica* showed that FHA was absolutely necessary for the colonization of the lower respiratory tract in rats and mice (67, 87). More recently, FHA has also been implicated in modulating the host immune response (63, 67). When applied to cultured macrophages, purified FHA can suppress IL-12, modulate the NF-κB pathway, and induce apoptosis (88, 89). Additionally, *B. bronchiseptica* that lack FHA

cause an infection that is hyperinflammatory, characterized by an influx of IL-17$^+$ macrophages, neutrophils, and CD4$^+$ T cells (63). FHA may also have synergistic effects with another important virulence factor, ACT. Several studies have shown that FHA and ACT can interact on the bacterial cell surface and can influence each other's secretion (90, 91). It has been proposed that FHA can enhance the delivery of ACT to host cells.

Although the function of FHA has been extensively investigated, there are still many conspicuous knowledge gaps. For example, the FHA host receptor(s) and cellular targets remain unknown. The secretion and processing of FhaB is still poorly understood and very little is known about the mechanism of release. Similarly, it has been impossible to determine the functions of released and cell-associated FHA because current knowledge prevents the creation of appropriate mutants. Testing these hypotheses directly has been a formidable challenge, but it is clear that FHA is multi-functional and largely influential to several aspects of infection.

References

1. **Mattoo S, Cherry JD**. 2005. Molecular Pathogenesis , Epidemiology , and Clinical Manifestations of Respiratory Infections Due to Bordetella pertussis and Other Bordetella Subspecies. clinical microbiology reviews **18**:326–382.

2. **Gerlach G, von Wintzingerode F, Middendorf B, Gross R**. 2001. Evolutionary trends in the genus Bordetella. Microbes and infection / Institut Pasteur **3**:61–72.

3. **Mattoo S, Foreman-Wykert AK, Cotter PA, Miller JF**. 2001. Mechanisms of Bordetella pathogenesis. Frontiers in bioscience a journal and virtual library **6**:E168–E186.

4. **Cotter PA, Miller JF**. 2001. Bordetella, p. 619–974. *In* Groisman, EA (ed.), Principles of Bacterial Pathogenesis. Academic Press, San Diego, CA.

5. **Cherry JD, Heininger U**. 2004. Pertussis and other Bordetella infections, p. 1588–1608. *In* Feign, RD, Cherry, JD, J, DG, S, K (eds.), Textbook of pediatric infectious diseases, 5th ed. The W. B. Saunders Co, Philadelphia, Pa.

6. **Goodnow RA**. 1980. Biology of Bordetella bronchiseptica. Microbiological reviews **44**:722–38.

7. **Woolfrey BF, Moody JA**. 1991. Human infections associated with Bordetella bronchiseptica. Clinical microbiology reviews **4**:243–55.

8. **Sebaihia M, Preston A, Maskell DJ, Kuzmiak H, Connell TD, King ND, Orndorff PE, Miyamoto DM, Thomson NR, Harris D, Goble A, Lord A, Murphy L, Quail MA, Rutter S, Squares R, Squares S, Woodward J, Parkhill J, Temple LM**. 2006. Comparison of the genome sequence of the poultry pathogen Bordetella avium with those of B. bronchiseptica, B. pertussis, and B. parapertussis reveals extensive diversity in surface structures associated with host interaction. Journal of bacteriology **188**:6002–15.

9. **Gross R, Keidel K, Schmitt K**. 2010. Resemblance and divergence: the “new” members of the genus Bordetella. Medical microbiology and immunology **199**:155–163.

10. **Gross R, Guzman CA, Sebaihia M, Santos VA, Pieper DH, Koebnik R, Lechner M, Bartels D, Buhrmester J, Choudhuri J, Ebensen T, Gaigalat L, Herrmann S, Khachane AN, Larisch C, Link S, Linke B, Meyer F, Mormann S, Nakunst D, Rückert C, Schneiker-Bekel S, Schulze K, Vorhölter F, Yevsa T, Engle JT, Goldman WE, Pühler A, Göbel UB, Goesmann A, Blöcker H, Kaiser O, Martinez-Arias R**. 2008. The missing link: Bordetella petrii is endowed with both the metabolic versatility of environmental bacteria and virulence traits of pathogenic Bordetellae. BMC genomics **9**:449.

11. **Cherry JD**. 1996. Historical review of pertussis and the classical vaccine. The Journal of infectious diseases **174 Suppl** :S259–63.

12. **Shah RC, Shah AR**. 2003. Pertussis vaccine controversies and acellular pertussis vaccine. Indian Journal of Pediatrics **70**:485–488.

13. **Sato Y, Sato H**. 1999. Development of acellular pertussis vaccines. Biologicals : journal of the International Association of Biological Standardization **27**:61–9.

14. **He Q, Mertsola J**. 2008. Factors contributing to pertussis resurgence. Future microbiology **3**:329–39.

15. 2012. Pertussis epidemic--Washington, 2012. MMWR. Morbidity and mortality weekly report **61**:517–22.

16. **Winter K, Harriman K, Zipprich J, Schechter R, Talarico J, Watt J, Chavez G**. 2012. California pertussis epidemic, 2010. The Journal of pediatrics **161**:1091–6.

17. **Caro JJ, Getsios D, Payne K, Annemans L, Neumann PJ, Trindade E**. 2005. Economic burden of pertussis and the impact of immunization. The Pediatric infectious disease journal **24**:S48–54.

18. **Parkhill J, Sebaihia M, Preston A, Murphy LD, Thomson N, Harris DE, Holden MTG, Churcher CM, Bentley SD, Mungall KL, Cerdeño-Tárraga AM, Temple L, James K, Harris B, Quail MA, Achtman M, Atkin R, Baker S, Basham D, Bason N, Cherevach I, Chillingworth T, Collins M, Cronin A, Davis P, Doggett J, Feltwell T, Goble A, Hamlin N, Hauser H, Holroyd S, Jagels K, Leather S, Moule S, Norberczak H, O'Neil S, Ormond D, Price C, Rabbinowitsch E, Rutter S, Sanders M, Saunders D, Seeger K, Sharp S, Simmonds M, Skelton J, Squares R, Squares S, Stevens K, Unwin L, Whitehead S, Barrell BG, Maskell DJ**. 2003. Comparative analysis of the genome sequences of Bordetella pertussis, Bordetella parapertussis and Bordetella bronchiseptica. Nature Genetics **35**:32–40.

19. **Diavatopoulos D a, Cummings C a, Schouls LM, Brinig MM, Relman D a, Mooi FR**. 2005. Bordetella pertussis, the causative agent of whooping cough, evolved from a distinct, human-associated lineage of B. bronchiseptica. PLoS pathogens **1**:e45.

20. **Cotter PA, Dirita VJ**. 2000. BACTERIAL VIRULENCE GENE REGULATION: An Evolutionary Perspective. Annual review of microbiology **54**:519–65.

21. **Uhl MA, Miller JF**. 1994. Autophosphorylation and phosphotransfer in the Bordetella pertussis BvgAS signal transduction cascade. Proceedings of the National Academy of Sciences of the United States of America **91**:1163–1167.

22. **Bock A, Gross R**. 2001. The BvgAS two-component system of Bordetella spp.: a versatile modulator of virulence gene expression. International journal of medical microbiology IJMM **291**:119–130.

23. **Cotter PA, Jones AM**. 2003. Phosphorelay control of virulence gene expression in Bordetella. Trends in microbiology **11**:367–373.

24. **Aricò B, Miller JF, Roy C, Stibitz S, Monack D, Falkow S, Gross R, Rappuoli R**. 1989. Sequences required for expression of Bordetella pertussis virulence factors share homology with prokaryotic signal transduction proteins. Proceedings of the National Academy of Sciences of the United States of America **86**:6671–6675.

25. **Roy CR, Falkow S**. 1991. Identification of Bordetella pertussis regulatory sequences required for transcriptional activation of the fhaB gene and autoregulation of the bvgAS operon. Journal of bacteriology **173**:2385–2392.

26. **Aricò B, Rappuoli R**. 1987. Bordetella parapertussis and Bordetella bronchiseptica contain transcriptionally silent pertussis toxin genes. Journal of bacteriology **169**:2847–53.

27. **Mattoo S, Yuk MH, Huang LL, Miller JF**. 2004. Regulation of type III secretion in Bordetella. Molecular microbiology **52**:1201–14.

28. **Williams CL, Haines R, Cotter PA**. 2008. Serendipitous discovery of an immunoglobulin-binding autotransporter in Bordetella species. Infection and immunity **76**:2966–2977.

29. **Akerley BJ, Monack DM, Falkow S, Miller JF**. 1992. The bvgAS locus negatively controls motility and synthesis of flagella in Bordetella bronchiseptica. Journal of bacteriology **174**:980–90.

30. **Graeff-Wohlleben H, Deppisch H, Gross R**. 1995. Global regulatory mechanisms affect virulence gene expression in Bordetella pertussis. Molecular & general genetics : MGG **247**:86–94.

31. **Cotter PA, Miller JF**. 1994. BvgAS-mediated signal transduction: analysis of phase-locked regulatory mutants of Bordetella bronchiseptica in a rabbit model. Infection and immunity **62**:3381–3390.

32. **Cotter PA, Miller JF**. 1997. A mutation in the Bordetella bronchiseptica bvgS gene results in reduced virulence and increased resistance to starvation, and identifies a new class of Bvg-regulated antigens. Molecular microbiology **24**:671–685.

33. **Peppler MS**. 1982. Isolation and characterization of isogenic pairs of domed hemolytic and flat nonhemolytic colony types of Bordetella pertussis. Infection and immunity **35**:840–51.

34. **LACEY BW**. 1960. Antigenic modulation of Bordetella pertussis. The Journal of hygiene **58**:57–93.

35. **Hulbert RR, Cotter PA**. 2009. Laboratory Maintenance of Bordetella pertussis. Current protocols in microbiology **Chapter 4**:Unit 4B.1.

36. **Cummings CA, Bootsma HJ, Relman DA, Miller JF**. 2006. Species- and strain-specific control of a complex, flexible regulon by Bordetella BvgAS. Journal of bacteriology **188**:1775–1785.

37. **Steffen P, Goyard S, Ullmann A**. 1996. Phosphorylated BvgA is sufficient for transcriptional activation of virulence-regulated genes in Bordetella pertussis. The EMBO Journal **15**:102–109.

38. **Boucher PE, Yang MS, Stibitz S**. 2001. Mutational analysis of the high-affinity BvgA binding site in the fha promoter of Bordetella pertussis. Molecular microbiology **40**:991–9.

39. **Jones AM, Boucher PE, Williams CL, Stibitz S, Cotter PA**. 2005. Role of BvgA phosphorylation and DNA binding affinity in control of Bvg-mediated phenotypic phase transition in Bordetella pertussis. Molecular microbiology **58**:700–713.

40. **Byrd MS, Mason E, Henderson MW, Scheller E V, Cotter PA**. 2013. An improved RIVET-like reporter system reveals differential cyaA gene activation in Bordetella species. Infection and immunity **81**:1295–1305.

41. **Williams CL, Boucher PE, Stibitz S, Cotter PA**. 2005. BvgA functions as both an activator and a repressor to control Bvg phase expression of bipA in Bordetella pertussis. Molecular microbiology **56**:700–13.

42. **Boucher PE, Menozzi FD, Locht C**. 1994. The modular architecture of bacterial response regulators. Insights into the activation mechanism of the BvgA transactivator of Bordetella pertussis. Journal of molecular biology **241**:363–77.

43. **Roy CR, Miller JF, Falkow S**. 1990. Autogenous regulation of the Bordetella pertussis bvgABC operon. Proceedings of the National Academy of Sciences of the United States of America **87**:3763–3767.

44. **Williams CL, Cotter PA**. 2007. Autoregulation is essential for precise temporal and steady-state regulation by the Bordetella BvgAS phosphorelay. Journal of bacteriology **189**:1974–82.

45. **Boulanger A, Chen Q, Hinton DM, Stibitz S**. 2013. In vivo phosphorylation dynamics of the Bordetella pertussis virulence-controlling response regulator BvgA. Molecular microbiology **88**:156–72.

46. **Scarlato, Prugnola A, Aricó B, Rappuoli R**. 1990. Positive transcriptional feedback at the bvg locus controls expression of virulence factors in Bordetella pertussis. Proceedings of the National Academy of Sciences of the United States of America **87**:6753–6757.

47. **Boucher PE, Yang M, Schmidt DM, Stibitz S**. 2001. Genetic and Biochemical Analyses of BvgA Interaction with the Secondary Binding Region of the fha Promoter of Bordetella pertussis **183**:536–544.

48. **Akerley BJ, Cotter PA, Miller JF**. 1995. Ectopic expression of the flagellar regulon alters development of the Bordetella-host interaction. Cell **80**:611–20.

49. **Tejada GM, Cotter PA, Heininger U, Camilli A, Akerley BJ, Mekalanos JJ, Miller JF**. 1998. Neither the Bvg- phase nor the vrg6 locus of Bordetella pertussis is required for respiratory infection in mice. Infection and immunity **66**:2762–8.

50. **Merkel TJ, Stibitz S, Keith JM, Leef M, Shahin R**. 1998. Contribution of regulation by the bvg locus to respiratory infection of mice by Bordetella pertussis. Infection and immunity **66**:4367–73.

51. **Vergara-Irigaray N, Chávarri-Martínez A, Rodríguez-Cuesta J, Miller JF, Cotter PA, Tejada GM**. 2005. Evaluation of the role of the Bvg intermediate phase in Bordetella pertussis during experimental respiratory infection. Infection and immunity **73**:748–60.

52. **Nicholson TL, Brockmeier SL, Loving CL, Register KB, Kehrli ME, Stibitz SE, Shore SM**. 2012. Phenotypic modulation of the virulent Bvg phase is not required for pathogenesis and transmission of Bordetella bronchiseptica in swine. Infection and immunity **80**:1025–1036.

53. **Julio SM, Inatsuka CS, Mazar J, Dieterich C, Relman DA, Cotter PA**. 2009. Natural-host animal models indicate functional interchangeability between the filamentous haemagglutinins of Bordetella pertussis and Bordetella bronchiseptica and reveal a role for the mature C-terminal domain, but not the RGD motif, during infection. Molecular microbiology **71**:1574–90.

54. **Inatsuka CS, Xu Q, Vujkovic-Cvijin I, Wong S, Stibitz S, Miller JF, Cotter P a**. 2010. Pertactin is required for Bordetella species to resist neutrophil-mediated clearance. Infection and immunity **78**:2901–9.

55. **Sukumar N, Sloan GP, Conover MS, Love CF, Mattoo S, Kock ND, Deora R**. 2010. Cross-species protection mediated by a Bordetella bronchiseptica strain lacking antigenic homologs present in acellular pertussis vaccines. Infection and immunity **78**:2008–16.

56. **Andreasen C, Carbonetti NH**. 2009. Role of Neutrophils in Response to Bordetella pertussis Infection in Mice. Infection and Immunity **77**:1182–1188.

57. **Carbonetti NH, Artamonova G V, Mays RM, Worthington ZE V**. 2003. Pertussis Toxin Plays an Early Role in Respiratory Tract Colonization by Bordetella pertussis. Infection and Immunity **71**:6358–6366.

58. **Warfel JM, Beren J, Kelly VK, Lee G, Merkel TJ**. 2012. Nonhuman primate model of pertussis. Infection and Immunity **80**:1530–1536.

59. **Warfel JM, Beren J, Merkel TJ**. 2012. Airborne Transmission of Bordetella pertussis. The Journal of infectious diseases **206**:902–6.

60. **Eby JC, Gray MC, Warfel JM, Paddock CD, Jones TF, Day SR, Bowden J, Poulter MD, Donato GM, Merkel TJ, Hewlett EL**. 2013. Quantifying Adenylate Cyclase Toxin of Bordetella pertussis in vitro and During Respiratory Infection. Infection and immunity **81**:1390–8.

61. **Warfel JM, Merkel TJ**. 2013. Bordetella pertussis infection induces a mucosal IL-17 response and long-lived Th17 and Th1 immune memory cells in nonhuman primates. Mucosal immunology **6**:787–96.

62. **Tejada GM, Miller JF, Cotter PA**. 1996. Comparative analysis of the virulence control systems of Bordetella pertussis and Bordetella bronchiseptica. Molecular microbiology **22**:895–908.

63. **Henderson MW, Inatsuka CS, Sheets AJ, Williams CL, Benaron DJ, Donato GM, Gray MC, Hewlett EL, Cotter P a**. 2012. Contribution of Bordetella filamentous hemagglutinin and adenylate cyclase toxin to suppression and evasion of IL-17-mediated inflammation. Infection and immunity **80**:2061–2075.

64. **Domenighini M, Relman D, Capiau C, Falkow S, Prugnola A, Scarlato, Rappuoli R**. 1990. Genetic characterization of Bordetella pertussis filamentous haemagglutinin: a protein processed from an unusually large precursor. Molecular microbiology **4**:787–800.

65. **Coutte L, Antoine R, Drobecq H, Locht C, Jacob-Dubuisson F**. 2001. Subtilisin-like autotransporter serves as maturation protease in a bacterial secretion pathway. The EMBO journal **20**:5040–8.

66. **Mazar J, Cotter PA**. 2006. Topology and maturation of filamentous haemagglutinin suggest a new model for two-partner secretion. Molecular microbiology **62**:641–654.

67. **Inatsuka CS, Julio SM, Cotter PA**. 2005. Bordetella filamentous hemagglutinin plays a critical role in immunomodulation, suggesting a mechanism for host

specificity. Proceedings of the National Academy of Sciences of the United States of America **102**:18578–18583.

68. **Noël CR, Mazar J, Melvin JA, Sexton JA, Cotter P a**. 2012. The prodomain of the Bordetella two-partner secretion pathway protein FhaB remains intracellular yet affects the conformation of the mature C-terminal domain. Molecular microbiology **86**:988–1006.

69. **Thanassi DG, Stathopoulos C, Karkal A, Li H**. 2005. Protein secretion in the absence of ATP: the autotransporter, two-partner secretion and chaperone/usher pathways of gram-negative bacteria (review). Molecular Membrane Biology **22**:63–72.

70. **Mazar J, Cotter PA**. 2007. New insight into the molecular mechanisms of two-partner secretion. Trends in Microbiology **15**:508–15.

71. **Jacob-Dubuisson F, Locht C, Antoine R**. 2001. Two-partner secretion in Gram-negative bacteria: a thrifty, specific pathway for large virulence proteins. Molecular microbiology **40**:306–13.

72. **Desvaux M, Cooper LM, Filenko NA, Scott-Tucker A, Turner SM, Cole JA, Henderson IR**. 2006. The unusual extended signal peptide region of the type V secretion system is phylogenetically restricted. FEMS Microbiology Letters **264**:22–30.

73. **Peterson JH, Szabady RL, Bernstein HD**. 2006. An unusual signal peptide extension inhibits the binding of bacterial presecretory proteins to the signal recognition particle, trigger factor, and the SecYEG complex. The Journal of Biological Chemistry **281**:9038–9048.

74. **Szabady RL, Peterson JH, Skillman KM, Bernstein HD**. 2005. An unusual signal peptide facilitates late steps in the biogenesis of a bacterial autotransporter. Proceedings of the National Academy of Sciences of the United States of America **102**:221–226.

75. **Kajava A V, Steven AC**. 2006. The turn of the screw: variations of the abundant beta-solenoid motif in passenger domains of Type V secretory proteins. Journal of structural biology **155**:306–15.

76. **Kajava A V, Cheng N, Cleaver R, Kessel M, Simon MN, Willery E, Jacob-Dubuisson F, Locht C, Steven AC**. 2001. Beta-helix model for the filamentous haemagglutinin adhesin of Bordetella pertussis and related bacterial secretory proteins. Molecular microbiology **42**:279–92.

77. **Makhov AM, Hannah JH, Brennan MJ, Trus BL, Kocsis E, Conway JF, Wingfield PT, Simon MN, Steven AC**. 1994. Filamentous hemagglutinin of

Bordetella pertussis. A bacterial adhesin formed as a 50-nm monomeric rigid rod based on a 19-residue repeat motif rich in beta strands and turns. Journal of molecular biology **241**:110–24.

78. **Lambert-Buisine C, Willery E, Locht C, Jacob-Dubuisson F**. 1998. N-terminal characterization of the Bordetella pertussis filamentous haemagglutinin. Molecular microbiology **28**:1283–93.

79. **Jacob-Dubuisson F oise, Kehoe B, Willery E, Reveneau N, Locht C, Relman DA**. 2000. Molecular characterization of Bordetella bronchiseptica filamentous haemagglutinin and its secretion machinery 1211–1221.

80. **Delattre A-S, Saint N, Clantin B, Willery E, Lippens G, Locht C, Villeret V, Jacob-Dubuisson F**. 2011. Substrate recognition by the POTRA domains of TpsB transporter FhaC. Molecular microbiology **81**:99–112.

81. **Hodak H, Clantin B, Willery E, Villeret V, Locht C, Jacob-Dubuisson F**. 2006. Secretion signal of the filamentous haemagglutinin, a model two-partner secretion substrate. Molecular microbiology **61**:368–82.

82. **Clantin B, Hodak H, Willery E, Locht C, Jacob-Dubuisson F, Villeret V**. 2004. The crystal structure of filamentous hemagglutinin secretion domain and its implications for the two-partner secretion pathway. Proceedings of the National Academy of Sciences of the United States of America **101**:6194–6199.

83. **Kimura A, Mountzouros KT, Relman DA, Falkow S, Cowell JL**. 1990. Bordetella pertussis Filamentous Hemagglutinin : Evaluation Protective Antigen and Colonization Factor in a Mouse Respiratory Infection. Infection and immunity **58**:7–16.

84. **Sato Y, Izumiya K, Sato H, Cowell JL, Manclark CR**. 1981. Role of antibody to leukocytosis-promoting factor hemagglutinin and to filamentous hemagglutinin in immunity to pertussis. Infection and immunity **31**:1223–31.

85. **Relman DA, Domenighini M, Tuomanen E, Rappuoli R, Falkow S**. 1989. Filamentous hemagglutinin of Bordetella pertussis: nucleotide sequence and crucial role in adherence. Proceedings of the National Academy of Sciences of the United States of America **86**:2637–41.

86. **Mattoo S, Miller JF, Cotter PA**. 2000. Role of Bordetella bronchiseptica fimbriae in tracheal colonization and development of a humoral immune response. Infection and immunity **68**:2024–33.

87. **Cotter PA, Yuk MH, Mattoo S, Akerley BJ, Boschwitz J, Relman DA, Miller JF**. 1998. Filamentous hemagglutinin of Bordetella bronchiseptica is required for efficient establishment of tracheal colonization. Infection and immunity **66**:5921–9.

88. **McGuirk P, Mills KH**. 2000. Direct anti-inflammatory effect of a bacterial virulence factor: IL-10-dependent suppression of IL-12 production by filamentous hemagglutinin from Bordetella pertussis. European journal of immunology **30**:415–22.

89. **Abramson T, Kedem H, Relman D**. 2001. Proinflammatory and proapoptotic activities associated with Bordetella pertussis filamentous hemagglutinin. Infection and immunity **69**:2650–2658.

90. **Zaretzky FR, Gray MC, Hewlett EL**. 2002. Mechanism of association of adenylate cyclase toxin with the surface of Bordetella pertussis: a role for toxin-filamentous haemagglutinin interaction. Molecular microbiology **45**:1589–98.

91. **Perez Vidakovics ML a, Lamberti Y, van der Pol W-L, Yantorno O, Rodriguez ME**. 2006. Adenylate cyclase influences filamentous haemagglutinin-mediated attachment of Bordetella pertussis to epithelial alveolar cells. FEMS immunology and medical microbiology **48**:140–7.

CHAPTER 2: An improved RIVET-like reporter system reveals differential *cyaA* gene activation in *Bordetella* species[1]

Introduction

Bordetella species are Gram-negative bacterial respiratory pathogens. The genus includes *Bordetella pertussis,* an obligate human pathogen and the causative agent of whooping cough, and the closely related *Bordetella bronchiseptica,* which can infect a wide range of mammals including several species that are commonly studied in the laboratory (1-3). These bacteria rely on the global two-component regulatory system BvgAS for virulence (1-3). The BvgAS phosphorelay regulates gene expression patterns according to environmental cues and controls at least three distinct phenotypic phases: Bvg minus (Bvg^-), Bvg plus (Bvg^+), and Bvg intermediate (Bvg^i) (4, 5). All evidence thus far suggests that the Bvg^+ phase is necessary and sufficient for infection, and that modulation to the Bvg^- or Bvg^i phase does not occur *in vivo* (6-8). Although it has been hypothesized that the Bvg^i phase and/or the Bvg^- phase is required for transmission or survival outside of a host (7, 9, 10), a recent study provided evidence that neither of these phenotypic phases is required for *B. bronchiseptica* transmission in swine (8).

---

[1]This chapter was originally published as an article in the journal *Infection and Immunity*. Citation is as follows: Byrd MS, Mason E, Henderson MW, Scheller E V, Cotter PA. 2013. An improved RIVET-like reporter system reveals differential cyaA gene activation in Bordetella species. Infection and immunity 81:1295–1305; M. S. B. and E. M. contributed equally to this article. Reprinted with permission.

Genes that define these three phenotypic phases have been divided into four classes based on their expression profile. Class 1 (late Bvg^+ phase) genes include *cyaA-E* (encoding the bifunctional hemolysin/adenylate cyclase toxin ACT) and *ptxA-E* (encoding the AB_5-type pertussis toxin) (4). Class 2 (early Bvg^+ phase) genes include those encoding filamentous hemagglutinin (*fhaB*), fimbriae (*fim2* and *fim3*), and *bvgAS* itself (4). *bipA* is the only class 3 (Bvg^i phase) gene that has been characterized. Class 4 (Bvg^- phase) genes include those encoding proteins involved in motility (*frlAB*) and chemotaxis in *B. bronchiseptica* (4).

Expression of genes that define the various Bvg-dependent phenotypic phases is determined mechanistically by the location and affinity of BvgA binding sites near the transcription start site (4). Class 1 genes contain multiple low affinity BvgA binding sites 5′ distal to the start of transcription (4, 11), while class 2 genes contain high-affinity BvgA binding sites proximal to the transcription start site (12-14). The promoter region of the class 3 gene *bipA* contains high affinity BvgA binding sites 5′ proximal to the transcription start site and low affinity sites 3′ to the transcription start site (10, 15). Although it has been hypothesized that BvgAS directly represses transcription of *frlAB* in *B. bronchiseptica* (16), BvgA binding to the *frlAB* promoter has not been demonstrated and BvgAS-mediated repression of at least some genes in *B. pertussis* is indirect (17).

In vitro transcription and DNA binding studies indicate that the phosphorylated form of BvgA (BvgA~P) is required to activate transcription of Bvg^+ phase genes and that a higher concentration of BvgA~P is necessary to bind "late" Bvg^+ phase promoters than "early" Bvg^+ phase promoters (11, 18). Although the natural signals that activate the BvgAS system are unknown, it is possible to modulate *Bordetella* spp. to the Bvg^- phase in the laboratory by adding a chemical modulator ($MgSO_4$ or nicotinic acid) to the growth medium, or by

growing bacteria at 25°C (15, 19-21). When grown under Bvg^- phase conditions, class 4 genes are expressed while class 1–3 genes are not expressed. When switched from Bvg^- phase to Bvg^+ phase conditions, transcription of class 4 genes ceases and transcription of class 2 genes, along with the sole class 3 gene *bipA*, is immediately activated. After several hours, class 1 genes are expressed and class 3 (*bipA*) genes are repressed. These data are consistent with the model in which the concentration of BvgA~P within the cell is nearly zero in the Bvg^- phase, low in the Bvg^i phase, and high in the Bvg^+ phase (4, 5, 11, 15, 18, 22, 23).

By contrast with the extensive *in vitro* characterization of the steady-state expression patterns of BvgAS-regulated genes in both *B. pertussis* and *B. bronchiseptica*, as well as kinetic analyses of gene expression upon switching from modulating to non-modulating conditions and vice versa (5, 10, 11, 15, 22-24), only one study has investigated BvgAS-dependent gene regulation *in vivo* (24). Veal-Carr et al. utilized recombination-based *in vivo* expression technology (RIVET) to analyze the kinetics of BvgAS-activated gene expression in *B. pertussis* both *in vitro* and following intranasal infection of mice (24, 25). They showed that the *in vivo* activation of Bvg^+ phase genes, including *ptxA*, *cyaA*, *fhaB*, and *prn*, temporally recapitulated the activation pattern of these genes upon switching *B. pertussis* from Bvg^- to Bvg^+ phase conditions *in vitro*; i.e., *fhaB* was activated early post-inoculation (~1 h), followed by *prn* (~4 h), then later by *cyaA* (~12 h) (24). Significantly, the fact that the pattern of gene activation was nearly identical in bacteria switched from Bvg^- to Bvg^+ phase conditions *in vitro* and post-inoculation of mice indicates that the mouse lung is a Bvg^+ phase environment (24).

We constructed a plasmid, pGFLIP, that encodes a Flp recombinase-based fluorescent reporter system to assess the activation kinetics of genes *in vivo* (26). The region of pGFLIP delivered to the chromosome contains *gfp* and *nptII* genes, encoding green fluorescent protein and neomycin phosphotransferase (conferring kanamycin resistance [Km^r]), respectively, flanked by *F*lp *r*ecombinase *t*arget (*FRT*) sites. The plasmid also contains a promoterless *flp* recombinase gene with a multiple cloning site (MCS) immediately 5′ to the start codon. Upon expression of *flp* under the control of a promoter of interest, the *gfp* and *nptII* genes are permanently excised from the bacterial chromosome.

To test our system, we cloned the promoter regions of several BvgAS-controlled genes, including the Bvg-activated genes *cyaA*, *fhaB*, and *ptxA* and the Bvg-repressed gene *flaA* (encoding flagellin) into pGFLIP and evaluated transcription activation *in vitro* and *in vivo* in *B. bronchiseptica*. Amongst other results, we found unexpectedly that the *cyaA* gene is expressed differently in *B. pertussis* and *B. bronchiseptica*.

Materials and Methods

Strains, reagents, and growth conditions. *Escherichia coli* were grown in lysogeny broth (LB; 10 g/l tryptone, 5 g/l yeast extract, 10 g/l NaCl) or on LB plates with 1.5% agar at 37°C. *Bordetella* were grown in Stainer-Scholte (SS) broth (27) or on Bordet-Gengou (BG) plates with 1.5% agar (BD Biosciences, San Jose, CA) supplemented with 7.5% (*B. bronchiseptica*) or 15.0% (*B. pertussis*) defibrinated sheep's blood (Colorado Serum Company, Denver, CO) at 37°C (28). As required, culture media were supplemented with kanamycin (Km; 50 or 100 μg/ml), ampicillin (100 μg/ml), streptomycin (25 μg/ml), $MgSO_4$ (20 mM or 50 mM), heptakis (1 mg/ml, Sigma), and for the Δ*asd* Δ*aphA* mobilizer strain RHO3 (29), diaminopimelic acid (DAP; 400 μg/ml). Unless otherwise noted, all restriction enzymes and T4 DNA ligase was purchased from New England Biolabs.

Construction of pGFLIP and derivatives containing *Bordetella* promoters. The Tn7 transposition plasmid pUC18T-mini-Tn7T-Km-*FRT* (30) was digested with BamHI, resulting in fragments of 3636 and 1299 bp in length containing the plasmid backbone and the *nptII* (Km^r) gene, respectively. Separately, a 797-bp fragment containing *gfp* driven by the constitutive *Burkholderia pseudomallei rpsL* promoter P_{S12} was amplified by PCR from mini-Tn7-*kan-gfp* (31) using Pfu Ultra II (Agilent) and primers GFP_UP and GFP_DN. This fragment was blunt-end ligated into the cloning vector pJET1.2/blunt (Fermentas) and was transformed into *E. coli* DH5α according to the manufacturer's instructions. Using restriction sites introduced by PCR, the P_{S12}-*gfp* fragment was digested from pJET using BamHI and was ligated together with the BamHI-digested pUC18T-mini-Tn7T-Km-*FRT* backbone and *nptII* fragment. As the *flp* gene would be sensitive to transcription read-through from either

the P_{S12} or the *nptII* promoter, primers specific to *gfp* (gfpseqR) and *nptII* (kanseqR) were used to confirm that both genes would be transcribed opposite the promoter of interest and would therefore not drive *flp* expression. Once the orientation of *gfp* and *nptII* was verified, the plasmid was digested with KpnI and StuI; a fragment containing promoterless *flp* amplified by PCR from pFLPe4 (30) using primers FLP_UP and FLP_DN was likewise digested with KpnI and StuI and was ligated into the digested vector. The resulting plasmid, pGFLIP, thus contained an MCS 5′ to *flp*, the *flp* recombinase gene, and constitutively expressed *nptII* and *gfp* genes flanked by *FRT* sites. pGFLIP was fully sequenced using a primer-walking approach with the primers listed in Table 2.

Promoters for five *Bordetella* genes (*cyaA*, $cyaA_{Bp}$, *fhaB*, *ptxA*, and *flaA*) were cloned into the MCS of pGFLIP as follows. For *cyaA* and $cyaA_{Bp}$, 605 and 604-bp fragments containing the *cyaA* promoter were amplified by PCR from *B. bronchiseptica* RB50 and *B. pertussis* BPSM, respectively, using primers cyaA_F and cyaA_R. These fragments were digested with SacI and KpnI and ligated into pGFLIP. For *fhaB*, a 426-bp fragment containing the *fhaB* promoter was amplified by PCR from RB50 using primers fhaprF2 and fhaprR2, digested with SacI and KpnI, and ligated into pGFLIP. For *ptxA*, a 454-bp fragment containing the *ptxA* promoter was amplified by PCR from BPSM using primers ptxprF and ptxprR, digested with SacI and ApaI, and ligated into pGFLIP. For *flaA*, a 514-bp fragment containing the *flaA* promoter was amplified by PCR from RB50 using primers flaA_F and flaA_R, digested with SacI and KpnI, and ligated into pGFLIP. These constructs were delivered to the chromosome by transposase-mediated insertion as described below.

Transposase-mediated delivery of pGFLIP to the *B. bronchiseptica att*Tn7 site. The pGFLIP plasmid was delivered to *Bordetella* by tri-parental mating using a procedure

modified from (28). *B. bronchiseptica* strains RB50 and RB52 were grown on BG agar for 48 h, and a portion of the cells was co-incubated with conjugation-competent *E. coli* RHO3 cells (29) harboring pGFLIP and RHO3 cells containing the helper plasmid pTNS3 (30), which expresses *tnsABCD* from a constitutive promoter, on BG agar supplemented with DAP for 6 h at 37°C. Following incubation, cells were restreaked onto BG/Km agar containing 20 mM $MgSO_4$ (to maintain strains containing pGFLIP with Bvg^+ phase promoters in the Bvg^- phase) or without $MgSO_4$ (to maintain RB50*flaA*FLP in the Bvg^+ phase) and were incubated an additional 48 h at 37°C. Delivery of pGFLIP to BPSM followed the same procedure except that incubations required four days at 37°C and plates were supplemented with 50 mM $MgSO_4$. pGFLIP without a promoter driving *flp* was used as a positive control for GFP production and as a negative control for *flp* activation. The delivery of all constructs to the *att*Tn7 site was confirmed by PCR using primers glmSF and gfpseqR (data not shown).

Evaluation of pGFLIP *in vitro*. We determined the functionality of pGFLIP using a plate-based assay in which RB50*cyaA*FLP and RB50*flaA*FLP were modulated between promoter-inactive and promoter-active conditions. BG agar containing 20 mM $MgSO_4$ was used to de-repress P_{flaA} and to deactivate P_{cyaA}, while BG agar without $MgSO_4$ was used to activate P_{cyaA} and to repress P_{flaA} (7). The pGFLIP strains were grown under promoter-inactive conditions for 48 h at 37°C and were determined to be GFP^+ using a G:BOX Chemi imaging system with an UltraBright-LED Blue transilluminator and a SW06 short-pass filter (495–600 nm; Syngene, Frederick, MD). A single GFP^+ colony was resuspended in PBS and was diluted and plated on BG agar under promoter-active and promoter-inactive conditions. To demonstrate the loss of Km^r upon promoter activation, Km (100 μg/ml) was added to some

plates. Plates were incubated for 48 h at 37°C, and white-light and fluorescent images were obtained using the G:BOX Chemi system.

For kinetic assays, strains containing pGFLIP were grown overnight with Km selection in SS under promoter-inactive conditions (20 mM $MgSO_4$ for RB50*cyaA*FLP, RB50*cyaA*$_{Bp}$FLP, RB50*fhaB*FLP, and RB50*ptxA*FLP; no added $MgSO_4$ for RB50*flaA*FLP). Cells were washed twice in PBS with or without 5 mM $MgSO_4$ to prevent the premature activation of Bvg^+ phase and *flaA* promoters, respectively, and were added to fresh SS medium under promoter-active conditions (20 mM $MgSO_4$ for RB50*flaA*FLP; no added $MgSO_4$ for RB50*cyaA*FLP, RB50*cyaA*$_{Bp}$FLP, RB50*fhaB*FLP, and RB50*ptxA*FLP) at the OD_{600} that was equivalent to 1×10^9 cfu/ml. Tubes were incubated on a roller at 37°C for 8 h. At each time point, an aliquot of cells was removed, diluted in PBS under promoter-inactive conditions, and was plated on BG agar under promoter-inactive conditions. Plates were incubated for 48 h at 37°C, and total cfu were enumerated. For kinetic assays with *B. pertussis*, cultures were inoculated at the cfu/ml corresponding to an OD_{600} of ~ 0.1, and cells were grown overnight in SS containing 50 mM $MgSO_4$, 100 μg/ml Km, and 1 mg/ml heptakis. Cells were washed in PBS containing 25 mM $MgSO_4$ to prevent premature *flp* activation. All other aspects of the assay were the same as for *B. bronchiseptica*, except that dilutions were plated on BG agar containing 50 mM $MgSO_4$ and plates were incubated four days at 37°C. GFP fluorescence was quantified using the G:BOX Chemi imaging system as described. The percent resolution (the ratio of GFP^- colonies to the total number of colonies × 100%) was calculated for each strain at each time point.

Evaluation of pGFLIP in a murine model of infection. Five- to seven-week-old BALB/c mice (Jackson Laboratories, Bar Harbor, ME) were inoculated intranasally with $1 \times$

10^5 cfu of *B. bronchiseptica* pGFLIP strains in 50 µl of PBS. For infections with RB50*cyaA*FLP, RB50*cyaA*$_{Bp}$FLP, RB50*fhaB*FLP, and RB50*ptxA*FLP, bacteria were grown overnight in SS medium containing Km (100 µg/ml) and 20 mM $MgSO_4$ to maintain cells in the Bvg^- phase. For infections with RB50*flaA*FLP, bacteria were grown overnight in SS media containing Km (100 µg/ml) to maintain cells in the Bvg^+ phase. Lungs were harvested from infected mice at 1 h and 30 h post-inoculation (p.i.). For RB50*flaA*FLP, right lungs were homogenized in 1 mL of PBS, diluted in PBS, and plated in duplicate on BG agar. For strains containing Bvg^+ phase promoters in pGFLIP, homogenization, dilution, and plating were carried out in the presence of 20 mM $MgSO_4$. Percent resolution was calculated for each strain at each time point. This study was done in strict accordance with the recommendations in the Guide for the Care and Use of Laboratory Animals of the National Institutes of Health. Our protocol was approved by the University of North Carolina IACUC (12-307.0). All animals were properly anesthetized for inoculations, monitored regularly, euthanized when moribund, and efforts were made to minimize suffering.

Statistical analyses. Statistical analyses were performed using Prism 5 (GraphPad Software, Inc.). Statistical significance was determined using the unpaired Student's *t*-test or analysis of variance (ANOVA). Images were formatted using Adobe Photoshop CS5 and figures were generated using Adobe Illustrator CS5 (Adobe Systems, Inc.).

Results

Design and Construction of pGFLIP. To study transcription activation of genes both *in vitro* and *in vivo*, we engineered a reporter system, pGFLIP, that provides both fluorescent and selectable markers. We designed our system for simplicity and ease of use. Therefore, all of the components necessary for pGFLIP function are contained on a single plasmid. The region of pGFLIP delivered to the chromosome includes *gfp* and *nptII*, each under the control of a strong constitutive promoter and together flanked by *FRT* sequences (Figure 3). The Flp recombinase gene *flp* is present in the opposite orientation from *gfp* and *nptII* with an immediate 5′ MCS to facilitate the insertion of a promoter of interest. In the absence of promoter activity *flp* is not transcribed and cells remain GFP^+ and Km^r. When the promoter of interest is activated, *flp* is transcribed and the gene product mediates recombination between *FRT* sites, permanently excising *gfp* and *nptII*.

To test the system, we cloned promoter regions from *B. bronchiseptica* and *B. pertussis* into the MCS to generate the strains described in Table 1. The region of pGFLIP between Tn7L and Tn7R ends was delivered to the *att*Tn7 site 3′ to the *glmS* gene in *Bordetella* spp. as described in Materials and Methods. Transcription terminators are present near the 5′ end of the transposon to prevent transcription read-through from *glmS*. Delivery of promoterless pGFLIP to *B. bronchiseptica* RB50 and *B. pertussis* BPSM resulted in strains that were stably GFP^+ and Km^r. These strains did not lose GFP fluorescence or Km^r when passaged multiple times *in vitro* in the absence of selection (data not shown).

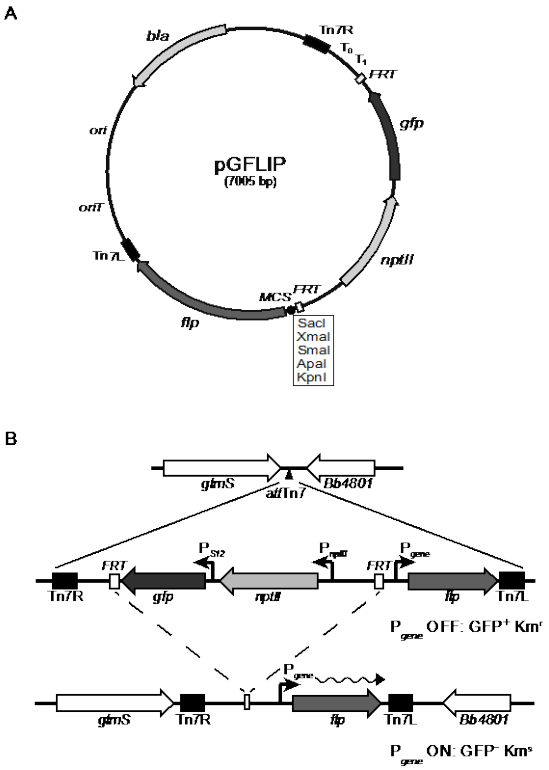

Figure 3. Design and mechanism of pGFLIP. (A) Diagram of pGFLIP. Tn7R and Tn7L, left and right ends of the Tn7 transposon, respectively; T_0 and T_1, bacteriophage λ and *E. coli rrnB* transcriptional terminators, respectively; *FRT*, Flp recombinase target; *gfp*, green fluorescent protein gene; *nptII*, neomycin phosophotransferase gene; MCS, multiple cloning site with restriction sites indicated; *flp*, Flp recombinase gene; *oriT*, origin of conjugative transfer; *ori*, ColE1 origin of replication; *bla*, β-lactamase gene. (B) Schematic illustration of Tn7-mediated delivery and Flp-mediated excision of pGFLIP in RB50. The region of pGFLIP flanked by Tn7L and Tn7R sequences is delivered to the *att*Tn7 site located between *glmS* and BB4801. While the promoter driving expression of the gene of interest (P_{gene}) remains inactive, *gfp* and *nptII* are expressed constitutively, resulting in fluorescent and Km^r bacteria. When P_{gene} is activated, *flp* is expressed and Flp recombinase mediates site-specific recombination between *FRT* sites, permanently excising *gfp* and *nptII* and yielding bacteria that are non-fluorescent and sensitive to Km.

Table 1. Strains and plasmids used in this study

Strain or Plasmid	Description	Source or reference
Strains		
E. coli		
DH5α	Molecular cloning strain	(28)
RHO3	Conjugation strain; Km^s, Δ*asd*, Δ*aphA*	(29)
Bordetella		
RB50	Wild-type *B. bronchiseptica* strain; Sm^r	(7)
RB52	RB50 containing *bvgAS* from BP338; Sm^r	(22)
BPSM	Sm^r Tohama I derivative	(29, 42)
RB50FLP	RB50 with promoterless pGFLIP integrated at *att*Tn7	This study
RB50*cyaA*FLP	RB50 with *flp* recombinase driven by P_{cyaA} integrated at *att*Tn7	This study
RB50$cyaA_{Bp}$FLP	RB50 with *flp* recombinase driven by P_{cyaA} from Tohama I integrated at *att*Tn7	This study
RB52$cyaA_{Bb}$FLP	RB52 with *flp* recombinase driven by P_{cyaA} from RB50 integrated at *att*Tn7	This study
RB52$cyaA_{Bp}$FLP	RB52 with *flp* recombinase driven by P_{cyaA} from Tohama I integrated at *att*Tn7	This study
RB50*fhaB*FLP	RB50 with *flp* recombinase driven by P_{fhaB} from RB50 integrated at *att*Tn7	This study
RB50*ptxA*FLP	RB50 with *flp* recombinase driven by P_{ptxA} from Tohama I integrated at *att*Tn7	This study
RB50*flaA*FLP	RB50 with *flp* recombinase driven by P_{flaA} integrated at *att*Tn7	This study
BPSMFLP	BPSM with promoterless pGFLIP integrated at *att*Tn7	This study
BPSM*cyaA*FLP	BPSM with *flp* recombinase driven by P_{cyaA} from RB50 integrated at *att*Tn7	This study
BPSM*fhaB*FLP	BPSM with *flp* recombinase driven by P_{fhaB} from RB50 integrated at *att*Tn7	This study
BPSM*ptxA*FLP	BPSM with *flp* recombinase driven by P_{ptxA} integrated at *att*Tn7	This study
Plasmids		
pUC18T-mini-Tn7T-Km-*FRT*	Mobilizable transposition vector; Ap^r, Km^r	(30)
pFLPe4	Site-specific excision vector, source of Flp recombinase; Ap^r, Km^r	(30)
mini-Tn7-*kan-gfp*	Mobilizable transposition vector, source of *gfp* driven by P_{S12}; Km^r	(31)
pTNS3	Tn7 transposase expression vector containing *tnsABCD*; Ap^r	(30)

pGFLIP	pUC18-based vector with P_{S12}-*gfp* and *nptII* flanked by *FRT* sequences and *flp* 3′ to the MCS; Ap^r, Km^r	This study
pGFLIP-P_{cyaA}	pGFLIP with *flp* recombinase driven by the RB50 *cyaA* promoter, Ap^r, $Km^{r a}$	This study
pGFLIP-P_{cyaABp}	pGFLIP with *flp* recombinase driven by the BPSM *cyaA* promoter, Ap^r, $Km^{r a}$	This study
pGFLIP-P_{fhaB}	pGFLIP with *flp* recombinase driven by the RB50 *fhaB* promoter, Ap^r, $Km^{r a}$	This study
pGFLIP-P_{ptxA}	pGFLIP with *flp* recombinase driven by the BPSM *ptxA* promoter, Ap^r, $Km^{r a}$	This study
pGFLIP-P_{flaA}	pGFLIP with *flp* recombinase driven by the RB50 *flaA* promoter, Ap^r, $Km^{r a}$	This study

[a] Km^r only under promoter-inactive conditions

Table 2. Primers used in this study

Primer	Sequence (5′-3′)[a]	Description
FLP_UP	ATCTACGGTACCATGAGCCAGTTCGATATCC	Forward and reverse primers to amplify *flp* from pFLPe4
FLP_DN	AGGTCCAGGCCTCTATATGCGTCTATTTATG	
GFP_UP	ATATATGGATCCCAGCTGTTGACTCGCTTG	Forward and reverse primers to amplify *gfp* from mini-Tn7-*kan-gfp*
GFP_DN	ACCTGGGGATCCTTATTTGTATAGTTCATCC	
Tn7seqF	GAGCGCTTTTGAAGCTGATGTGCT	Forward sequencing primer annealing within Tn7R
gfpseqR	GATGACGGGAACTACAAGACACGT	Reverse sequencing primer annealing within *gfp*
kanseqR	ATCGCCTTCTATCGCCTTCTTGAC	Reverse sequencing primer annealing within *nptII*
GFLseq1	ACGGTGAAAACCTCTGACACATGC	Forward sequencing primers for sequencing pGFLIP by primer-walking
GFLseq2	CTGAAATCAGTCCAGTTATGCTGTG	
GFLseq3	AAATCCGCCGCTAGGAGCTT	
GFLseq4	GTCTGCCATGATGTATACATTGTGTG	
GFLseq5	GGGACAACTCCAGTGAAAAGTTCTTC	
GFLseq6	CTGATGCTCTTCGTCCAGATCATC	
GFLseq7	CCTGCGTGCAATCCATCTTGTTCA	
GFLseq8	CAGGGGATCTTGAAGTTCCTATTCCG	
GFLseq9	GCAACAATTCTGGAAGCCTCATT	
GFLseq10	TCTTTAGCGCAAGGGGTAGGATCG	
GFLseq11	TCCAATTGAGGAGTGGCAGCAT	
GFLseq12	TATCAGAGCTTATCGGCCAGCCT	
GFLseq13	ATAAAGATACCAGGCGTTTCCCCC	
GFLseq14	AAACAAACCACCGCTGGTAGC	
GFLseq15	CGCAGAAGTGGTCCTGCAACTTTA	
GFLseq16	CCGCGCCACATAGCAGAACTTTAA	
gflpmcsF	GTTGACAAAGGGAATCAGGGGATC	Forward sequencing primer for inserts in the MCS
gflpmcsR	GAACTGGGTGTAGCGTCGTAAGCT	Reverse sequencing primer for inserts in

		the MCS
glmSF	CAGCTGCTGTCGTACCACACGG	Forward primer to confirm Tn7 insertion at *glmS* by PCR
cyaA_F	ATTATAGAGCTCTGCGAGCAGATGCAC	Forward and reverse primers to amplify P_{cyaA} from RB50 and BPSM
cyaA_R	TATAATGGTACCGTGGATCTGTCGATAAGTAG	
ptxprF	AGCTTCGAGCTCCAAGATAATCGTCCTGCTC	Forward and reverse primers to amplify P_{ptxA} from BPSM
ptxprR	ATATATGGGCCCTCCCGTCTTCCCCTCT	
fhaprF2	AGGCCTGAGCTCGATAAGAAGAATATGCTT	Forward and reverse primers to amplify P_{fhaB} from RB50
fhaprR2	ATATTCGGTACCATTCCGACCAGCGAAGTG	
flaA_F	AATGAGCTCGCCGTGCTCAACGTCA	Forward and reverse primers to amplify P_{flaA} from RB50
flaA_R	ATTATAGGTACCAGGCTCCCAAGAGAGAAA	

Functional evaluation of pGFLIP *in vitro*. To evaluate the functionality of pGFLIP, we used two *B. bronchiseptica* promoters for which activity can readily be induced *in vitro*: P_{cyaA} and P_{flaA}. In *B. bronchiseptica*, the *flaA* promoter is highly transcribed in the Bvg^- phase, while the *cyaA* promoter is transcribed strongly in the Bvg^+ phase (9, 10, 15, 22, 32). Therefore, RB50*flaA*FLP was constructed under Bvg^+ phase conditions to prevent expression of *flaA*, while RB50*cyaA*FLP was maintained under Bvg^- phase conditions to prevent expression of *cyaA*. Km was added to the media during construction of these strains to select against any bacteria that had activated *flp*, thus ensuring that the population only contained GFP^+ and Km^r cells. To test these strains for pGFLIP functionality, we suspended a single GFP^+ colony of each strain in PBS and plated on BG, BG/Km, BG/$MgSO_4$, and BG/Km/$MgSO_4$ agar and observed colony formation and GFP fluorescence after two (*B. bronchiseptica*) or four (*B. pertussis*) days incubation at 37°C.

When plated under promoter-active conditions (20 mM $MgSO_4$ for RB50*flaA*FLP; no added $MgSO_4$ for RB50*cyaA*FLP) in the absence of Km, all RB50*flaA*FLP and RB50*cyaA*FLP colonies examined had lost fluorescence, and when tested subsequently for growth on agar containing Km, all colonies had lost Km^r (Figure 4 A and D). As expected, plating either strain under promoter-active conditions and in the presence of Km resulted in a lack of growth due to loss of *nptII* from the chromosome (Figure 4 E and H). Conversely, when plated under promoter-inactive conditions (no added $MgSO_4$ for RB50*flaA*FLP; 20 mM $MgSO_4$ for RB50*cyaA*FLP) *in the presence of Km*, all RB50*flaA*FLP and RB50*cyaA*FLP colonies maintained fluorescence (Figure 4 F and G). Likewise, under promoter-inactive conditions in the absence of Km, all RB50*flaA*FLP colonies maintained fluorescence (Figure 4

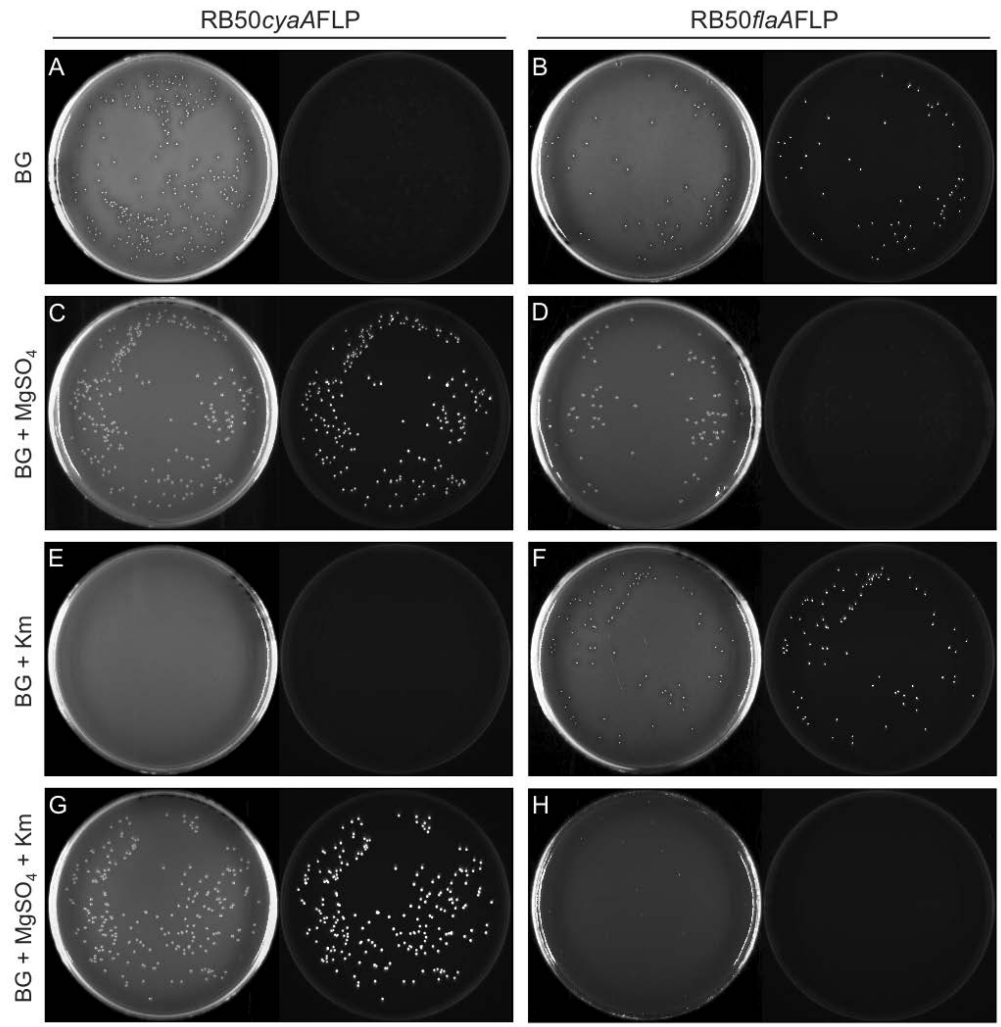

Figure 4. Plate-based validation of the pGFLIP reporter system using P_{cyaA} and P_{flaA}. Left column, images of RB50*cyaA*FLP plated under (A) Bvg^+ phase and (C) Bvg^- phase conditions (achieved by supplementing BG agar with 20 mM $MgSO_4$) in the (E) presence or (G) absence of 100 µg/ml Km. Right column, images of RB50*flaA*FLP plated under (B) Bvg^+ phase and (D) Bvg^- phase conditions in the (F) presence or (H) absence of 100 µg/ml Km. White light photographs are on the left and fluorescent images are on the right in each pair of images.

B), indicating that *flaA* is not expressed under these conditions. Unexpectedly, however, when RB50*cyaA*FLP was plated under promoter-inactive conditions *in the absence of Km selection*, approximately 14% of the colonies had lost fluorescence at the time of imaging (Figure 4C). These colonies did not grow when restreaked onto BG/Km/$MgSO_4$, indicating

that cells in these colonies were not *gfp* mutants but had lost fluorescence and Km^r due to Flp-mediated recombination. These results suggest that the transcription activity of P_{cyaA} under Bvg^- phase conditions *in vitro* is close to the threshold level of *flp* transcription required for Flp-mediated recombination between *FRT* sites. These plate-based assays for fluorescence and Km^r demonstrated that pGFLIP is indeed functional and that both markers (*gfp* and *nptII*) can be used to document promoter activation under active and inactive conditions.

Kinetic analysis of *Bordetella* gene activation using pGFLIP. We next assessed the ability of this system to monitor gene activation over time in bacteria grown in liquid culture. Strains containing pGFLIP plasmids with *cyaA*, *fhaB*, *ptxA*, and *flaA* promoters were grown overnight under promoter-inactive conditions, switched to promoter-active conditions, and the percent resolution (i.e., loss of GFP fluorescence and Km^r) was calculated over 8 h. For the first 4 h after switching from Bvg^+ phase to Bvg^- phase conditions, the percentage of RB50*flaA*FLP colonies that had lost fluorescence remained below 20% (Figure 5A), indicating that less than 20% of the bacteria had reached or surpassed the threshold of *flp* expression to result in recombination during this time. Approximately 75% of cells had lost fluorescence at 6 h, and this proportion was maintained at 8 h (Figure 5A). When grown under Bvg^- phase conditions for 24 h, greater than 85% of cells demonstrated a loss of fluorescence and Km^r (data not shown). The fact that resolution did not reach 100% suggests that the maximum

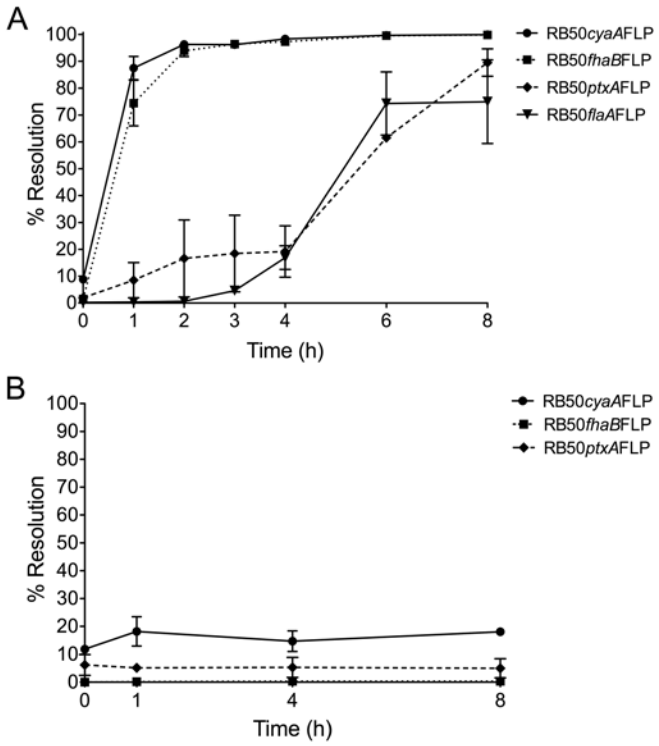

Figure 5. Kinetic analysis of *Bordetella* gene activation *in vitro*. *B. bronchiseptica* strains grown under promoter-off conditions and in the presence of 100 µg/ml Km were washed and placed in fresh SS medium under (A) promoter-on conditions or (B) promoter-off conditions. Colonies arising from aliquots plated over 8 h were monitored for loss of fluorescence and the percent resolution was calculated. Results are the mean ± SEM for experiments performed in duplicate or triplicate.

level of *flaA* expression under *in vitro* Bvg^- phase conditions (SS medium containing 20 mM $MgSO_4$) is just at or above the threshold of *flp* expression needed for Flp-mediated recombination between *FRT* sites. The relatively long amount of time required for the majority of RB50*flaA*FLP cells to cross the threshold of *flp* expression is in agreement with a previous study that examined the expression kinetics of the BvgAS-regulated operon *frlAB*, which encodes the *E. coli* FlhDC homologs FrlAB that are at the top of the flagella transcription cascade in *B. bronchiseptica* (16). Upon shifting from Bvg^+ phase to Bvg^- phase conditions, a *frlAB-lacZ* fusion strain exhibited a gradual increase in β-galactosidase

activity over time, reaching approximately 40% of the maximum overnight expression level by 7.5 h (15).

In contrast, when RB50*fhaB*FLP were switched from Bvg^- phase to Bvg^+ phase conditions, the *fhaB* promoter was apparently activated as early as 1 h, at which time approximately 75% of cells had lost fluorescence (Figure 5A). At 2 h and later time points, nearly 100% of RB50*fhaB*FLP cells had lost fluorescence, consistent with the classification of *fhaB* as a class 2 gene requiring a relatively low level of BvgA~P for activation. As a canonical class 1 (or "late") gene, *ptxA* had only been activated in approximately 8% of cells at 1 h (Fig. 3A). Approximately 20% of cells had activated *ptxA* by 4 h, increasing to 90% of cells by 8 h. Surprisingly, *cyaA*, which is also considered to be a class 1 gene, was activated in over 85% of cells at 1 h, and in greater than 95% of cells at 2 h and later time points (Fig. 3A). These data suggest that at early time points after switching to promoter-active conditions, the *cyaA* promoter is activated to a level sufficient to drive *flp*-mediated recombination. This result was unexpected based on *cyaA* transcription results in studies of *B. pertussis* (5, 11, 18, 23, 24).

At the initiation of each kinetic experiment, we observed a consistent background resolution (i.e., the percent resolution at 0 h) for each Bvg^+ phase promoter in pGFLIP. RB50*cyaA*FLP displayed the highest background resolution at 8.9%, while the background resolution for *fhaB* and *ptxA* was significantly lower at 1.54% and 1.99%, respectively ($p < 0.01$). The background resolution for RB50*flaA*FLP was the lowest of the pGFLIP constructs at 0.23% (Figure 5A). The fact that a portion of RB50*cyaA*FLP cells had lost fluorescence at 0 h suggests that low-level expression of *cyaA* might be occurring in a BvgAS-independent manner, which could interfere with measuring BvgAS-dependent P_{cyaA} activation over time.

Therefore, to test the sensitivity of pGFLIP to background resolution we grew RB50*cyaA*FLP, RB50*fhaB*FLP, and RB50*ptxA*FLP strains overnight as in Fig. 3A, washed the cells to remove Km, and maintained the cultures under Bvg^- conditions in the absence of selection for 8 h. At 0, 1, 4, and 8 h, the percent resolution was determined for each strain. We hypothesized that if P_{cyaA} was indeed active under Bvg^- conditions we would observe a steady increase in resolution over time for RB50*cyaA*FLP but not for RB50*fhaB*FLP or RB50*ptxA*FLP. As expected, RB50*cyaA*FLP displayed the greatest background resolution at 11.9%, increasing to 18.1% at 8 h (Figure 5B). Loss of fluorescence for RB50*fhaB*FLP and RB50*ptxA*FLP remained essentially unchanged over 8 h, averaging 0.22% and 5.4%, respectively (Figure 5B). Although *cyaA* had been activated in approximately one-fifth of the population at 8 h, these data do not account for the >85% resolution observed for RB50*cyaA*FLP as early as 1 h following the switch to Bvg^+ phase conditions.

Neither the *B. bronchiseptica bvgAS* allele nor P_{cyaA} accounts for the unexpectedly early activation of *cyaA*. As *cyaA* expression in RB50 was activated unexpectedly early compared to what has been observed for *B. pertussis* (5, 11, 18, 23, 24), we sought to determine whether differences in the *cyaA* promoter or in the *bvgAS* allele between *B. bronchiseptica* and *B. pertussis* accounted for this difference. There are five single nucleotide changes and one nucleotide insertion in the sequence 5′ to *cyaA* in *B. bronchiseptica* RB50 compared to *B. pertussis* BPSM. We hypothesized that replacing the *cyaA* promoter of RB50 with that of BPSM would delay the activation of P_{cyaA} relative to P_{fhaB}, similar to what was observed by Veal-Carr et al. (24). We cloned the *cyaA* promoter from *B. pertussis* BPSM into pGFLIP and introduced this plasmid into RB50, generating strain RB50$cyaA_{Bp}$FLP. When evaluated

in the kinetic assay, there was no difference in the rate of resolution between RB50*cyaA*FLP and RB50$cyaA_{Bp}$FLP, suggesting that differences in the *cyaA* promoter do not account for the rapid resolution observed in *B. bronchiseptica* (Figure 6).

Some strains of *B. pertussis*, such as BP338 and BPSM, exhibit decreased sensitivity to chemical modulation compared to *B. bronchiseptica* RB50 due to amino acid differences in BvgS, which causes these strains to remain in the Bvg^+ phase at a lower concentration of modulator compared to RB50 (22). We hypothesized, therefore, that the *bvgAS* allele from BP338 would permit activation of *cyaA* more quickly and in a greater percentage of cells compared to the *B. bronchiseptica* RB50 *bvgAS* allele. To assess this, we utilized strain RB52, which contains the entire *bvgAS* locus and *bvgA* promoter from *B. pertussis* BP338 in place of *bvgAS* in RB50 (22). RB52 recapitulates the decreased sensitivity to modulation characteristic of both BP338 and BPSM, requiring ≥ 40 mM $MgSO_4$ to modulate to the Bvg^- phase, in contrast to RB50, which requires ≥ 10 mM $MgSO_4$ to fully modulate (15, 22). We introduced pGFLIP containing the RB50 *cyaA* promoter driving *flp* expression into RB52, producing strain RB52$cyaA_{Bb}$FLP. We evaluated the kinetics of *cyaA* activation in RB52$cyaA_{Bb}$FLP compared to RB50*cyaA*FLP and did not observe any difference. Likewise, when we evaluated an RB52 derivative containing the BPSM *cyaA* promoter driving *flp* expression (RB52$cyaA_{Bp}$FLP) in the kinetic assay, there was no impact on *cyaA* activation compared to RB50*cyaA*FLP. Together, these data suggest that neither the *cyaA* promoter nor the *bvgAS* allele significantly affects the kinetics of *cyaA* activation in *B. bronchiseptica* as reported by the P_{cyaA}-*flp* promoter fusion in pGFLIP (Figure 6).

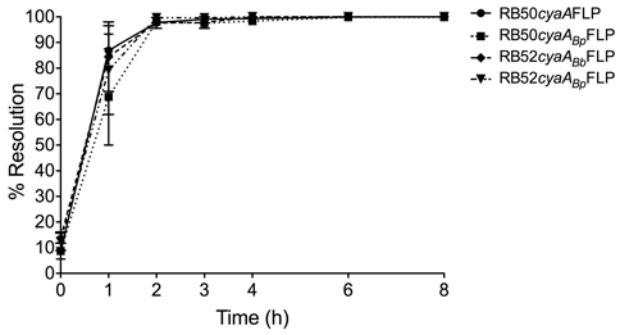

Figure 6. Effect of P_{cyaA} and *bvgAS* alleles on *cyaA* activation in *B. bronchiseptica*. RB50 and RB52, an RB50 derivative carrying the *bvgAS* allele from *B. pertussis* BP338 in place of the native *bvgAS* allele, each with pGFLIP containing RB50 and BPSM P_{cyaA}, were grown as in Fig. 3 and were switched to promoter-on conditions for 8 h. Loss of fluorescence was calculated for each strain as described in Materials and Methods. Results are the mean ± SEM for experiments performed in duplicate.

Evaluation of *Bordetella* promoter activation *in vivo*. Although the kinetics of Bvg^+ phase gene activation *in vivo* have been examined for *B. pertussis* (24), these experiments have not been done in *B. bronchiseptica* or in the context of a natural bacteria-host interaction. To address BvgAS-regulated gene activation in *B. bronchiseptica in vivo*, we infected BALB/c mice intranasally with 1×10^5 cfu of the RB50 pGFLIP strains shown in Figure 5A, grown under promoter-inactive conditions (100 μg/ml Km, 20 mM $MgSO_4$). Mice were sacrificed and lungs were harvested at 1 h and 30 h p.i. Lungs were homogenized and dilutions were plated on BG agar containing 20 mM $MgSO_4$ to prevent further recombination. Total cfu were enumerated and the percentage of colonies that had lost fluorescence (% resolution) was calculated for each strain and time point. The percentage of RB50*fhaB*FLP that had lost fluorescence at 1 h was 95.3 ± 0.60%, while only 5.4 ± 0.69% of RB50*ptxA*FLP had lost fluorescence at this time (Figure 7). Similar to the *in vitro* kinetic assay (Figure 5A), the majority (85.3 ± 3.3%) of RB50*cyaA*FLP cells had lost fluorescence at 1 h. At 30 h p.i., essentially all cells had lost fluorescence, indicating that the environment in the mouse

induces the expression of Bvg$^+$ phase genes to a level at or above that required to activate *flp* expression (Figure 7). The fact that the pGFLIP system functions *in vivo* much the same as *in vitro* when switched from Bvg$^-$ to Bvg$^+$ phase conditions suggests that the pattern of Bvg$^+$ phase gene activation is similar between these two conditions and that the unexpectedly early expression from the *cyaA* promoter *in vitro* was not due to an artifact of that assay.

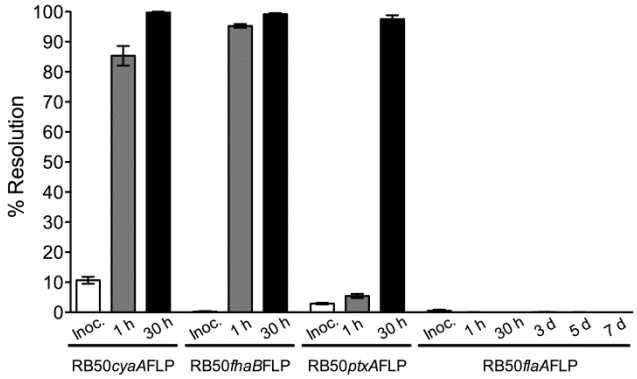

Figure 7. Analysis of *Bordetella* gene activation *in vivo* using pGFLIP. RB50*cyaA*FLP, RB50*fhaB*FLP, RB50*ptxA*FLP, and RB50*flaA*FLP were grown as in Fig. 3 and 1×10^5 cfu was inoculated intranasally into mice in a total volume of 50 µl. Mice were sacrificed at 0, 1, and 30 h p.i., with additional time points at 3, 5, and 7 days for RB50*flaA*FLP, and lungs were homogenized and plated on BG agar supplemented with 20 mM $MgSO_4$ and Sm (for RB50*cyaA*FLP, RB50*fhaB*FLP, and RB50*ptxA*FLP) or on BG agar supplemented only with Sm (for RB50*flaA*FLP). Loss of fluorescence was calculated for each strain as described in Materials and Methods. Results are the mean ± SEM for experiments performed in duplicate with three mice per time point

Although all evidence thus far suggests that the Bvg$^+$ phase is necessary and sufficient for *Bordetella* spp. to cause respiratory infection in rats and mice (6, 7, 22, 33), it is possible that rare *in vivo* environments exist that induce modulation to the Bvg$^-$ phase. Therefore, using the activation of the *flaA* promoter as an indicator of the Bvg$^-$ phase, we infected mice as described above and evaluated the loss of fluorescence at 1 h and 30 h p.i. We did not observe activation of *flaA* in any RB50*flaA*FLP cells at 1 h, 30 h, 3 d, 5 d, or 7 d (Figure 7).

These data suggest that *B. bronchiseptica* do not enter the Bvg^- phase in the mouse during the time period that we examined.

Kinetic analysis of *Bordetella* gene activation in *B. pertussis* reveals delayed activation of *cyaA* compared to *B. bronchiseptica.* Due to the observation that neither the *cyaA* promoter nor the *bvgAS* allele affects the kinetics of *cyaA* activation in *B. bronchiseptica*, we hypothesized that additional, species-specific factors account for the differences in the activation of *cyaA*. To evaluate this possibility, we delivered the same pGFLIP plasmids as those used in *B. bronchiseptica* to the chromosome of *B. pertussis* BPSM and evaluated loss of fluorescence in the kinetic assay. We reasoned that if the activation of *cyaA*, *fhaB*, and *ptxA* in *B. pertussis* resembled the pattern seen in *B. bronchiseptica*, then the discrepancy with was likely due to differences in resolvase/recombinase expression sensitivity between pGFLIP and RIVET (i.e., Flp recombinase is activated at a lower threshold of P_{cyaA} activity than TnpR, making *cyaA* appear to be activated sooner in the Flp-*FRT* system). Alternatively, if activation of *cyaA*, *fhaB*, and *ptxA* was canonical as in Veal-Carr et al. (24), then the difference in *cyaA* activation would be attributed to species-specific gene regulation.

In contrast to what we observed in *B. bronchiseptica*, the proportion of BPSM*cyaA*FLP that had lost fluorescence at 1 h was less than 10%, essentially equal to the level of background resolution (Figure 8). There was a steady loss of fluorescence in BPSM*cyaA*FLP beginning at 2 h post-switch and continuing until 6 h, at which time greater than 90% of colonies had lost fluorescence. The pattern of P_{cyaA} activation in *B. pertussis* matched that of P_{ptxA}, which displayed similar but somewhat earlier activation in *B. pertussis* compared to *B. bronchiseptica* (Figure 8). Interestingly, the loss of fluorescence in

BPSM*fhaB*FLP occurred more slowly compared to RB50*fhaB*FLP, with approximately 55% of cells having lost fluorescence at 1 h. At 2 h post-switch the proportion of GFP^- BPSM*fhaB*FLP equaled that of RB50*fhaB*FLP at 1 h, indicating that the activation of P_{fhaB} may be delayed in *B. pertussis* compared to *B. bronchiseptica*; however, the background resolution for BPSM*fhaB*FLP (29.5 ± 11.3%) was substantially higher compared to RB50*fhaB*FLP. At 1.99%, the background resolution for BPSM*ptxA*FLP was identical to that seen for RB50*ptxA*FLP, while the background for BPSM*cyaA*FLP (4.8 ± 2.2%) was not significantly different compared to RB50*cyaA*FLP (Figure 8).

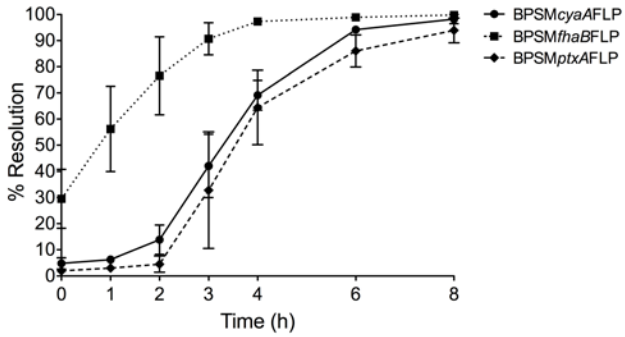

Figure 8. Kinetic analysis of Bordetella gene activation *in vitro* in *B. pertussis.* Strains grown under promoter-off conditions and in the presence of 100 µg/ml Km were washed and placed in fresh SS medium under promoter-on conditions. Colonies arising from aliquots plated over 8 h were monitored for loss of fluorescence and the percent resolution was calculated. Results are the mean ± SEM for experiments performed in triplicate.

Discussion

Evaluating bacterial gene expression within the host is critical for understanding the complex host-pathogen interactions that result in disease, clearance, or asymptomatic colonization. One approach that has been developed to evaluate gene expression in the host is *in vivo* expression technology (IVET) (34). In IVET, promoter sequences are cloned 5′ to a gene that either confers resistance to an antibiotic or complements a specific auxotrophy (34-36). Under conditions in which the promoter is active, these genes are expressed and permit the survival of bacteria in hosts that have either been dosed with the relevant antibiotic (for antibiotic resistance-based selection) or naturally lack the ability to complement the auxotrophy (for auxotrophy-based selection) (34). A drawback of using IVET is that promoters that are activated transiently or at a low level may not be identified due to insufficient production of the missing survival factor (34). In RIVET, a modification of IVET, a promoter of interest drives the expression of a site-specific recombinase that irreversibly excises a genetic marker, often an antibiotic resistance gene (24, 34, 37). By selective plating it is possible to determine if the promoter of interest was active at some time during infection. Unlike IVET, RIVET permits the detection of transiently or weakly expressed genes because the recombinase-mediated loss of a marker need only occur once to document promoter activation (34).

pGFLIP is a pUC18-based plasmid that, while conceptually similar to RIVET, possesses several advantages over this well-characterized genetic tool. The Tn7 transposon system specifically delivers sequences to the *att*Tn7 site located 3′ to the highly conserved *glmS* gene, which provides pGFLIP with an especially broad host range that includes many

Gram-negative bacteria (38). As a result of this specific recombination at the *att*Tn7 site, only one integration event is required for all components of pGFLIP to be delivered in single copy to the bacterial chromosome. Single-copy delivery eliminates potential gene dosage issues inherent to multi-copy plasmid systems, and integration at the *att*Tn7 site does not disturb the native locus of the gene to be tested. Once delivered, a Tn7 transposon is stable in the absence of selection, unlike suicide plasmids that have been integrated into the chromosome via single-crossover homologous recombination, which can spontaneously resolve in the absence of selection. In contrast with other published systems, pGFLIP also possesses two markers—*gfp* and *nptII*—allowing either the loss of fluorescence or Km^r to indicate promoter activation.

In this study, we used pGFLIP to analyze the transcription activation of Bvg-regulated genes in both *B. bronchiseptica* RB50 and *B. pertussis* BPSM. Our results showed that, *in vitro*, *fhaB* and *ptxA* promoters were activated early and late, respectively, following a switch from Bvg^- to Bvg^+ phase conditions, which is in agreement with previous reports for both *Bordetella* species (15, 23, 24). However, the *cyaA* promoter was activated unexpectedly early in our assay; these results appear to stand in contradiction to the established view that *cyaA* is transcribed solely as a late gene. Using *B. bronchiseptica* RB50 in a BALB/c mouse model, we found that the pattern of gene activation for *cyaA*, *fhaB*, and *ptxA* was nearly identical to that observed *in vitro* at early time points. Veal-Carr et al. reported similar agreement between *in vitro* and *in vivo* gene activation patterns using RIVET (24), although in that study, maximal activation of *fhaB*, *cyaA*, and *prn* occurred over a much greater time scale (approximately 24 h to full activation), likely a result of differences in sensitivity between the TnpR-*res* and Flp-*FRT* systems. Our use of pGFLIP to evaluate

gene activation in *B. bronchiseptica* is both the first kinetic analysis of P_{cyaA} and the first *in vivo* kinetic analysis of any promoter to be reported for this organism.

Although we expected P_{cyaA} to behave like a class 1 promoter in *B. bronchiseptica*, based on gene activation and expression data obtained by us and others for *B. pertussis* (5, 11, 18, 23, 24), our data nevertheless suggest that P_{cyaA} acts more like a class 2 promoter in this organism. However, it is not necessarily the case that *cyaA* reaches maximal expression at 1–2 h following a switch from Bvg^- phase to Bvg^+ phase; it is possible that *cyaA* activation occurs in a stepwise manner, i.e., P_{cyaA} may rapidly reach a level of expression necessary to activate *flp* transcription in our system, but may not reach maximal expression until much later. This scenario would account for the apparently rapid activation of P_{cyaA} without requiring a bacterium to be producing and secreting a significant amount of ACT immediately upon switching to non-modulating conditions. Evidence exists to support *cyaA* activation and ACT production, albeit at a reduced level, in the Bvg^i phase, as strains RB50i and RB53i are slightly hemolytic on BG agar (a consequence of the hemolysin activity of ACT), and RB53i produces measurable levels of *cyaA* transcript (9). We were able to determine that neither differences in the *cyaA* promoter nor in the *bvgAS* allele between the two species accounted for the difference in *cyaA* activation (see Fig. 4), suggesting that other, potentially Bvg-independent, factors may be influencing *cyaA* activation in *B. bronchiseptica* compared to *B. pertussis*.

In *B. pertussis* BPSM, P_{cyaA} demonstrated an activation pattern consistent with both indirect (RIVET) and direct (RNA hybridization) assessments, reinforcing the conclusion that *cyaA* activation is indeed different between RB50 and BPSM (23, 24). Given the differences in host range and the ability of *B. bronchiseptica* to survive outside of a host (7,

9, 10, 33), it is possible that the relatively early activation of *cyaA* in *B. bronchiseptica* is advantageous during the establishment of infection in a mammalian host or in transmission between hosts. Previous studies have shown that RB50 *cyaA* deletion mutants are more susceptible to clearance from the mouse respiratory tract, presumably as a result of neutrophil-mediated killing, and that ACT may interact with FHA (an "early" Bvg^+ gene) on the cell surface and modulate cytokine production by the host (39, 40). All strains of *B. bronchiseptica* that have been tested show the same modulation characteristics *in vitro* (i.e., the same relatively low concentration of modulator is required for inducing the Bvg^- phase), while *B. pertussis* isolates exhibit variable resistance to modulation at concentrations of modulator equal to or greater than for *B. bronchiseptica* (22). These observations suggest that early expression of *cyaA* may not be detrimental to human-adapted *B. pertussis* but may be necessary for *B. bronchiseptica* to establish an infection.

For both *B. bronchiseptica* and *B. pertussis* it has been shown that the Bvg^+ phase is necessary and sufficient for infection (6, 7, 9, 16, 22). Our results do not contradict these observations for *B. bronchiseptica*, but demonstrate that once inside the host, bacteria begin to transcribe Bvg^+ phase genes within 1 h p.i., with essentially every cell having activated *fhaB*, *cyaA*, and *ptxA* by 30 h p.i. The transition of *B. bronchiseptica* from Bvg^- phase to Bvg^+ phase upon inoculation also indicates that the mouse lung is a Bvg^+ phase environment. We likewise provided evidence that *B. bronchiseptica* does not modulate to the Bvg^- phase *in vivo*, supporting studies conducted using Bvg^- phase-locked mutants that were unable to establish an infection and were quickly cleared from the respiratory tract and those using Bvg^+ phase-locked mutants that displayed no colonization defect (7, 8). Moreover, ectopic expression of flagellin in Bvg^+ phase *B. bronchiseptica* results in impaired persistence in the

rat respiratory tract, possibly due to an immune response to this antigen (16). Therefore, modulation to the Bvg$^-$ phase likely does not occur *in vivo* as it would be disadvantageous to bacterial survival. We cannot rule out the possibility, however, that some Bvg$^+$ RB50*flaA*FLP bacteria did modulate to the Bvg$^-$ phase and were quickly eliminated by the immune response, or were present in a niche other than the lung (such as the trachea or nasopharnx) and were not represented in the lung homogenates that we analyzed. It is also conceivable that *B. bronchiseptica* is able to partially modulate, perhaps to the Bvg^i phase, which would not be documented using RB50*flaA*FLP. We are currently constructing additional strains to test this possibility.

The pGFLIP plasmid has proven to be useful in understanding the regulation of gene activation in *Bordetella*. However, there remain caveats for the use of this system in other applications. As with other IVET and RIVET systems, pGFLIP requires that strains be manipulated under strict promoter-inactive conditions to prevent unwanted Flp-mediated resolution. This requirement poses problems for studying genes for which conditions of repression or lack of activation are unknown, genes that are essential for growth, and for genes that may not be fully transcriptionally inactive *in vitro*. And, like other systems that have been developed to monitor transcription, pGFLIP cannot provide information about post-transcriptional or post-translational regulation of target genes. Finally, as was shown by the variable background resolution of Bvg-regulated promoters in our study, pGFLIP appears to be sensitive to low-level promoter activation even under "repressed" conditions for certain genes. Lee et al. were able to modulate the sensitivity of RIVET by mutating the ribosome-binding site (RBS) of *tnpR*, effectively raising the threshold of promoter activity required for resolution (41). pGFLIP does not possess an RBS 5′ to *flp*, instead relying on the RBS of the

promoter of interest, though it would be feasible to develop a modified pGFLIP plasmid that contains an RBS with reduced sensitivity to permit the study of genes that are not fully inactive or are constitutively active at a low level.

In this study we used pGFLIP to detect the activation of BvgAS-regulated genes in *Bordetella*, but there are additional uses for this system to measure transcription activation at the population or single cell level. Using pGFLIP, fluorescence can be used to quickly differentiate cells that have activated the promoter of interest from those that have not. Over time, stochastic and/or transient promoter activation can result in sectoring of fluorescent colonies, permitting spatiotemporal observation of gene activation within a single colony (M. S. Byrd and E. Mason, unpublished observation). The addition of a second, non-*gfp* fluorescent label (e.g., a constitutively expressed fluorescent protein or a fluorescently labeled antibody) to cells already containing pGFLIP would allow cells that had activated the promoter of interest to be differentiated from cells that had not. Cells labeled using such an approach could be visualized using fluorescence-activated cell sorting or by microscopy. We are currently developing an improved pGFLIP plasmid that contains a constitutively expressed fluorescent protein gene not flanked by *FRT* sites that will provide a two-color to one-color readout upon activation of *flp* by the promoter of interest. The development of pGFLIP has resulted in a sensitive genetic tool that can be used to document promoter activation in a broad range of Gram-negative bacteria both *in vitro* and *in vivo*. Our use of pGFLIP to document the activation of Bvg-regulated promoters revealed unexpectedly early activation of *cyaA* in *B. bronchiseptica*, suggesting a possible explanation for the less restrictive host range of this organism compared to *B. pertussis*, and is the first *in vivo* use of a recombination-based genetic reporter of *B. bronchiseptica* gene activation.

We thank Megan Ray for technical assistance and members of the Cotter laboratory for helpful discussions of this manuscript. This work was supported by grants from the National Institutes of Health (U54 AI065359, AI43986, and AI094991 to P.A.C.).

References

1. **Gross R**, **Keidel K**, **Schmitt K**. 2010. Resemblance and divergence: the “new” members of the genus Bordetella. Med Microbiol Immunol **199**:155–163.

2. **Gerlach G**, **Wintzingerode von F**, **Middendorf B**, **Gross R**. 2001. Evolutionary trends in the genus Bordetella. Microbes and Infection **3**:61–72.

3. **Cotter PA**, **Miller JF**. 2001. *Bordetella*, pp. 619–674. *In* Groisman, EA (ed.), *Principles of Bacterial Pathogenesis*. Academic Press, San Diego, CA.

4. **Cotter PA**, **Jones AM**. 2003. Phosphorelay control of virulence gene expression in Bordetella. Trends Microbiol. **11**:367–373.

5. **Cummings CA**, **Bootsma HJ**, **Relman DA**, **Miller JF**. 2006. Species- and strain-specific control of a complex, flexible regulon by Bordetella BvgAS. J. Bacteriol. **188**:1775–1785.

6. **Martinez de Tejada G**, **Cotter PA**, **Heininger U**, **Camilli A**, **Akerley BJ**, **Mekalanos JJ**, **Miller JF**. 1998. Neither the Bvg- phase nor the vrg6 locus of Bordetella pertussis is required for respiratory infection in mice. Infect. Immun. **66**:2762–2768.

7. **Cotter PA**, **Miller JF**. 1994. BvgAS-mediated signal transduction: analysis of phase-locked regulatory mutants of Bordetella bronchiseptica in a rabbit model. Infect. Immun. **62**:3381–3390.

8. **Nicholson TL**, **Brockmeier SL**, **Loving CL**, **Register KB**, **Kehrli ME**, **Stibitz SE**, **Shore SM**. 2012. Phenotypic modulation of the virulent Bvg phase is not required for pathogenesis and transmission of Bordetella bronchiseptica in swine. Infect. Immun. **80**:1025–1036.

9. **Cotter PA**, **Miller JF**. 1997. A mutation in the Bordetella bronchiseptica bvgS gene results in reduced virulence and increased resistance to starvation, and identifies a new class of Bvg-regulated antigens. Mol. Microbiol. **24**:671–685.

10. **Stockbauer KE**, **Fuchslocher B**, **Miller JF**, **Cotter PA**. 2001. Identification and characterization of BipA, a Bordetella Bvg-intermediate phase protein. Mol. Microbiol. **39**:65–78.

11. **Jones AM**, **Boucher PE**, **Williams CL**, **Stibitz S**, **Cotter PA**. 2005. Role of BvgA phosphorylation and DNA binding affinity in control of Bvg-mediated phenotypic phase transition in Bordetella pertussis. Mol. Microbiol. **58**:700–713.

12. **Boucher PE**, **Murakami K**, **Ishihama A**, **Stibitz S**. 1997. Nature of DNA binding and RNA polymerase interaction of the Bordetella pertussis BvgA transcriptional

activator at the fha promoter. J. Bacteriol. **179**:1755–1763.

13. **Boucher PE**, **Yang MS**, **Stibitz S**. 2001. Mutational analysis of the high-affinity BvgA binding site in the fha promoter of Bordetella pertussis. Mol. Microbiol. **40**:991–999.

14. **Chen Q**, **Decker KB**, **Boucher PE**, **Hinton D**, **Stibitz S**. 2010. Novel architectural features of Bordetella pertussis fimbrial subunit promoters and their activation by the global virulence regulator BvgA. Mol. Microbiol. **77**:1326–1340.

15. **Williams CL**, **Cotter PA**. 2007. Autoregulation is essential for precise temporal and steady-state regulation by the Bordetella BvgAS phosphorelay. J. Bacteriol. **189**:1974–1982.

16. **Akerley BJ**, **Cotter PA**, **Miller JF**. 1995. Ectopic expression of the flagellar regulon alters development of the bordetella-host interaction. Cell **80**:611–620.

17. **Cróinín TÓ**, **Grippe VK**, **Merkel TJ**. 2005. Activation of the vrg6 promoter of Bordetella pertussis by RisA. J. Bacteriol. **187**:1648–1658.

18. **Steffen P**, **Goyard S**, **Ullmann A**. 1996. Phosphorylated BvgA is sufficient for transcriptional activation of virulence-regulated genes in Bordetella pertussis. The EMBO Journal **15**:102.

19. **Miller JF**, **Roy CR**, **Falkow S**. 1989. Analysis of Bordetella pertussis virulence gene regulation by use of transcriptional fusions in Escherichia coli. J. Bacteriol. **171**:6345–6348.

20. **Scarlato V**, **Prugnola A**, **Aricó B**, **Rappuoli R**. 1990. Positive transcriptional feedback at the bvg locus controls expression of virulence factors in Bordetella pertussis. Proc. Natl. Acad. Sci. USA **87**:6753–6757.

21. **McPheat WL**, **Wardlaw AC**, **Novotny P**. 1983. Modulation of Bordetella pertussis by nicotinic acid. Infect. Immun. **41**:516–522.

22. **Martinez de Tejada G**, **Miller JF**, **Cotter PA**. 1996. Comparative analysis of the virulence control systems of Bordetella pertussis and Bordetella bronchiseptica. Mol. Microbiol. **22**:895–908.

23. **Aricó B**, **Scarlato V**, **Prugnola A**, **Rappuoli R**. 1991. Sequential activation and environmental regulation of virulence genes in Bordetella pertussis. The EMBO Journal **10**:3971.

24. **Veal-Carr WL**, **Stibitz S**. 2005. Demonstration of differential virulence gene promoter activation in vivo in Bordetella pertussis using RIVET. Mol. Microbiol. **55**:788–798.

25. **Camilli A**, **Beattie DT**, **Mekalanos JJ**. 1994. Use of genetic recombination as a reporter of gene expression. Proc. Natl. Acad. Sci. USA **91**:2634–2638.

26. **Hoang TT**, **Karkhoff-Schweizer RR**, **Kutchma AJ**, **Schweizer HP**. 1998. A broad-host-range Flp-FRT recombination system for site-specific excision of chromosomally-located DNA sequences: application for isolation of unmarked Pseudomonas aeruginosa mutants. Gene **212**:77–86.

27. **Stainer DW**, **Scholte MJ**. 1970. A simple chemically defined medium for the production of phase I Bordetella pertussis. J. Gen. Microbiol. **63**:211–220.

28. **Inatsuka CS**, **Xu Q**, **Vujkovic-Cvijin I**, **Wong S**, **Stibitz S**, **Miller JF**, **Cotter PA**. 2010. Pertactin is required for Bordetella species to resist neutrophil-mediated clearance. Infect. Immun. **78**:2901–2909.

29. **Lopez CM**, **Rholl DA**, **Trunck LA**, **Schweizer HP**. 2009. Versatile dual-technology system for markerless allele replacement in Burkholderia pseudomallei. Appl. Environ. Microbiol. **75**:6496–6503.

30. **Choi KH**, **Mima T**, **Casart Y**, **Rholl D**, **Kumar A**, **Beacham IR**, **Schweizer HP**. 2008. Genetic tools for select-agent-compliant manipulation of Burkholderia pseudomallei. Appl. Environ. Microbiol. **74**:1064–1075.

31. **Norris MH**, **Kang Y**, **Wilcox B**, **Hoang TT**. 2010. Stable, site-specific fluorescent tagging constructs optimized for burkholderia species. Appl. Environ. Microbiol. **76**:7635–7640.

32. **Akerley BJ**, **Miller JF**. 1993. Flagellin gene transcription in Bordetella bronchiseptica is regulated by the BvgAS virulence control system. J. Bacteriol. **175**:3468–3479.

33. **Merkel TJ**, **Stibitz S**, **Keith JM**, **Leef M**, **Shahin R**. 1998. Contribution of regulation by the bvg locus to respiratory infection of mice by Bordetella pertussis. Infect. Immun. **66**:4367–4373.

34. **Rediers H**, **Rainey PB**, **Vanderleyden J**, **De Mot R**. 2005. Unraveling the secret lives of bacteria: use of in vivo expression technology and differential fluorescence induction promoter traps as tools for exploring niche-specific gene expression. Microbiol. Mol. Biol. Rev. **69**:217–261.

35. **Gort AS**, **Miller VL**. 2000. Identification and characterization of Yersinia enterocolitica genes induced during systemic infection. Infect. Immun. **68**:6633–6642.

36. **Wang J**, **Mushegian A**, **Lory S**, **Jin S**. 1996. Large-scale isolation of candidate virulence genes of Pseudomonas aeruginosa by in vivo selection. Proc. Natl. Acad. Sci. USA **93**:10434–10439.

37. **Bron PA**, **Grangette C**, **Mercenier A**, **de Vos WM**, **Kleerebezem M**. 2004. Identification of Lactobacillus plantarum genes that are induced in the gastrointestinal tract of mice. J. Bacteriol. **186**:5721–5729.

38. **Choi KH**, **Gaynor JB**, **White KG**, **Lopez C**, **Bosio CM**, **Karkhoff-Schweizer RR**, **Schweizer HP**. 2005. A Tn7-based broad-range bacterial cloning and expression system. Nat Methods **2**:443–448.

39. **Zaretzky FR**, **Gray MC**, **Hewlett EL**. 2002. Mechanism of association of adenylate cyclase toxin with the surface of Bordetella pertussis: a role for toxin-filamentous haemagglutinin interaction. Mol. Microbiol. **45**:1589–1598.

40. **Henderson MW**, **Inatsuka CS**, **Sheets AJ**, **Williams CL**, **Benaron DJ**, **Donato GM**, **Gray MC**, **Hewlett EL**, **Cotter PA**. 2012. Contribution of Bordetella filamentous hemagglutinin and adenylate cyclase toxin to suppression and evasion of interleukin-17-mediated inflammation. Infect. Immun. **80**:2061–2075.

41. **Lee SH**, **Hava DL**, **Waldor MK**, **Camilli A**. 1999. Regulation and Temporal Expression Patterns of Vibrio cholerae Virulence Genes during Infection. Cell **99**:625–634.

42. **Menozzi FD**, **Mutombo R**, **Renauld G**, **Gantiez C**, **Hannah JH**, **Leininger E**, **Brennan MJ**, **Locht C**. 1994. Heparin-inhibitable lectin activity of the filamentous hemagglutinin adhesin of Bordetella pertussis. Infect. Immun. **62**:769–778.

CHAPTER 3: Evidence for phenotypic bistability resulting from transcriptional interference of *bvgAS* in *Bordetella bronchiseptica*[1]

Introduction:

The genus *Bordetella* includes Gram-negative bacteria that cause respiratory infections. *Bordetella pertussis* and *Bordetella parapertussis*$_{hu}$ are strictly human-specific pathogens that cause whooping cough, an acute disease that has experienced a recent resurgence despite widespread vaccination (1–3). Phylogenetic analyses indicate that *B. pertussis* and *B. parapertussis*$_{hu}$ have recently evolved from *Bordetella bronchiseptica,* which infects a wide range of mammals and can also survive naturally for long periods of time outside of the host (4–6). Although the factors that determine host specificity remain unknown, the presence and regulation of virulence factor-encoding genes is highly conserved between these three sub-species (7, 8).

Filamentous hemagglutinin (FHA), encoded by the *fhaB* gene, is a well-characterized virulence factor of *Bordetella* and is a primary component of acellular pertussis vaccines (1, 9, 10). A prototypical member of the Two Partner Secretion family of proteins, FHA is a large, surface-exposed protein that is produced and secreted at a high level during growth *in vitro* (10–12). In *B. bronchiseptica,* FHA mediates adherence to a wide range of cell lines and is required for colonization of the lower respiratory tract in both rats and mice (13–15).

---

[1]This chapter was originally written as an article for the journal *Molecular Microbiology*. It was accepted September 3, 2013. PMID: 24007341. Reprinted with permission.

Although FHA was first characterized as an adhesin, it has subsequently been reported to perform several other important functions. For example, exposure of lipopolysaccharide and IFN-γ-stimulated macrophages to purified *B. pertussis* FHA suppresses interleukin-12 (IL-12) production, and macrophages treated with FHA exhibit higher rates of apoptosis compared to untreated controls (16, 17). FHA-deficient *B. bronchiseptica* causes an infection that is hyperinflammatory compared to infection caused by wild-type bacteria and is characterized by increased influx of interleukin-17 (IL-17)-positive neutrophils, macrophages, and $CD4^+$ Tcells, suggesting that FHA plays an immunomodulatory role *in vivo* (15, 18). Additionally, there is strong evidence that FHA interacts with another important virulence factor, adenylate cyclase toxin ACT (19, 20).

In *Bordetella,* the master regulator that controls the expression of all known virulence factor-encoding genes is called BvgAS (21). A two-component sensory transduction system, BvgAS controls at least three distinct phenotypic phases (Bvg^+, Bvg^i, and Bvg^-) by altering gene expression patterns in response to environmental stimuli (Figure 9A) (22). The Bvg^+ phase is induced during standard laboratory growth conditions at 37ºC on Bordet Gengou (BG) blood agar or in Stainer-Scholte broth. Bvg^+ phase bacteria are non-motile and form small, dome-shaped, hemolytic colonies on BG blood agar. Bacteria can be induced (or *modulated*) to the Bvg^- phase in the laboratory by growth at room temperature or by supplementing media with millimolar concentrations of chemical modulators such as $MgSO_4$ or nicotinic acid. Bacteria in the Bvg^- phase are motile (*B. bronchiseptica* only) and form large, flat, non-hemolytic colonies. The Bvg^i phase can be induced in the laboratory with intermediate concentrations of chemical modulators and these bacteria form colonies that appear phenotypically intermediate compared to Bvg^- and Bvg^+ phase colonies. Each

phenotypic phase is defined by a unique pattern of gene expression (Figure 9B) (7, 22, 23). For example, bacteria in the Bvg^+ phase are characterized by maximal expression of virulence-activated genes (*vags)* such as *fhaB*, *cyaA-E* (encoding adenylate cyclase toxin ACT), *ptxA-E* (encoding pertussis toxin in *B. pertussis*), and *bvgAS* itself (which is positively autoregulated). In contrast, Bvg^- phase bacteria maximally express virulence-repressed genes (*vrgs*) including those required for motility (i.e., *flaA,* encoding flagellin and *frlAB*, the *Bordetella flhDC* homolog) and chemotaxis (*B. bronchiseptica* only) but do not express *vags*. The *vags* fall into two classes: those expressed in the Bvg^i phase *and* the Bvg^+ phase, and those expressed maximally only in the Bvg^+ phase. Additionally, some genes, such as *bipA*, are expressed maximally only in the Bvg^i phase (24, 25). Thus, Bvg^i phase bacteria are characterized by maximal expression of *bipA*, *bvgAS*, and *fhaB*, and minimal expression of *vrgs*, *cyaA*, and *ptxA* (*B. pertussis* only) (Figure 9B) (7, 23–26).

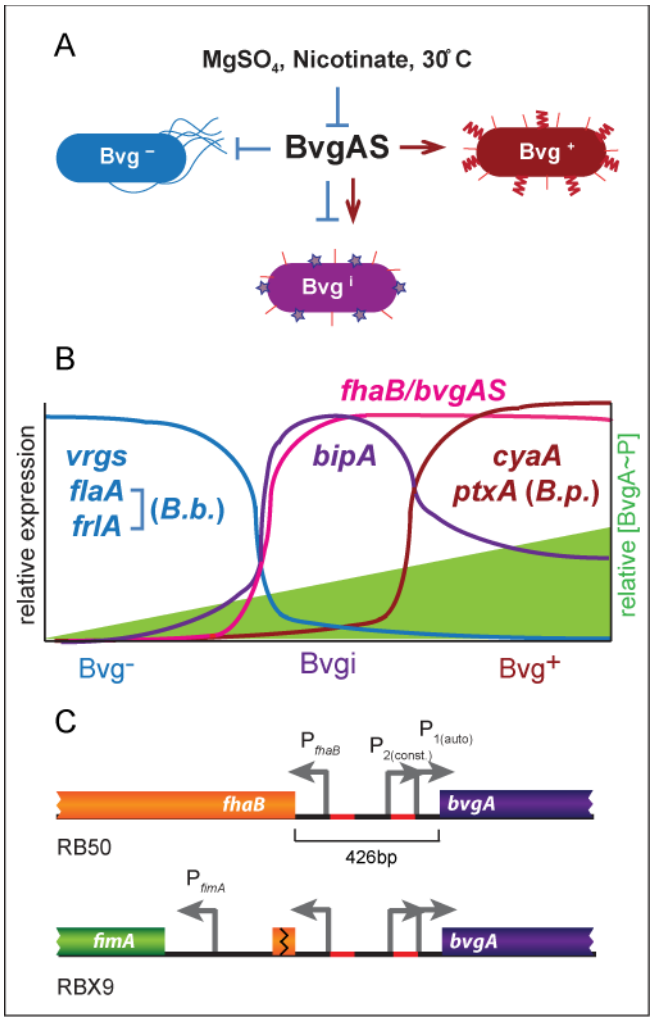

Figure 9. The *Bordetella* BvgAS system controls at least four different classes of genes and three different phenotypic phases in response to environmental stimuli. A, BvgAS is responsible for the Bvg^{+}, Bvg^{i}, and Bvg^{-} phases and is repressed by chemical modulators or low temperature. B, The three phenotypic phases are defined by unique patterns of gene expression as indicated, and rely on the intracellular concentration of BvgA~P. C, The chromosomal organization of the *fhaB* and *bvgAS* loci in RB50 (top) and RBX9 (Δ*fhaB*, bottom). Red regions indicate relative BvgA binding regions.

Upon activation of the BvgAS phosphorelay in response to environmental signals, BvgS (the sensor kinase) autophosphorylates, becoming the substrate for BvgA (the response regulator). BvgA-phosphate (BvgA~P) binds DNA and activates or represses transcription (22, 25, 27–30). *In vitro* transcription and DNA binding experiments have identified both high and low affinity BvgA binding sites located at various positions relative to the

transcription start sites of BvgAS-regulated genes (22, 25, 27, 30, 31). These data, together with a recent report describing a direct assessment of BvgA~P levels in *B. pertussis* cultures (32), support a model in which BvgA~P levels are extremely low under Bvg^- phase conditions, moderate under Bvg^i phase conditions, and high under Bvg^+ phase conditions (22, 32). In addition to controlling distinct phenotypic phases in response to steady-state conditions, BvgAS can regulate gene expression in a temporal manner (27, 33–35). Because *bvgAS* is positively autoregulated, both the concentration of BvgA and the proportion that is phosphorylated increase when bacteria sense activating signals. Therefore, gene expression patterns change temporally as the total concentration of BvgA~P gradually increases when bacteria are switched from Bvg^- to Bvg^+ phase conditions (27, 33–35).

The *bvgAS* and *fhaB* genes are adjacent and transcribed divergently. The 426 bp intergenic region contains at least three promoters (with at least two that control *bvgAS*, called P_2 and P_1) and multiple high-affinity BvgA binding sites (29, 30, 36, 37) (Figure 9C). In the Bvg^- phase, *bvgAS* transcription is driven by the BvgAS-independent promoter P_2 that is responsible for basal levels of BvgA (which likely remain unphosphorylated) (36, 37). When switched to the Bvg^+ phase, BvgA becomes phosphorylated and activates *fhaB* and *bvgAS* via binding to high-affinity sites near P_{fhaB} and P_1 (36, 38). Once a relatively high concentration of BvgA~P is achieved, genes with low-affinity BvgA binding sites at their promoters, such as *cyaA* and *ptxA* in *B. pertussis*, are activated and the bacteria transition into the Bvg^+ phase (27, 35, 39). The Bvg^+ phase, and therefore high levels of BvgA~P, is maintained as long as bacteria sense a Bvg^+ phase environment. Without *bvgAS* positive autoregulation, the ability of *B. bronchiseptica* to transition between and maintain each phenotypic phase is compromised (35).

Data obtained thus far indicate that the Bvg$^+$ phase is necessary and sufficient to cause respiratory infection, the Bvg$^-$ phase facilitates survival outside of the host, and BvgAS modulation to the Bvg^i or Bvg$^-$ phase does not occur during infection (40–45). For example, several groups have shown that Bvg$^+$ phase-locked bacteria behave identically to wild-type bacteria in colonization, persistence, and contribution to lung pathology (40, 42–44). In contrast, Bvg$^-$ phase-locked bacteria cannot establish an infection and Bvg^i phase-locked bacteria are severely limited in colonization and persistence (23, 40–43). Additionally, we recently demonstrated that *flaA* is not expressed at a detectable level when mice are infected with the *B. bronchiseptica* wild-type strain RB50 (46) and Akerley *et. al* showed that production of flagella in the Bvg$^+$ phase is detrimental to infection (44). Although the natural signals that affect BvgAS activity and the role of modulation in nature remain unknown, all of these data suggest that wild-type *Bordetella* do not modulate to the Bvg$^-$ phase within the mammalian host.

B. bronchiseptica strain RBX9, which contains an in-frame deletion mutation of *fhaB* (Figure 1C), has been used extensively to characterize the function of FHA *in vitro* and *in vivo* (11, 13, 15, 18, 47, 48). RBX9 is defective in adherence to multiple cell lines, is unable to autoaggregate in liquid culture, and causes hyperinflammation in the murine lung infection model (13–15, 18, 48). We isolated large colony variants (LCVs) from mice infected with RBX9 and also by modulating RBX9 to the Bvg$^-$ phase *in vitro*. We determined that the LCVs were a product of transcriptional interference that influenced *bvgAS* and produced an unusual bistable phenotype. Additionally, and despite evidence suggesting that *Bordetella* do not modulate during infection, the discovery of LCVs indicates that a subpopulation of RBX9 bacteria modulates *in vivo*.

Materials and Methods

Strains and growth conditions. *Escherichia coli* were grown in lysogeny broth (LB; 10 g l^{-1} tryptone, 5 g l^{-1} yeast extract, 2.5 g l^{-1} NaCl) or on LB with agar (1.5%) at 37°C. *Bordetella* were grown in Stainer-Scholte (SS) broth or on Bordet-Gengou (BG) agar (1.5%) (BD Biosciences, San Jose, CA) supplemented with 7.5% defibrinated sheep's blood (Colorado Serum Company, Denver, CO) at 37°C. As required, culture media were supplemented with kanamycin (Km; 50 μg ml^{-1}), ampicillin (Ap; 100 μg ml^{-1}), streptomycin (Sm; 25 μg ml^{-1}), magnesium sulfate ($MgSO_4$; 50 mM in plates and 20 mM in liquid), and diaminopimelic acid (DAP; 400 μg ml^{-1}) for the *E. coli* mobilizer strain RHO3 (Δ*asd* Δ*aphA*). Unless otherwise noted, all restriction enzymes and T4 DNA ligase was purchased from New England Biolabs. For a complete list of strains and plasmids used in this study, please see Table S4.

Construction of bacterial strains. Allelic exchange and Campbell-type integrations were done by matings using parental *Bordetella* and *E. coli* strain RHO3 harboring the appropriate suicide plasmid. The pGFLIP plasmid was delivered to the *att*Tn7 site using tri-parental mating with the above strains and with RHO3 cells harboring pTNS3, which encodes the transposase genes *tnsABCD*. Integration at the *att*Tn7 locus was confirmed via PCR. For details on specific strain constructions see the Supplemental text.

Immunofluorescence. HA epitopes on the surface of RBX9BatB-HA*flaA-gfp* bacteria were stained and visualized using indirect immunofluorescence. After 72h of growth at 37˚C, five to twenty colonies of each morphology including Bvg^+, Bvg^-, Bvg^i, and LCV, were scraped off of BG blood agar plates and resuspended into 1ml of 4% paraformaldehyde

and were allowed to fix on ice for 30 min. Cells were pelleted and washed with 1% BSA in PBS in a microcentrifuge tube. Primary antibody (mouse monoclonal anti-HA IgG diluted 1:2000 in 1% BSA in PBS) was used to resuspend the pellet and this mixture was incubated for 1h at room temperature (RT). The pellets were washed twice in 1% BSA for 5 min. Secondary antibody (Alexa Fluor 594-conjugated goat anti-mouse IgG, diluted 1:250 in 1% BSA in PBS; Invitrogen) was used to resuspend the pellet and this mixture was then incubated for 30 min at RT in the dark. The pellets were washed twice with 1% BSA for 5 min. Four microliters of the leftover pellet and liquid was pipetted onto a slide for visualization.

Confocal Microscopy. Immunofluorescent RBX9BatB-HA*flaA-gfp* bacteria were visualized using a Zeiss LSM 710 confocal microscope. Secondary antibody (Alexa Fluor 594-conjugated goat anti-mouse IgG) was detected using a 594 nm laser and GFP was detected at 488 nm. We used the 63× oil objective with 3× digital zoom. Images were viewed and saved with the Zen software from Carl Zeiss Microscopy.

pGFLIP assays. For RBX9*cyaA*FLP, RB50P*bvgA*$_{short}$*FLP* and RB50P*bvgA*$_{long}$*FLP*, strains were grown on BG blood agar plates under promoter-inactive conditions (Bvg$^-$ phase) with Km for 48h at 37°C and were determined to be GFP positive (GFP$^+$) using a G:BOX Chemi imaging system with an UltraBright-LED blue transilluminator and an SW06 short-pass filter (495 to 600 nm; Syngene, Frederick, MD). Single GFP$^+$ colonies were then resuspended in PBS, diluted, and plated onto Bvg$^+$ or Bvg$^-$ phase conditions (promoter-active and promoter-inactive conditions, respectively) in the absence of Km selection. For RBX9*cyaA*FLP, GFP$^+$ LCVs were picked, diluted, and plated onto Bvg$^+$ and Bvg$^-$ phase

conditions in the absence of Km selection. Percent resolution was determined by averaging the ratio of GFP^- cfu/total cfu for at least three plates.

Intranasal inoculation of mice. Four- to eight-week-old BALB/c mice (Jackson Laboratories, Bar Harbor, ME) were inoculated intranasally with 1×10^5 cfu of *B. bronchiseptica* in 50 µl of PBS. For all infections, bacteria were grown overnight in SS medium. Lungs were harvested at 1h and 72h p.i. Right lungs were homogenized in 1 ml of PBS, diluted in PBS, and plated in at least duplicate on BG agar. Figure 16 represents data from three independent experiments performed with at least two mice per strain per time point.

This study was carried out in strict accordance with the recommendations in the Guide for the Care and Use of Laboratory Animals of the National Institutes of Health. Our protocol was approved by the University of North Carolina IACUC (10-134, 12-307). All animals were properly anesthetized for inoculations, monitored regularly, euthanized when moribund, and efforts were made to minimize suffering.

Statistical analyses. Statistical analyses were performed using Prism 5.0 (GraphPad Software, Inc.). Statistical significance was determined using the unpaired Student's t-test or analysis of variance (ANOVA) followed by Tukey's multiple comparison test. Images were formatted using Adobe Photoshop CS5 and figures were generated using Adobe Illustrator CS5 (Adobe Systems, Inc.).

Results

Isolation and characterization of LCVs. While comparing wild-type *B. bronchiseptica* strain RB50 with its Δ*fhaB* derivative RBX9 in a murine lung infection model, we noticed that at early time points post-inoculation (12 and 24 h), a small proportion (~1%) of cfus recovered from the lungs of RBX9-inoculated mice formed colonies on BG blood agar (Bvg^+ phase conditions) that were larger, flatter, and less hemolytic than colonies typically formed by RBX9 and RB50 () (Figure 10D). These Large Colony Variants (LCVs) were not recovered from RB50-infected mice. When LCVs were picked, diluted, and replated on BG blood agar, approximately 95% of the resulting colonies were phenotypically Bvg^+ phase, and approximately 5% were LCVs (Table 3) (Figure 10H). When replated again, LCVs continued to yield 95% Bvg^+ phase colonies and 5% LCVs. All phenotypically Bvg^+ phase colonies yielded only phenotypically Bvg^+ phase colonies after replating onto BG agar.

Table 3 LCV recovery frequency

Condition	%[a] LCVs recovered on BG blood agar
Plating murine lung homogenate after 30 hours	0.39 ± 0.13
Replating any RBX9 Bvg^- phase colony	5.43 ± 0.98
Replating an LCV from BG agar (derived *in vitro*)	3.90 ± 0.80
Replating an LCV from BG agar (derived *in vivo*)	6.03 ± 1.26
Replating any RBX9 Bvg^+ phase colony	0

[a]Values are means ± standard errors for experiments performed at least in triplicate

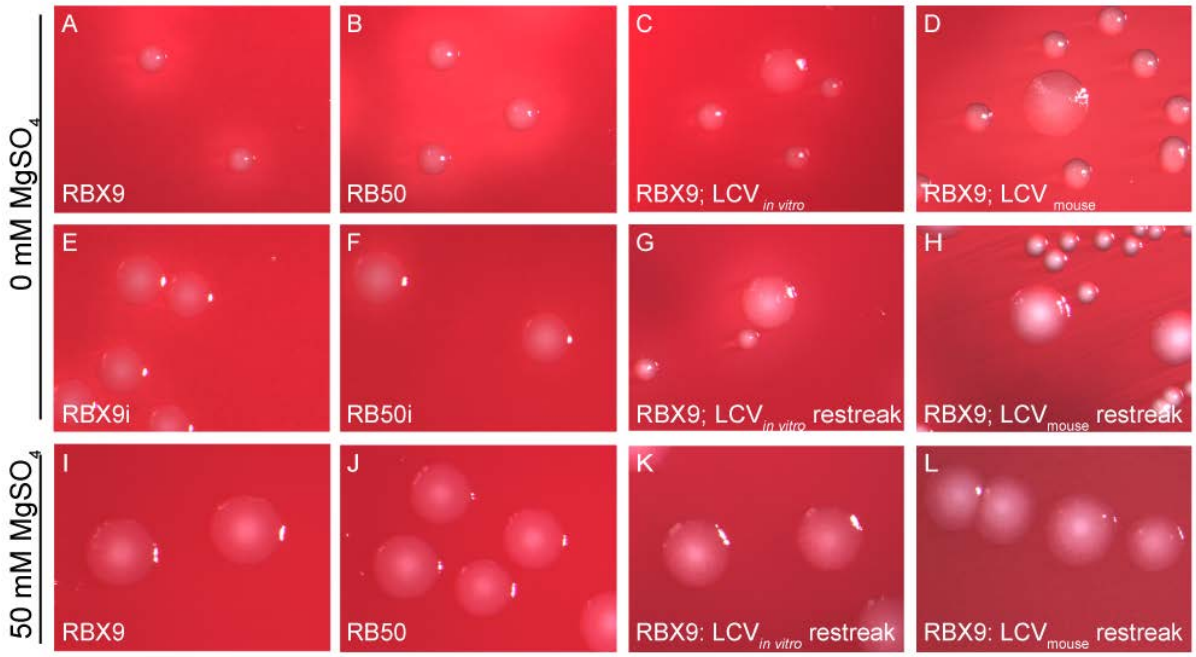

Figure 10. RB50 and RBX9 colony morphology. Bacteria were plated on either BG agar or BG agar + 50mM $MgSO_4$ and were imaged after 48h. A, RB50; B, RBX9; C, RBX9 LCV produced after *in vitro* modulation: D, RBX9 LCV recovered from mouse lung homogenate; E, RB50i (a Bvg-intermediate phase-locked strain in the RB50 background); F, RBX9i (a Bvg-intermediate phase-locked strain in the RBX9 background); G, RBX9 restreak of an LCV produced after modulation; H, RBX9 restreak of an LCV recovered from the mouse lung; I, RB50; J, RBX9; K, RBX9 restreak of an LCV produced after modulation; L, RBX9 restreak of an LCV recovered from the mouse lung.

We found serendipitously that LCVs were also induced *in vitro* under certain conditions. Specifically, when RBX9 was grown on BG blood agar + 50mM $MgSO_4$ (Bvg^- phase conditions) and then replated onto BG blood agar—effectively switching the bacteria from Bvg^- to Bvg^+ phase conditions—approximately 95% of the colonies were phenotypically Bvg^+ phase and 5% were LCVs (Table 3) (Figure 10C). When these LCVs were picked, diluted, and replated onto BG blood agar, approximately 95% of colonies displayed the Bvg^+ phase morphology and approximately 5% of colonies were LCVs (Table 3) (Figure 10G). Again, all phenotypically Bvg^+ phase colonies yielded only phenotypically

Bvg^+ phase colonies after replating onto BG agar. When RBX9 was streaked onto BG agar supplemented with 50mM $MgSO_4$, or passaged continuously under Bvg^- phase conditions, all colonies displayed typical Bvg^- phase morphology.

To determine if the generation of LCVs in RBX9 was due to the Δ*fhaB* mutation and not an unknown secondary mutation, we reconstructed strain RBX9 by allelic exchange. The newly constructed strain behaved identically to RBX9, producing LCVs following BvgAS modulation and generating a similar proportion of LCVs upon restreaking an LCV onto BG blood agar. Although LCVs appear morphologically similar to Bvg^i phase colonies (Figure 10), the fact that restreaking LCVs yielded a heterogeneous population of morphologically different colonies indicates that the Δ*fhaB* mutation does not lock bacteria into one particular phenotypic phase (such as the Bvg^i phase.)

LCVs are composed of both Bvg^- and Bvg^+ phase bacteria. To better understand the properties of LCVs, we investigated specific gene expression patterns within the bacteria that composed them. The fact that LCVs are hemolytic suggests that *cyaA*, a Bvg^+ phase gene, is expressed because ACT is responsible for hemolysis on BG blood agar (49). Additionally, electron micrographs of negatively stained LCVs revealed the presence of numerous flagella, which are only produced in the Bvg^- phase (data not shown). To determine if bacteria within LCVs were motile, we grew bacteria on Stainer-Scholte plates with 0.3% agar (Bvg^+ phase conditions). LCVs stab-inoculated into this agar produced a zone of migration that was smaller than that produced by Bvg^- phase-locked bacteria, but larger than Bvg^+ and Bvg^i phase bacteria, which do not produce a zone of migration (data not shown), suggesting that at least some bacteria within LCVs are motile. Together, our observations indicate that both

cyaA and *flaA* are expressed within each LCV. However, expression data have shown that expression of *vags*, such as *cya*, and *vrgs*, such as *flaA*, is mutually exclusive (7). Therefore, we hypothesized that LCVs are composed of at least two phenotypically distinct populations of bacteria: a population in the Bvg^+ phase and a population in the Bvg^- phase.

To determine the phenotypes of individual bacteria present in each LCV, we created RBX9BatB-HA*fla-gfp*, a strain that contains two unique tags that permit the distinction between Bvg^+ and Bvg^- phase bacteria. RBX9BatB-HA*flaA-gfp* contains an HA epitope-encoding sequence introduced into *batB* (encoding the Bvg^+ phase surface-exposed protein BatB) as well as *gfp* driven by the *flaA* promoter at a neutral site in the chromosome. The *batB* gene is expressed maximally in the Bvg^+ phase and minimally in the Bvg^i and Bvg^- phases (50). The *flaA* gene, as described previously, is a typical *vrg* and contains a strong promoter that is active only in the Bvg^- phase (22, 51). Therefore, Bvg^+ phase bacteria should produce a surface-exposed HA-tagged BatB protein and be GFP^- and Bvg^- phase bacteria should be GFP^+ and lack a surface-exposed HA epitope.

We used Alexa-Fluor 594-conjugated antibodies to indirectly recognize HA epitopes so that BatB-producing bacteria displayed red fluorescence. Bacteria expressing *fla-gfp* produced GFP and displayed green fluorescence. When Bvg^+ phase colonies of RBX9BatB-HA*fla*-gfp were stained with anti-HA and an Alexa-Fluor 594-conjugated secondary antibody, only red-fluorescing bacteria were observed and no green fluorescence was detected (Figure 11.)

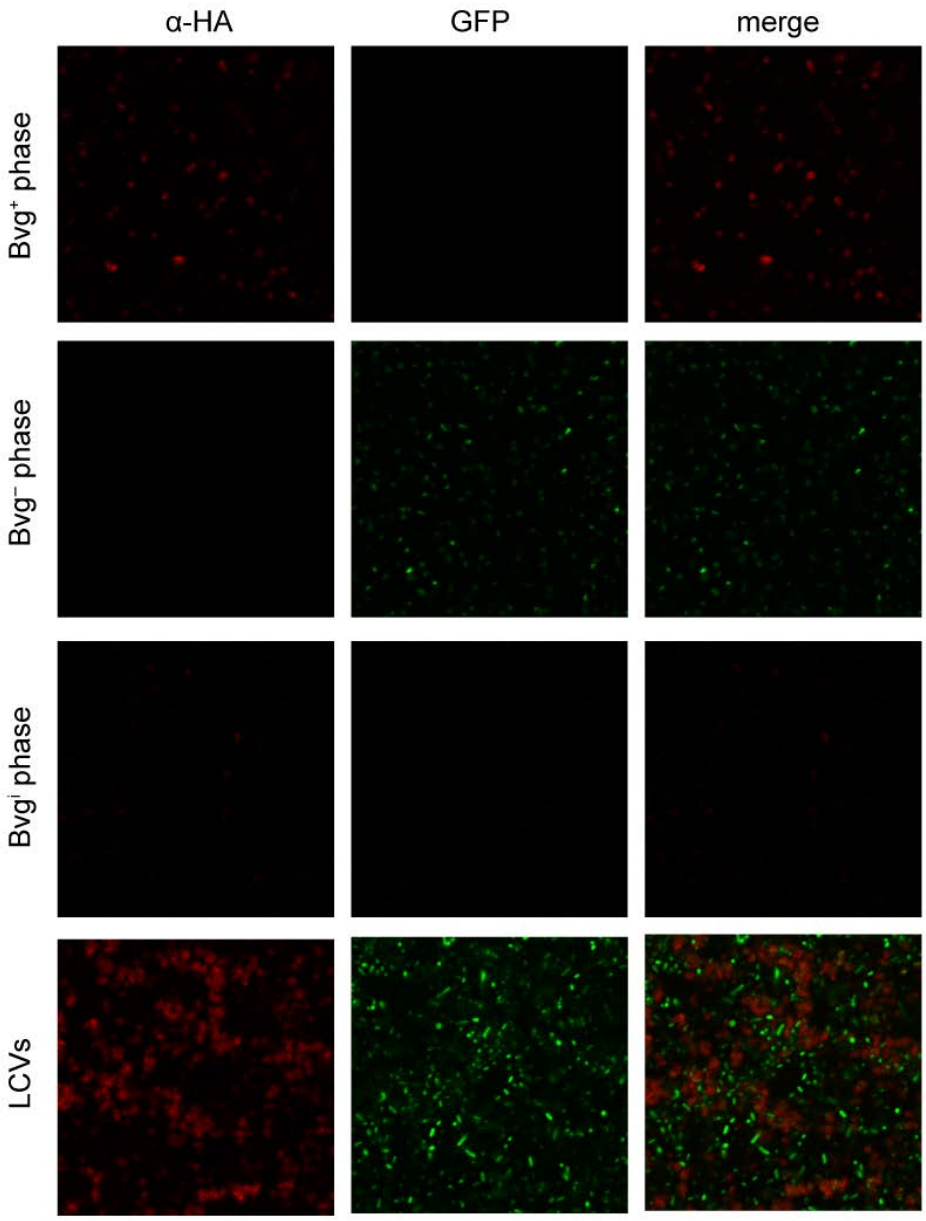

Figure 11. Detection of Bvg$^+$ (α-HA, red) and Bvg$^-$ phase (*flaA-gfp*, green) bacteria in typical RBX9 colonies and LCVs. RBX9BatBN-HA*flaA-gfp* was grown on BG blood agar (Bvg$^+$ phase conditions), BG blood agar + 50 mM $MgSO_4$ (Bvg$^-$ phase conditions), or BG blood agar + 6 mM $MgSO_4$ (Bvg^i phase conditions). Several colonies of each phenotype were combined and stained with mouse monoclonal α-HA IgG followed by an Alexa Fluor 594-conjugated goat anti-mouse IgG secondary antibody. Fluorescence was detected using a Zeiss LSM 710 confocal microscope.

When Bvg$^-$ phase colonies were stained, only green-fluorescing bacteria were observed and no red fluorescence was detected. When Bvg^i phase colonies were stained, a

small proportion of cells displayed red or green fluorescence, but the majority of cells were not fluorescent and no bacteria displayed both red and green fluorescence (Figure 11). In contrast, when LCVs from RBX9BatB-HA*fla*-gfp were stained, approximately half of the bacteria fluoresced red and approximately half fluoresced green (Figure 11). No co-localization of red and green fluorescence from either LCVs or Bvg^{i} phase colonies was observed, confirming that the expression of *vags* and *vrgs* is mutually exclusive under these conditions. These data demonstrate that LCVs are composed of both Bvg^{+} and Bvg^{-} phase bacteria and are not a homogeneous population of Bvg^{i} phase bacteria.

The Δ*fhaB* mutation in RBX9, but not lack of FHA protein, is responsible for the LCV phenotype. To determine if the generation of LCVs was due to lack of FHA protein production or the specific genetic architecture created by the Δ*fhaB* mutation in RBX9, we first determined if other *fhaB* mutants yielded LCVs. Strain RB50ΔP_{fhaB} contains a deletion mutation of the *fhaB* promoter, strain RB50ΔSP_{fhaB} contains a deletion mutation in *fhaB* such that the extended signal peptide of FHA is missing, and strain RB50Δβ$helix_{fhaB}$ contains a large deletion mutation in the region of *fhaB* encoding the β-helix structure (Figure S17). These strains were analysed for FHA production by Western blot, and either produced no FHA protein (RB50 Δ P*fhaB* and RB50 Δ SP*fhaB*) or a severely truncated FHA protein (RB50 Δ β -helix) (data not shown). We grew these strains under Bvg^{-} phase conditions and plated single colonies onto Bvg^{+} phase conditions to determine if they would produce LCVs similar to RBX9. No LCVs were observed, suggesting that a lack of wild-type FHA protein is not sufficient to produce the LCV phenotype.

To investigate the contribution of the genetic architecture created by the *fhaB* deletion to the LCV phenotype, we created RB50::pBam, a strain that produces FHA and contains an altered *fhaB-bvgAS* locus (Figure S17). RB50::pBam was created by integrating pBam, a suicide plasmid containing the *fhaB-bvgAS* intergenic region, into the RB50 chromosome. Therefore, RB50::pBam has a complete *fhaB* ORF in addition to non-native plasmid DNA 5′ to the *fhaB-bvgAS* intergenic region. After modulation, RB50::pBam produced LCVs similar to RBX9. These data suggest that the LCV phenotype can be produced by altering the genetic architecture 5′ to the *fhaB-bvgAS* intergenic region and is independent of FHA production.

The LCV phenotype results from a defect in *bvgAS* positive autoregulation. In addition to activating all of the known virulence factor-encoding genes in *Bordetella*, BvgAS activates *bvgAS* expression though positive autoregulation. Williams *et al.* demonstrated that positive autoregulation is required for the precise transition between and maintenance of the Bvg^+, Bvg^i, and Bvg^- phases (35). Three observations suggested that LCVs resulted from defective *bvgAS* autoregulation in RBX9. First, the mutations that cause LCVs are genetically linked (immediately 5′) to *bvgAS*; second, LCVs consist of bacteria in least two separate BvgAS-controlled phenotypic phases; and third, LCVs were induced *in vitro* following a switch from Bvg^- to Bvg^+ phase growth conditions.

We hypothesized that when RBX9 (or RB50::pBam) bacteria are switched to Bvg^+ phase conditions from Bvg^- phase conditions, most, like all wild-type bacteria, are able to activate transcription at the *bvgAS* P_1 promoter, leading to increased BvgAS levels and resulting in the transition to and maintenance of the Bvg^+ phase. According to our hypothesis, however, a small subset of RBX9 and RB50::pBam bacteria are unable to activate *bvgAS* transcription, possibly due to insufficient levels of BvgA and/or BvgS, and

these bacteria are therefore "trapped" in the Bvg$^-$ phase. We hypothesized further that although some descendants of these "Bvg$^-$ phase-trapped" bacteria will be able to activate *bvgAS* transcription and hence "escape" to the Bvg$^+$ phase, many will remain Bvg$^-$ phase-trapped and thus a substantial Bvg$^-$ phase population will be maintained in the LCV. An alternate hypothesis is that LCVs arise from spontaneous or transient shifting of bacteria between the Bvg$^+$ and Bvg$^-$ phases, which would also result in a mixture of Bvg$^+$ and Bvg$^-$ phase bacteria within a single colony.

To determine if LCVs contain Bvg$^-$ phase-trapped bacteria, we used the recombinase-based reporter system pGFLIP, which creates a permanent genetic change in response to gene activation (46). In this system, a promoter of interest drives expression of the site-specific recombinase-encoding gene *flp*, which when activated, results in recombination between Flp recombinase target (*FRT*) sites that flank *gfp* and the kanamycin (Km) resistance gene *nptII*. Therefore, any activation (even transient, low-level expression) of *flp* results in a permanent loss of Km resistance and GFP fluorescence. This system targets the reporter construct to the neutral *att*Tn7 site 3' to *glmS*. We created strain RBX9*cyaA*FLP by mating the plasmid pGFLIP-P$_{cyaA}$, in which the *B. bronchiseptica cyaA* promoter drives *flp* expression, into RBX9. The *cyaA* gene is exclusively controlled by BvgAS, is highly expressed in the Bvg$^+$ phase, and is expressed minimally in the Bvg$^-$ phase (22). In RBX9*cyaA*FLP, bacteria that have never expressed *cyaA* should remain GFP$^+$ and Km^r, whereas bacteria that have expressed *cyaA* should convert to GFP$^-$ and Km^s. If *gfp* is lost due to P$_{cyaA}$ activation, all descendent cells will also be GFP$^-$ and Km^s.

Previously, we demonstrated that RB50*cyaA*FLP bacteria remain GFP$^+$ under Bvg$^-$ phase conditions with Km selection and that they reach 100% resolution (GFP$^-$ cfu/total cfu)

when grown under Bvg^+ phase conditions (46). When RBX9*cyaA*FLP was plated under Bvg^- phase conditions with Km selection, each colony was morphologically identical and fluorescent, indicating that *cyaA* had not been activated to a level required for sufficient *flp* expression to lead to recombination between *FRT* sites (Figure 12A).

In contrast, when a colony of RBX9*cyaA*FLP that was grown under Bvg^- phase conditions was plated and grown under Bvg^+ phase conditions, approximately 15% of the colonies were LCVs and approximately 80% of those LCVs were GFP^+ (Figure 12B). None of the Bvg^+ phase colonies were GFP^+. When a GFP^+ LCV was replated and grown under Bvg^+ phase conditions, approximately 5% of the colonies were LCVs and approximately 80% of those were GFP^+ (Figure 12C). We serially replated GFP^+ LCVs eight times and in all cases, additional GFP^+ LCVs were generated (data not shown). These data indicate that a significant proportion of bacteria within a GFP^+ LCV had never activated *cyaA* and had therefore failed to switch to Bvg^+ phase in response to a change in conditions; i.e., they were Bvg^- phase-trapped. Moreover, our data suggest that all LCVs arise from a Bvg^- phase-trapped bacterium and that upon subsequent multiplication, most descendants have "escaped" to the Bvg^+ phase but a small proportion remain trapped in the Bvg^- phase. These data do not support a model in which LCVs consist of bacteria that transiently fluctuate between Bvg^+ and Bvg^- phase, because if this was true, LCVs would not be GFP^+.

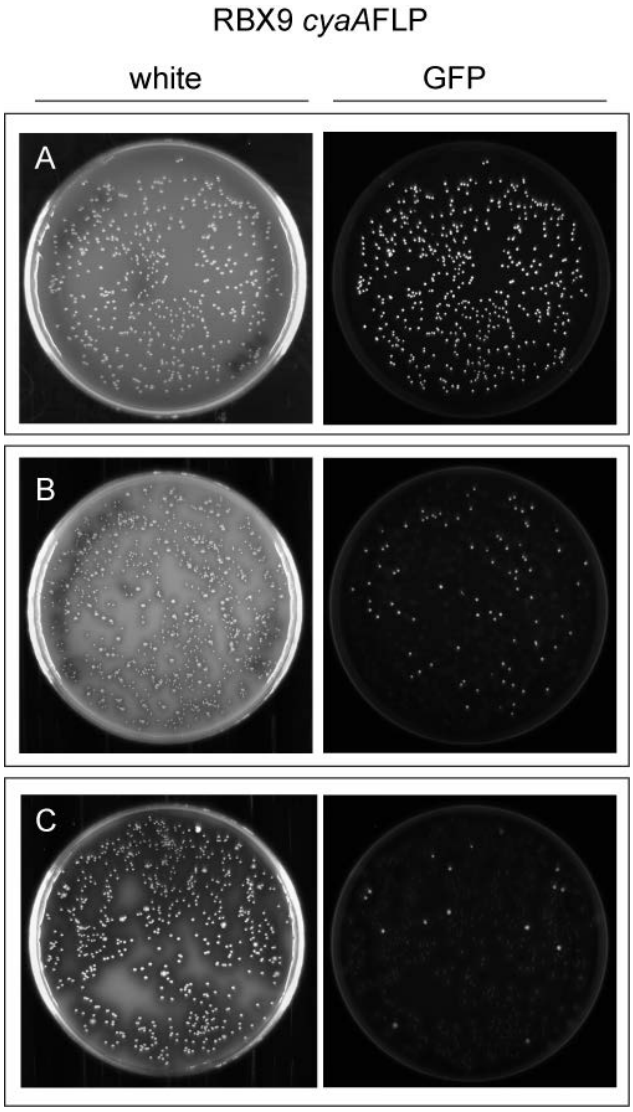

Figure 12. LCVs from the strain RBX9P*cyaA*FLP are GFP$^+$, indicating that *cyaA* has not been activated in a substantial proportion of these colonies. A, RBX9P*cyaA*FLP on BG blood agar + 50mM $MgsO_4$ (Bvg$^-$ phase conditions); B, a GFP$^+$ colony from A plated onto BG blood agar (Bvg$^+$ phase conditions); C, a GFP$^+$ LCV from B plated onto BG blood agar (Bvg$^+$ phase conditions). Colonies were visualized after 48h of growth.

Approximately 20% of the LCV colonies were GFP$^-$, indicating that P_{cyaA}-*flp* expression was sufficient to mediate recombination in the bacterium that founded the LCV or in its early descendants. Although this result appears inconsistent with our model, we have observed previously that when RB50*cyaA*FLP is grown under Bvg$^-$ phase conditions (when *cyaA* expression is minimal) and without Km selection, P_{cyaA}-*flp* is expressed sufficiently in

approximately 15% of bacteria such that they convert to GFP^- and Km^S (46). These data indicate that the *cyaA* promoter activity under Bvg^- phase conditions is near the threshold level required for *flp* expression and subsequent recombination. Therefore, GFP^- LCVs are most likely due to the activity level of the *cyaA* promoter under Bvg^- phase conditions and not due to bacteria switching to the Bvg^+ phase and then back to the Bvg^- phase. Nonetheless, our data indicate that in approximately 80% of LCVs, appear to have a defect in *bvgAS* positive autoregulation, leading to the observed Bvg− phasetrapped population.

Sequences upstream of the *fhaB-bvgAS* intergenic region affect the efficiency of *bvgAS* activation in the Bvg^- phase. Our data indicate that *bvgAS* autoregulation is defective in RBX9 and specifically, that LCVs are composed of a subpopulation of Bvg^- phase-trapped bacteria. As stated in the introduction, *bvgAS* is controlled primarily by two promoters. Studies with *B. pertussis* have shown that under Bvg− phase conditions, P_2 is transcribed at a low basal level. This level of transcription results in BvgS levels that are sufficient to respond to Bvg^+ phase conditions by autophosphorylating and mediating phosphorylation of BvgA. The resulting BvgA∼P levels are sufficient to bind at the bvgAS P_1 promoter, recruit RNAP, and activate transcription (38). (Although similar transcriptional analyses have not been conducted with *B. bronchiseptica*, the nucleotide sequence of the *fhaB-bvgAS* intergenic region in *B. bronchiseptica* is 91.1% identical and most of those differences are located in regions that, based on *B. pertussis* studies, are not bound by either BvgAS or RNAP.) We considered two hypotheses: 1) the level of transcription from P_2 in RBX9 is lower than in RB50 such that in some bacteria the levels of BvgAS are too low to activate transcription at P_1 in response to Bvg^+ phase conditions, and 2) transcription activation at P_1 by BvgA~P is

somehow defective in RBX9 compared to RB50. Moreover, our data suggest that defective autoregulation in RBX9 is due to the lack of native sequences or presence of non-native sequences 5′ to the *fhaB-bvgAS* intergenic region.

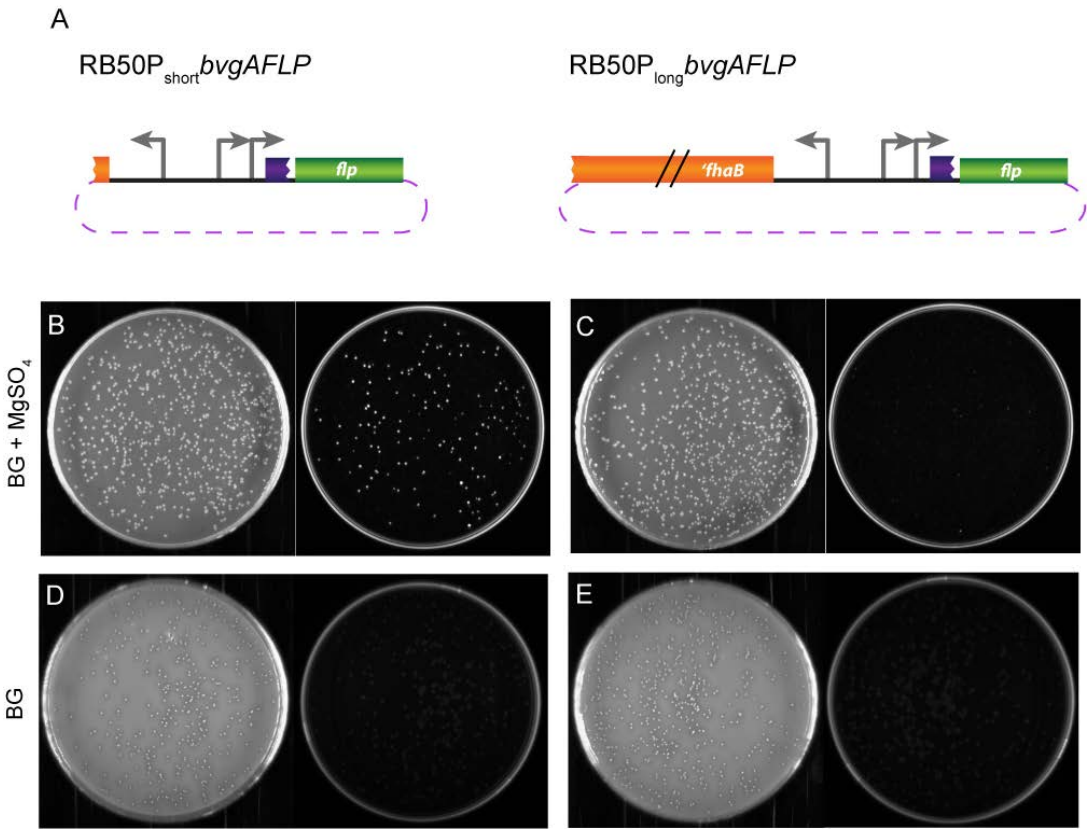

Figure 13. Sequences upstream of *bvgAS* affect transcription efficiency under Bvg⁻ phase conditions. A, Schematics of RB50P$_{short}$*bvgAFLP* and RB50P$_{long}$*bvgAFLP* showing the sequences 5′ to *flp* inserted at the *att*Tn7 site (not drawn to scale); B and C, strains were first grown on BG blood agar + 50 mM $MgSO_4$ + Km and one colony was plated onto BG blood agar + 50 mM $MgSO_4$ (Bvg⁻ phase conditions) without Km selection; D and E, strains were grown on BG blood agar + 50 mM $MgSO_4$ + Km selection and then one colony of each was plated onto BG blood agar (Bvg⁺ phase conditions) without selection. Representative white light (left) and fluorescent (right) images are shown for panels B, C, D, and E.

To test our hypotheses, we constructed RB50P$_{short}$*bvgAFLP* and RB50P$_{long}$*bvgAFLP*, where RB50P$_{short}$*bvgAFLP* contains only the *fhaB-bvgAS* intergenic region driving *flp* and

RB50P$_{long}$*bvgAFLP* contains this region plus an additional 1200 bp of *fhaB* sequences driving *flp* (Figure 13A). These strains were constructed under Bvg$^-$ phase conditions in the presence of Km. To investigate P_2 expression, we determined the percent resolution (the percentage of cfu that had activated *flp*) of each strain grown under Bvg$^-$ phase conditions by counting the ratio of GFP$^-$ cfu to total cfu when one colony was plated from Bvg$^-$ phase conditions with Km selection to Bvg$^-$ phase conditions without Km selection. The average resolution under Bvg$^-$ phase conditions in RB50P$_{short}$*bvgAFLP* was 68% whereas the average resolution in RB50P$_{long}$*bvgAFLP* was 97%. Plates are shown from one representative experiment (Figure 13B, C). Our data indicate that the per-cell activation of RB50P$_{short}$*bvgAFLP* is lower than the per-cell activation of RB50P$_{long}$*bvgA*FLP under Bvg$^-$ phase conditions, and demonstrate that either a lack of native *fhaB* sequences or the presence of non-native sequences has a direct effect on the efficiency of *bvgAS* transcription in the Bvg$^-$ phase.

When a colony from each strain was grown on Bvg$^-$ phase conditions with Km selection and then plated onto Bvg$^+$ phase conditions without Km selection, maximum resolution was achieved and there were no GFP$^+$ colonies in either strain (Figure 13D, E). These data suggest that RBX9 does not have a defect in transcription activation at P_1.

The LCV phenotype is caused by a (divergent) promoter in proximity to *bvgAS*. Based on our results, we hypothesized that sequences within *fhaB* (1-1200 nucleotides of the coding region) 5′ to the *fhaB-bvgAS* intergenic region effect the low level of transcription from P_2 that occurs under Bvg$^-$ phase conditions. To test this hypothesis, we constructed a strain containing a deletion mutation from nt 8 to 1256 of *fhaB* (Figure S17 C). This mutant did not

produce LCVs when switched from the Bvg^- to the Bvg^+ phase. We conclude that the lack of specific sequences within the first 1200bp of *fhaB* do not cause the LCV phenotype.

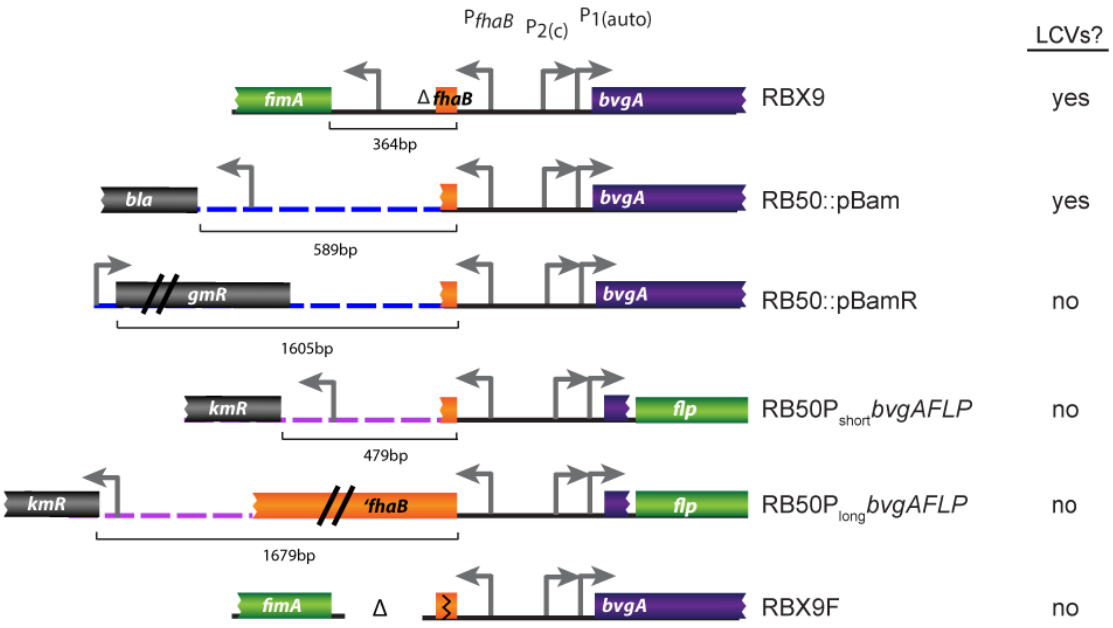

Figure 14. The genetic architecture of the *bvgAS-fhaB* intergenic region of strains that do and do not produce LCVs. Strains that produce LCVs or demonstrate a defect in *bvgA-flp* activation have divergent promoters 5´ to the *bvgAS-fhaB* intergenic region. Schematics for RB50P$_{short}$*bvgAFLP* and RB50P$_{long}$*bvgAFLP* represent sequences inserted at the *att*Tn7 site. Dotted lines represent non-coding plasmid DNA. Sequence lengths from the ATG of *fhaB* to the nearest 5' ATG are indicated. Not drawn to scale.

These data led us to closely reexamine the genetic architecture of each strain that produced LCVs (RBX9 and RB50::pBam) as well as the strains that showed a difference in *bvgAS-flp* reporter activation (RB50P$_{short}$*bvgAFLP* and RB50P$_{long}$*bvgAFLP*). A comparison of these strains revealed the presence of a divergent promoter 5´ to the *fhaB-bvgAS* intergenic region in RBX9, RB50::pBam, and RB50P$_{short}$*bvgAFLP* (Figure 14). In RBX9, the *fimA* promoter is very close to the *fhaB-bvgAS* intergenic region, in contrast to RB50 in which it is separated by the entire (>12kb) *fhaB* gene. In RB50::pBam, the *bla* promoter (driving expression of the ampicillin resistance gene on the plasmid) is adjacent to the *fhaB-bvgAS*

intergenic region. In the strain RB50P*bvgA*$_{short}$*FLP*, the *npt* promoter (driving expression of the kanamycin resistance gene on the plasmid) is proximal to P$_{bvgA}$-*flp*, whereas the RB50P*bvgA*$_{long}$*FLP* reporter is "buffered" from the same *npt* promoter by an additional 1200bp of *fhaB* (Figure 14). We hypothesized that the presence of a promoter 5′ to the *bvgAS-fhaB* intergenic region was interfering with *bvgAS* P_2 transcription, possibly by sequestering RNA polymerase away from P_2. To test the hypothesis that nearby promoters affect P_2 transcription, we reversed the orientation of the insert in the plasmid pBam. In the resulting plasmid, pBamR, the *bla* promoter is no longer proximal to the *bvgAS* homology region. Instead, the closest promoter 5' to *bvgAS* on the plasmid is the *aaC1* promoter (driving expression of the gentamicin resistance gene), which is more than 1.5kb away (Figure 14). We created RB50::pBamR by integrating the pBamR plasmid into the RB50 chromsome. Modulating RB50::pBamR and plating bacteria onto Bvg$^+$ phase conditions resulted in all colonies having the typical Bvg$^+$ phase morphology, and no LCVs were observed. The LCV phenotype was therefore abolished by changing the sequences upstream of the *bvgAS-fhaB* region, presumably by increasing the distance between a promoter and *bvgAS*. Additionally, we deleted the intergenic region between *fhaB* and *fimA* (which includes the *fimA* promoter) in RBX9. The resulting strain RBX9F did not produce LCVs after modulation. These data strongly support a model in which a promoter upstream of *bvgAS* interferes with normal P_2 transcription efficiency, resulting in some cells having an insufficient quantity of BvgAS to activate transcription at P_1.

Each Bvg$^-$ phase-trapped bacterium within an LCV initiates the formation of a new LCV and the proportion of Bvg$^-$ phase-trapped bacteria within an LCV decreases over time. Our data indicate that LCVs are founded by a single Bvg$^-$ phase-trapped bacterium and that each LCV harbors Bvg$^-$ phase-trapped bacteria that can propagate additional LCVs. However, it is unclear whether all Bvg$^-$ phase-trapped bacteria, or only a subset of these cells, yield LCVs upon replating. To address this question, we needed two pieces of information: the proportion of Bvg$^-$ phase-trapped bacteria within one LCV and the frequency of new LCV formation from the same parent colony when replated. We used RBX9*cyaA*FLP to evaluate the composition and LCV-forming capacity of single LCVs.

Plating a GFP$^+$ LCV onto Bvg$^-$ phase conditions, in which *cyaA* expression is minimal, will minimize further Flp-mediated recombination due to *cyaA* activation, permitting us to determine the proportion of GFP$^+$ bacteria (and hence Bvg$^-$ phase-trapped) existing within the LCV at that time. Plating the same GFP$^+$ LCV onto Bvg$^+$ phase conditions will allow us to determine the number of new LCVs generated from the subpopulation of Bvg$^-$ phase-trapped bacteria in the parent LCV. Comparing the frequency of newly generated LCVs under Bvg$^+$ phase conditions to the frequency of GFP$^+$ cfu under Bvg$^-$ phase conditions will reveal the proportion of Bvg$^-$ phase bacteria that form LCVs when replated.

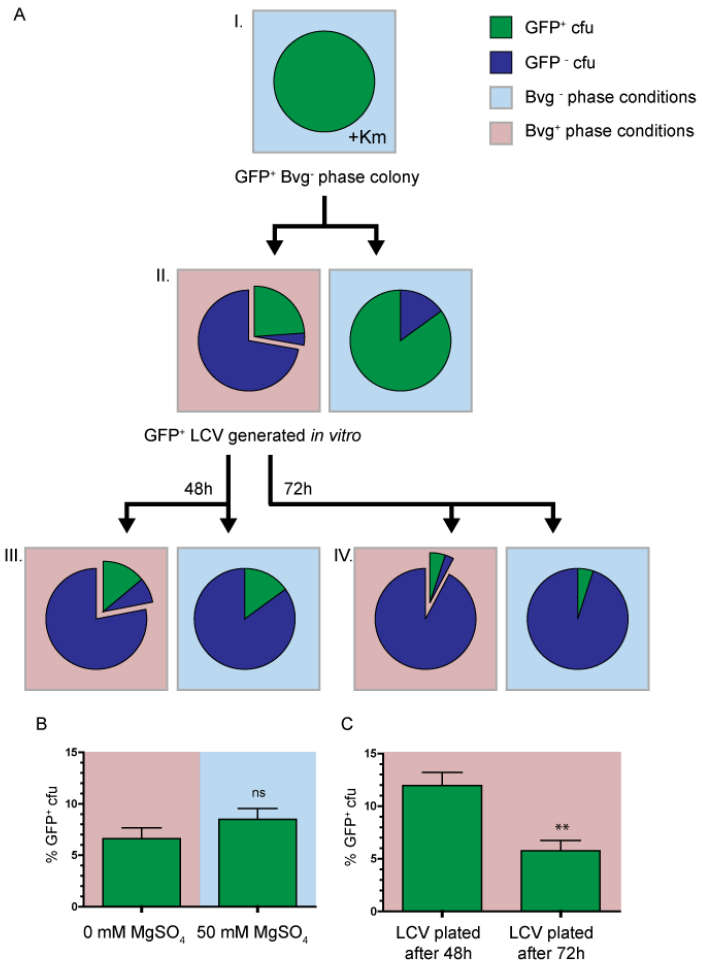

Figure 15. A, Schematic of RBX9*cyaA*FLP experimental design, including a data set from one replicate. Each pie chart represents the population obtained from plating a single GFP$^+$ colony from the previous plate (see text for details). Blue sectors in pie charts represent the frequency of GFP$^-$ cfu; Green sectors in pie charts represent the frequency of GFP$^+$ cfu; offset regions of pie charts represent the frequency of LCVs. B, Comparison of GFP$^+$ cfu frequencies obtained from plating a single GFP$^+$ LCV onto Bvg$^+$ and Bvg$^-$ phase conditions. C, Comparison of GFP$^+$ cfu frequencies obtained from plating a GFP$^+$ LCV grown after 48h and 72h. Background color represents BvgAS conditions, where red is Bvg$^+$ phase conditions and blue is Bvg$^-$ phase conditions. **, P = 0.005 by Student's Unpaired T-test.

We first grew RBX9*cyaA*FLP on Bvg$^-$ phase conditions with Km selection to maintain the *gfp* and Km^r markers (Figure 15A I). Then we took single GFP$^+$ (Bvg$^-$ phase) colonies and plated them onto Bvg$^+$ and Bvg$^-$ phase conditions (Figure 15A II). GFP$^+$ LCVs that were recovered from Bvg$^+$ phase plates were then plated again onto Bvg$^+$ and Bvg$^-$

phase conditions (Figure 15A III). The numbers of GFP^+ cfu, LCVs, and Bvg^+ phase colonies from each plate were recorded. The results from one representative experiment are shown in Figure 15A. When the GFP^+ LCVs were plated onto Bvg^+ and Bvg^- phase conditions, there was no significant difference in the average number of GFP^+ cfu under Bvg^- phase conditions compared to the average number of GFP^+ LCVs on the corresponding BG blood agar plate (Figure 15B). These data suggest that each Bvg^- phase bacterium within an LCV is Bvg^- phase-trapped and forms an LCV when replated onto Bvg^+ phase conditions.

Additionally, we asked if the composition of LCVs (i.e., the ratio of Bvg^- to Bvg^+ phase bacteria) changed over time. We hypothesized that this ratio would change due to bacterial division as well as the rate of conversion of Bvg^- phase-trapped bacteria to Bvg^+ phase bacteria. Because we expected a unidirectional conversion of phenotypes (Bvg^- to Bvg^+ phase only) under Bvg^+ phase conditions, we predicted that the ratio of Bvg^- to Bvg^+ phase bacteria would decrease as the bacterial population increased. To determine if the compositions would change after an additional day of growth, we compared GFP^+ LCVs plated after our standard incubation time (48h) (Figure 15A III) to GFP^+ LCVs plated after 72 h (Figure 15A IV). When GFP^+ LCVs were plated after 48h of incubation, we obtained an average of 12 ± 1.2% GFP^+ cfu under Bvg^- phase conditions, whereas after 72h, we obtained an average of 5.75 ± 1% GFP^+ cfu under the same conditions (P=0.005) (Figure 15C). These data indicate that the frequency of GFP^+ (and therefore Bvg^- phase-trapped) bacteria in an LCV decreases over time.

These data also strongly suggest (as discussed in a previous result) that GFP^- LCVs are a result of the background activation of *cyaA* in RBX9P*cyaA*flp, as the background *cyaA*-

flp activation under conditions of inactivity (Bvg^- phase conditions) was the same as the frequency of GFP^- LCVs (to total LCVs) under Bvg^+ phase conditions (Figure 15A II).

Modulation of RBX9 *in vivo* occurs at a very low frequency. All data published thus far strongly suggest that wild-type *Bordetella* do not modulate to the Bvg^i or Bvg^- phase *in vivo* and that the Bvg^+ phase is necessary and sufficient for infection (40–45). The recovery of LCVs from mouse lung homogenates and the fact that LCVs were recovered *in vitro* only following modulation, however, supports the hypothesis that RBX9 modulates during infection. To test this hypothesis, we constructed strain RBX9*flaA*FLP, a strain containing the pGFLIP cassette in which the *flaA* promoter drives expression of *flp* (46). Previously, using the same P_{flaA}-*flp*-containing cassette in wild-type RB50, we showed that *flaA* was not activated to a detectable level in RB50 during murine infection (46). RB50*flaA*FLP and RBX9*flaA*FLP bacteria were grown under Bvg^+ phase conditions with Km selection to minimize background resolution prior to inoculation. Mice were inoculated intranasally with $7.5x10^4$ – $1x10^5$ cfu and lungs were harvested at 3, 24, 30, and 72 hours post-inoculation. We conducted this experiment several times. In all experiments, a low proportion (≤1%) of GFP^- bacteria was recovered from the lungs of both RB50*flaA*FLP- and RBX9*flaA*FLP-inoculated animals (data not shown). This low proportion was not significantly different, however, from the proportion of GFP^- bacteria present in the samples used for inoculation (plated after inoculating the animals). Data from previous work with RB50*flaA*FLP (46) and our experiments with RBX9*flaA*FLP indicate that resolution of the P_{flaA}-*flp* cassette is BvgAS-dependent because GFP^- bacteria are never recovered from strains containing the *bvgS-C3* mutation, which locks the bacteria in the Bvg^+ phase (data not shown). For the

RBX9*flaA*FLP-inoculated animals, most of the GFP$^-$ colonies recovered from the mouse lungs were LCVs and no GFP$^+$ LCVs were recovered, indicating that formation of LCVs *in vivo* correlates with, and is most likely caused by, BvgAS modulation. Together, these data suggest that a very small proportion of RBX9 modulates to the Bvg$^-$ phase during infection. However, our data neither support nor refute the possibility that RB50 modulates as well.

To determine if bacteria modulate to the Bvg^i phase during infection, we attempted to construct strains with Bvg^i phase promoters, including the *bipA* promoter, driving *flp*. However, we were unable to construct these strains, presumably because the level of expression of these genes in Bvg$^+$ phase conditions was above the threshold of *flp* activation required for recombination and loss of GFP and Km^R.

If BvgAS modulation occurs in vivo, it does not alter the outcome of infection. Our data suggest that a small proportion RBX9 (and possibly RB50) bacteria may modulate to the Bvg$^-$ phase during infection. Although several previous experiments have shown that wild-type and Bvg$^+$ phase-locked *B. bronchiseptica* strains are indistinguishable in animal models (40–43, 45), we considered the possibility that the proportion of RBX9 bacteria that modulate *in vivo* could actually be greater than that of RB50, but not apparent from the P_{flaA}-*flp* data because modulated RBX9 bacteria are killed in the host (i.e., that modulated bacteria, and perhaps specifically modulated RBX9 bacteria are more susceptible to host-mediated clearance than modulated RB50 bacteria). To test this hypothesis, we compared RBX9, RBX9c (the Bvg$^+$ phase-locked derivative of RBX9), RBX9F (the ΔP_{fimA} derivative of RBX9 which is not defective for *bvgAS* autoregulation), and RBX9cF (a Bvg$^+$ phase-locked derivative of RBX9F) in mice. The results of three independent experiments are shown in

Figure 16. In no case did a statistically significant difference in bacterial burden occur amongst the various strains. These data negate our hypothesis and provide strong evidence that the low level of BvgAS modulation that occurs *in vivo* (based on the recovery of LCVs) does not impact the outcome of infection.

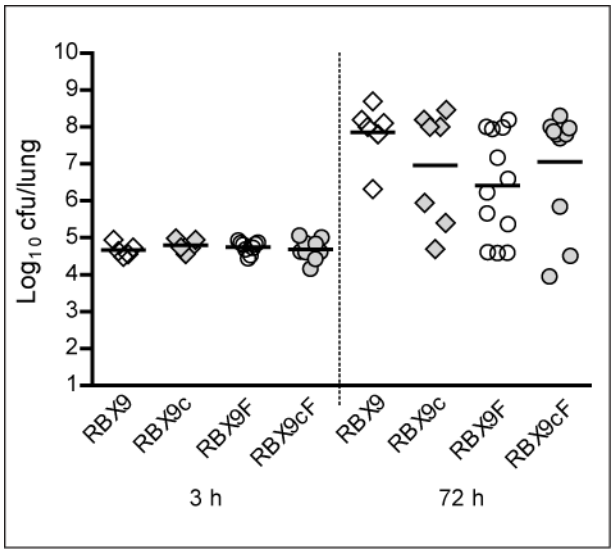

Figure 16. Comparison of RBX9, RBX9c, RBX9F, and RBX9cF burdens in the mouse lung after 3h and 72h p.i. RBX9c and RBX9cF are Bvg$^+$ phase-locked derivatives of RBX9 and RBX9F, respectively; four-to eight-week-old BALB/C mice were intranasally infected with 1×10^5 cfu in 50µl and lungs were harvested at each time point; each diamond or circle indicates the number of cfu recovered from a single animal and each horizontal line indicates the geometric mean for each group; these data represent three independent experiments with at least two mice per strain per time point.

Discussion

The discovery and characterization of LCVs in *B. bronchiseptica* yielded several interesting findings, the most significant being evidence that transcriptional interference can result from activity at a promoter located several hundred nucleotides 5′ to the affected promoter. Given this relatively large distance between promoters, the mechanism of interference likely does not involve direct blocking of transcription; therefore, we suggest the name 'passive transcriptional interference' for this phenomenon. Our data indicate that the *bvgAS* P_2 promoter is sensitive to passive transcriptional interference and that it results in the emergence of a bistable phenotype, apparent as LCVs, when bacteria are switched from Bvg^- phase conditions to Bvg^+ phase conditions. The fact that LCVs, which contain Bvg^- phase-trapped bacteria, were recovered from the lungs of infected mice, provided evidence that BvgAS modulation occurs *in vivo*. Our experiments indicate, however, that although a small proportion of bacteria may modulate during infection, this level of modulation does not alter the outcome of infection.

Bacterial populations often exhibit phenotypic heterogeneity. A common mechanism by which bacteria can generate this heterogeneity is phase variation, a reversible and heritable change in phenotype (due to either genetic or epigenetic modifications) often manifested as different colony morphologies (52, 53). Phase variation frequently alters the production of surface-exposed epitopes such as pilli, capsule, flagella, lipopolysaccharide (LPS), and adhesins (52). Coincidently, phase variation is often associated with virulence and is an important strategy used by pathogens to avoid immune selection. Some well-characterized examples of phase variation include the *opa* operon encoding adhesin proteins in *Neisseria* species, the *pap* operon encoding fimbrae in *E. coli*, and the flagella subunits

encoded by *fljBA* and *fliC* in *Salmonella enterica* serotype Typhimurium (54–56). In *Bordetella*, phase variation in both *fim3* and *bvgAS* has been described (57, 58).

More recently, a phenomenon that generates bistable populations at the single-cell level has been discovered, called feedback-based multistability (FBM) (59). FBM is distinct from phase variation in that it is not based on genetic mutations but is instead based on feedback loops of regulatory networks (59). In isogenic populations, these feedback networks can result in bistability, which occurs when individuals in a population exhibit either one of two alternative stable steady-states (but not intermediate states) (60). A well-characterized example of FBM is in *Bacillius subtilis*, in the regulation of competence orchestrated by the transcription factor ComK (61). Competence is a cellular state induced by nutrient depletion, but only occurs in a fraction of the *B. subtilis* population due to oscillating levels of ComK at the single-cell level (62, 63). In one study, Smits *et al*. removed the external regulation of *comK*, leaving only positive autoregulation, and showed that ComK levels continued to exhibit bistability. Therefore, the authors argue that ComK bistability can be reduced to a positive autoregulatory loop in concert with random transcriptional and translational fluctuations or "noise" (64). This claim is supported by other examples, in which feedback regulation and a non-linear input are the only required components for a bistable system (60, 65).

We discovered LCVs of *B. bronchiseptica* after plating lung homogenates of mice infected with strain RBX9 and found that they yielded a heterogeneous population upon restreaking onto BG blood agar. We did not find evidence of classical phase variation in RBX9. Instead, the mechanism by which LCVs are generated appears more similar to FBM, in which the concentration of BvgA under Bvg^- phase conditions varies in the population and

results in only some bacteria committing to a positive feedback loop when switched to Bvg^+ phase conditions. In support of this, we were able to label bacteria within LCVs with tags unique to the Bvg^+ and Bvg^- phase and demonstrate the existence of two phenotypically distinct populations (Figure 11). The dual-tagged RBX9 strain also provided the first direct evidence that Bvg^i phase cultures are not simply a mixture of Bvg^+ and Bvg^- phase bacteria.

Use of the recombinase-based reporter system pGFLIP (46) showed that the Δ*fhaB* mutation in RBX9 causes a decrease in the efficiency of *bvgAS* positive autoregulation and results in Bvg^- phase-trapped bacteria that decline in proportion over time and can initiate the formation of new LCVs (Figure 12, 13, and 15). Based on these results and previous data, we postulate a model of LCV formation and propagation (Figure S18). According to our model, the concentration of BvgA varies in a population and also in individual cells as they grow and divide. In RB50, the average concentration of BvgA under Bvg^- phase conditions is such that 100% of the bacteria are able to respond to Bvg^+ phase conditions and transition to the Bvg^+ phase phenotype (Figure S18 A,B). In RBX9 however, the average concentration of BvgA is decreased under Bvg^- phase conditions compared to wild-type bacteria (curve shifted to the left in Figure S18A, such that a subpopulation is below the threshold level required to respond to Bvg^+ phase conditions. These bacteria are thus Bvg^- phase trapped and remain phenotypically Bvg^- phase even under Bvg^+ phase conditions. Under Bvg^+ phase conditions, these bacteria form LCVs, which continue to harbor Bvg^- phase-trapped bacteria. The Bvg^- phase-trapped bacteria within LCVs occasionally escape to become Bvg^+ phase descendants, possibly through unequal division or stochastic accumulation of BvgA (Figure S18C). Therefore, in this system, a mutation that decreases the basal concentration of the

positively autoregulated factor (BvgA) results in an FBM-like phenotype, whereas in other systems, FBM is the natural mechanism by which bacteria reach a bistable state.

Our pGFLIP data indicated that the *bvgAS* positive autoregulation defect is due to decreased activity of P_2. This result explains why RBX9 has lower levels of BvgA: it has decreased transcription of *bvgAS*. Our data suggest that the reason for decreased transcription is the presence of a promoter located 5′ to the P_2 promoter. This upstream divergent promoter is exerting its negative effects on *bvgAS* from relatively far away (~800 bp) and appears to represent a previously undescribed form of transcriptional interference (the suppressive influence of one transcriptional process on another), (66). It is unclear whether this promoter must be highly active or divergently transcribed. However, as with other examples of transcription interference, we predict that increasing this promoter's strength would also increase the degree of interference (67). Additionally, we predict that the orientation of the promoter may not be important and that reversing its orientation would not abolish interference if transcription read through was prevented. We do not understand mechanistically how this "passive" transcriptional interference occurs. One possibility is that the divergent promoter sequesters RNA polymerase away from the sensitive promoter (P_2) or that transcription at this site influences DNA topology in a way that is prohibitive to P_2 activation. Although the LCV phenotype appeared as an artifact of genetic manipulation, our results are important as they demonstrate an undescribed form of transcriptional interference and also because they reveal a mechanism by which in-frame deletion mutations that can have unanticipated polar effects on neighboring genes. Furthermore, RBX9 and its derivatives constitute a genetically tractable system for studying additional mechanisms of transcriptional interference and details of FBM.

The LCVs also provided insight into the behavior of BvgAS during infection. The role of BvgAS-dependent modulation in the *Bordetella* life cycle is not completely understood and remains an important area of investigation. Several studies have attempted to determine if Bvg^{i} or Bvg^{-} phase bacteria exist at any point during *Bordetella* infection, and so far none have yielded positive results (40–43, 45). These data, together with those demonstrating that Bvg^{-} phase bacteria transition rapidly to the Bvg^{+} phase following intranasal inoculation (46, 68), have led to the conclusion that not only is the Bvg^{+} phase necessary and sufficient for infection, but that bacteria switch to and remain in the Bvg^{+} phase *in vivo*. The Bvg^{i} and Bvg^{-} phases are hypothesized to be important for transmission and survival *ex vivo*, however, no role for these phenotypic phases in a natural setting has been demonstrated. For *B. pertussis* particularly, which appears to survive outside the host only briefly during transmission to a new host, the role of BvgAS modulation remains mysterious. The isolation of LCVs from mouse lungs provides strong evidence that at least some RBX9 bacteria modulate during infection. However, the proportion of bacteria that modulated and that could be recovered from the animals was very low. Because the P_{flaA}-*flp* system was unable to reliably distinguish this low proportion of modulated bacteria from background resolution, we could not determine if wild type bacteria modulate *in vivo*. If they do not, our data would suggest that only FHA-deficient bacteria modulate *in vivo*, which would suggest that FHA functions to prevent the bacteria from experiencing a Bvg^{-} phase environment during infection. In pilot experiments, we also recovered LCVs from mice infected with ΔfhaB, ΔcyaA double mutants – in higher proportions, in some cases, than in

mice infected with RBX9. These preliminary data suggest the intriguing possibility that FHA and ACT function together to prevent Bordetella from creating or entering a modulating environment in the host. Our future experiments will be aimed at testing this hypothesis.

We thank members of our laboratory, especially Jeffrey Melvin, for many insightful discussions. Research reported in this publication was supported by the National Institute of Allergy and Infectious Diseases of the National Institutes of Health under award numbers R01AI43986, RO1AI094991, and U54AI065359 to P.A.C. The content is solely the responsibility of the authors and does not necessarily represent the official views of the National Institutes of Health. The authors have no conflicts of interest to declare.

References

1. **Mattoo S, Cherry JD**. 2005. Molecular Pathogenesis , Epidemiology , and Clinical Manifestations of Respiratory Infections Due to Bordetella pertussis and Other Bordetella Subspecies. clinical microbiology reviews **18**:326–382.

2. **Marconi GP, Ross LA, Nager AL**. 2012. An upsurge in pertussis: epidemiology and trends. Pediatric emergency care **28**:215–9.

3. **Campos-Outcalt D**. 2005. Pertussis: a disease re-emerges. The Journal of family practice **54**:699–703.

4. **Gross R, Keidel K, Schmitt K**. 2010. Resemblance and divergence: the “new” members of the genus Bordetella. Medical microbiology and immunology **199**:155–163.

5. **Gerlach G, Von Wintzingerode F, Middendorf B, Gross R**. 2001. Evolutionary trends in the genus Bordetella. Microbes and infection / Institut Pasteur **3**:61–72.

6. **Diavatopoulos D a, Cummings C a, Schouls LM, Brinig MM, Relman D a, Mooi FR**. 2005. Bordetella pertussis, the causative agent of whooping cough, evolved from a distinct, human-associated lineage of B. bronchiseptica. PLoS pathogens **1**:e45.

7. **Cummings CA, Bootsma HJ, Relman DA, Miller JF**. 2006. Species- and strain-specific control of a complex, flexible regulon by Bordetella BvgAS. Journal of bacteriology **188**:1775–1785.

8. **Tejada GM, Miller JF, Cotter PA**. 1996. Comparative analysis of the virulence control systems of Bordetella pertussis and Bordetella bronchiseptica. Molecular **22**:895–908.

9. **Sato Y, Sato H**. 1999. Development of acellular pertussis vaccines. Biologicals : journal of the International Association of Biological Standardization **27**:61–9.

10. **Domenighini M, Relman D, Capiau C, Falkow S, Prugnola A, Scarlato, Rappuoli R**. 1990. Genetic characterization of Bordetella pertussis filamentous haemagglutinin: a protein processed from an unusually large precursor. Molecular microbiology **4**:787-800.

11. **Mazar J, Cotter PA**. 2006. Topology and maturation of filamentous haemagglutinin suggest a new model for two-partner secretion. Molecular microbiology **62**:641–654.

12. **Coutte L, Antoine R, Drobecq H, Locht C, Jacob-Dubuisson F**. 2001. Subtilisin-like autotransporter serves as maturation protease in a bacterial secretion pathway. The EMBO journal **20**:5040–8.

13. **Cotter PA, Yuk MH, Mattoo S, Akerley BJ, Boschwitz J, Relman DA, Miller JF**. 1998. Filamentous hemagglutinin of Bordetella bronchiseptica is required for efficient establishment of tracheal colonization. Infection and immunity **66**:5921-9.

14. **Mattoo S, Miller JF, Cotter PA**. 2000. Role of Bordetella bronchiseptica fimbriae in tracheal colonization and development of a humoral immune response. Infection and immunity **68**:2024-33.

15. **Inatsuka CS, Julio SM, Cotter PA**. 2005. Bordetella filamentous hemagglutinin plays a critical role in immunomodulation, suggesting a mechanism for host specificity. Proceedings of the National Academy of Sciences of the United States of America **102**:18578–18583.

16. **McGuirk P, Mills KH**. 2000. Direct anti-inflammatory effect of a bacterial virulence factor: IL-10-dependent suppression of IL-12 production by filamentous hemagglutinin from Bordetella pertussis. European journal of immunology **30**:415–22.

17. **Abramson T, Kedem H, Relman D**. 2001. Proinflammatory and proapoptotic activities associated with Bordetella pertussis filamentous hemagglutinin. Infection and immunity **69**:2650–2658.

18. **Henderson MW, Inatsuka CS, Sheets AJ, Williams CL, Benaron DJ, Donato GM, Gray MC, Hewlett EL, Cotter P a**. 2012. Contribution of Bordetella filamentous hemagglutinin and adenylate cyclase toxin to suppression and evasion of IL-17-mediated inflammation. Infection and immunity **80**:2061–2075.

19. **Perez Vidakovics ML a, Lamberti Y, Van der Pol W-L, Yantorno O, Rodriguez ME**. 2006. Adenylate cyclase influences filamentous haemagglutinin-mediated attachment of Bordetella pertussis to epithelial alveolar cells. FEMS immunology and medical microbiology **48**:140–7.

20. **Zaretzky FR, Gray MC, Hewlett EL**. 2002. Mechanism of association of adenylate cyclase toxin with the surface of Bordetella pertussis: a role for toxin-filamentous haemagglutinin interaction. Molecular microbiology **45**:1589–98.

21. **Aricò B, Miller JF, Roy C, Stibitz S, Monack D, Falkow S, Gross R, Rappuoli R**. 1989. Sequences required for expression of Bordetella pertussis virulence factors share homology with prokaryotic signal transduction proteins. Proceedings of the National Academy of Sciences of the United States of America **86**:6671–6675.

22. **Cotter PA, Jones AM**. 2003. Phosphorelay control of virulence gene expression in Bordetella. Trends in microbiology **11**:367-373.

23. **Cotter PA, Miller JF**. 1997. A mutation in the Bordetella bronchiseptica bvgS gene results in reduced virulence and increased resistance to starvation, and identifies a new class of Bvg-regulated antigens. Molecular microbiology **24**:671–685.

24. **Deora R, Bootsma HJ, Miller JF, Cotter PA**. 2001. Diversity in the Bordetella virulence regulon: transcriptional control of a Bvg-intermediate phase gene. Molecular microbiology **40**:669-683.

25. **Williams CL, Boucher PE, Stibitz S, Cotter PA**. 2005. BvgA functions as both an activator and a repressor to control Bvg phase expression of bipA in Bordetella pertussis. Molecular microbiology **56**:700-13.

26. **Stockbauer KE, Fuchslocher B, Miller JF, Cotter PA**. 2001. Identification and characterization of BipA, a Bordetella Bvg-intermediate phase protein. Molecular microbiology **39**:65-78.

27. **Jones AM, Boucher PE, Williams CL, Stibitz S, Cotter PA**. 2005. Role of BvgA phosphorylation and DNA binding affinity in control of Bvg-mediated phenotypic phase transition in Bordetella pertussis. Molecular microbiology **58**:700–713.

28. **Boucher PE, Maris AE, Yang M-S, Stibitz S**. 2003. The response regulator BvgA and RNA polymerase alpha subunit C-terminal domain bind simultaneously to different faces of the same segment of promoter DNA. Molecular cell **11**:163–73.

29. **Boucher PE, Yang M, Schmidt DM, Stibitz S**. 2001. Genetic and Biochemical Analyses of BvgA Interaction with the Secondary Binding Region of the fha Promoter of Bordetella pertussis **183**:536–544.

30. **Boucher PE, Yang MS, Stibitz S**. 2001. Mutational analysis of the high-affinity BvgA binding site in the fha promoter of Bordetella pertussis. Molecular microbiology **40**:991–9.

31. **Steffen P, Goyard S, Ullmann A**. 1996. Phosphorylated BvgA is sufficient for transcriptional activation of virulence-regulated genes in Bordetella pertussis. The EMBO Journal **15**:102–109.

32. **Boulanger A, Chen Q, Hinton DM, Stibitz S**. 2013. In vivo phosphorylation dynamics of the Bordetella pertussis virulence-controlling response regulator BvgA. Molecular microbiology **88**:156–72.

33. **V. Scarlato, Rappuoli R.** 1991. Differential response of the bvg virulence regulon of Bordetella pertussis to MgSO4. Journal of bacteriology **173**:7401-7404.

34. **Prugnola A, Aricò B, Manetti R, Rappuoli R, Scarlato, V**. 1995. Response of the bvg regulon of Bordetella pertussis to different temperatures and short-term temperature shifts. Microbiology (Reading, England) **141:**2529-2534.

35. **Williams CL, Cotter PA**. 2007. Autoregulation is essential for precise temporal and steady-state regulation by the Bordetella BvgAS phosphorelay. Journal of bacteriology **189**:1974–82.

36. **Roy CR, Falkow S**. 1991. Identification of Bordetella pertussis regulatory sequences required for transcriptional activation of the fhaB gene and autoregulation of the bvgAS operon. Journal of bacteriology **173**:2385-2392.

37. **Scarlato, Prugnola A, Aricó B, Rappuoli R**. 1990. Positive transcriptional feedback at the bvg locus controls expression of virulence factors in Bordetella pertussis. Proceedings of the National Academy of Sciences of the United States of America **87**: 6753-6757.

38. **Zu T, Manetti R, Rappuoli R, Scarlato**. 1996. Differential binding of BvgA to two classes of virulence genes of Bordetella pertussis directs promoter selectivity by RNA polymerase. Molecular microbiology **21**:557-565.

39. **Karimova G, Bellalou J, Ullmann A**. 1996. Phosphorylation-dependent binding of BvgA to the upstream region of the cyaA gene of Bordetella pertussis. Molecular microbiology **20**:489–496.

40. **Tejada GM, Cotter PA, Heininger U, Camilli A, Akerley BJ, Mekalanos JJ, Miller JF**. 1998. Neither the Bvg- phase nor the vrg6 locus of Bordetella pertussis is required for respiratory infection in mice. Infection and immunity **66**:2762-8.

41. **Vergara-Irigaray N, Chávarri-Martínez A, Rodríguez-Cuesta J, Miller JF, Cotter PA, Tejada GM**. 2005. Evaluation of the role of the Bvg intermediate phase in Bordetella pertussis during experimental respiratory infection. Infection and immunity **73**:748-60.

42. **Nicholson TL, Brockmeier SL, Loving CL, Register KB, Kehrli ME, Stibitz SE, Shore SM**. 2012. Phenotypic modulation of the virulent Bvg phase is not required for pathogenesis and transmission of Bordetella bronchiseptica in swine. Infection and immunity **80**:1025–1036.

43. **Cotter PA, Miller JF**. 1994. BvgAS-mediated signal transduction: analysis of phase-locked regulatory mutants of Bordetella bronchiseptica in a rabbit model. Infection and immunity **62**:3381-3390.

44. **Akerley BJ, Cotter PA, Miller JF**. 1995. Ectopic expression of the flagellar regulon alters development of the Bordetella-host interaction. Cell **80**:611-20.

45. **Merkel TJ, Stibitz S, Keith JM, Leef M, Shahin R**. 1998. Contribution of regulation by the bvg locus to respiratory infection of mice by Bordetella pertussis. Infection and immunity **66**:4367–73.

46. **Byrd MS, Mason E, Henderson MW, Scheller E V, Cotter P a**. 2013. An improved RIVET-like reporter system reveals differential cyaA gene activation in Bordetella species. Infection and immunity **81**:1295–1305.

47. **Irie Y, Mattoo S, Yuk MH**. 2004. The Bvg Virulence Control System Regulates Biofilm Formation in Bordetella bronchiseptica. Journal of bacteriology **186**:5692–5698.

48. **Julio SM, Inatsuka CS, Mazar J, Dieterich C, Relman DA, Cotter PA**. 2009. Natural-host animal models indicate functional interchangeability between the filamentous haemagglutinins of Bordetella pertussis and Bordetella bronchiseptica and reveal a role for the mature C-terminal domain, but not the RGD motif, during infection. Molecular microbiology **71**:1574–90.

49. **Bellalou J, Sakamoto H, Ladant D, Geoffroy C, Ullmann A**. 1990. Deletions affecting hemolytic and toxin Deletions Affecting Hemolytic and Toxin Activities of Bordetella pertussis Adenylate Cyclase **58**:3242-3247.

50. **Williams CL, Haines R, Cotter PA**. 2008. Serendipitous discovery of an immunoglobulin-binding autotransporter in Bordetella species. Infection and immunity **76**:2966–2977.

51. **Akerley BJ, Monack DM, Falkow S, Miller JF**. 1992. The bvgAS locus negatively controls motility and synthesis of flagella in Bordetella bronchiseptica. Journal of bacteriology **174**:980–90.

52. **Woude MW Van Der, Bäumler AJ**. 2004. Phase and Antigenic Variation in Bacteria. clinical microbiology reviews **17**: 581–611.

53. **Hallet B**. 2001. Playing Dr Jekyll and Mr Hyde: combined mechanisms of phase variation in bacteria. Current opinion in microbiology **4**:570–81.

54. **Stern A, Meyer TF**. 1987. Common mechanism controlling phase and antigenic variation in pathogenic neisseriae. Molecular microbiology **1**:5–12.

55. **Simon M, Zieg J, Silverman M, Mandel G, Doolittle R**. 1980. Phase variation: evolution of a controlling element. Science (New York, N.Y.) **209**:1370–4.

56. **Hernday A, Krabbe M, Braaten B, Low D**. 2002. Self-perpetuating epigenetic pili switches in bacteria. Proceedings of the National Academy of Sciences of the United States of America **99 Suppl 4**:16470–6.

57. **Willems R, Paul A, Van der Heide HGJ, Ter Avest AR, Mooi FR**. 1990. Fimbrial phase variation in Bordetella pertussis: a novel mechanism for transcriptional regulation. The EMBO journal **9**:2803–2809.

58. **Stibitz S, Aaronson W, Monack D, Falkow S**. 1989. Phase variation in Bordetella pertussis by frameshift mutation in a gene for a novel two-component system. Nature **338**:266–9.

59. **Smits WK, Kuipers OP, Veening J-W**. 2006. Phenotypic variation in bacteria: the role of feedback regulation. Nature reviews. Microbiology **4**:259–71.

60. **Ferrell JE**. 2002. Self-perpetuating states in signal transduction: positive feedback, double-negative feedback and bistability. Current Opinion in Cell Biology **14**:140–148.

61. **Sinderen D Van, Luttinger A, Kong U, Kong L, Dubnau D, Venema G, Hamoen L**. 1995. comK encodes the competence transcription factor, the key regulatory protein for competence development in Bacillus subtilis. Molecular Microbiology **15**:455–462.

62. **Espinar L, Dies M, Cagatay T, Suel GM, Garcia-Ojalvo J**. 2013. Circuit-level input integration in bacterial gene regulation. Proceedings of the National Academy of Sciences. **110**: 7091–7096.

63. **Veening J-W, Smits WK, Kuipers OP**. 2008. Bistability, epigenetics, and bet-hedging in bacteria. Annual review of microbiology **62**:193–210.

64. **Smits WK, Eschevins CC, Susanna K a, Bron S, Kuipers OP, Hamoen LW**. 2005. Stripping Bacillus: ComK auto-stimulation is responsible for the bistable response in competence development. Molecular microbiology **56**:604–14.

65. **Maamar H, Dubnau D**. 2005. Bistability in the Bacillus subtilis K-state (competence) system requires a positive feedback loop. Molecular microbiology **56**:615–24.

66. **Shearwin KE, Callen BP, Egan JB**. 2005. Transcriptional interference--a crash course. Trends in genetics : TIG **21**:339–45.

67. **Sneppen K, Dodd IB, Shearwin KE, Palmer AC, Schubert R a, Callen BP, Egan JB**. 2005. A mathematical model for transcriptional interference by RNA polymerase traffic in Escherichia coli. Journal of molecular biology **346**:399–409.

68. **Veal-Carr WL, Stibitz S**. 2005. Demonstration of differential virulence gene promoter activation in vivo in Bordetella pertussis using RIVET. Molecular microbiology **55**: 788–798.

Supplemental Information

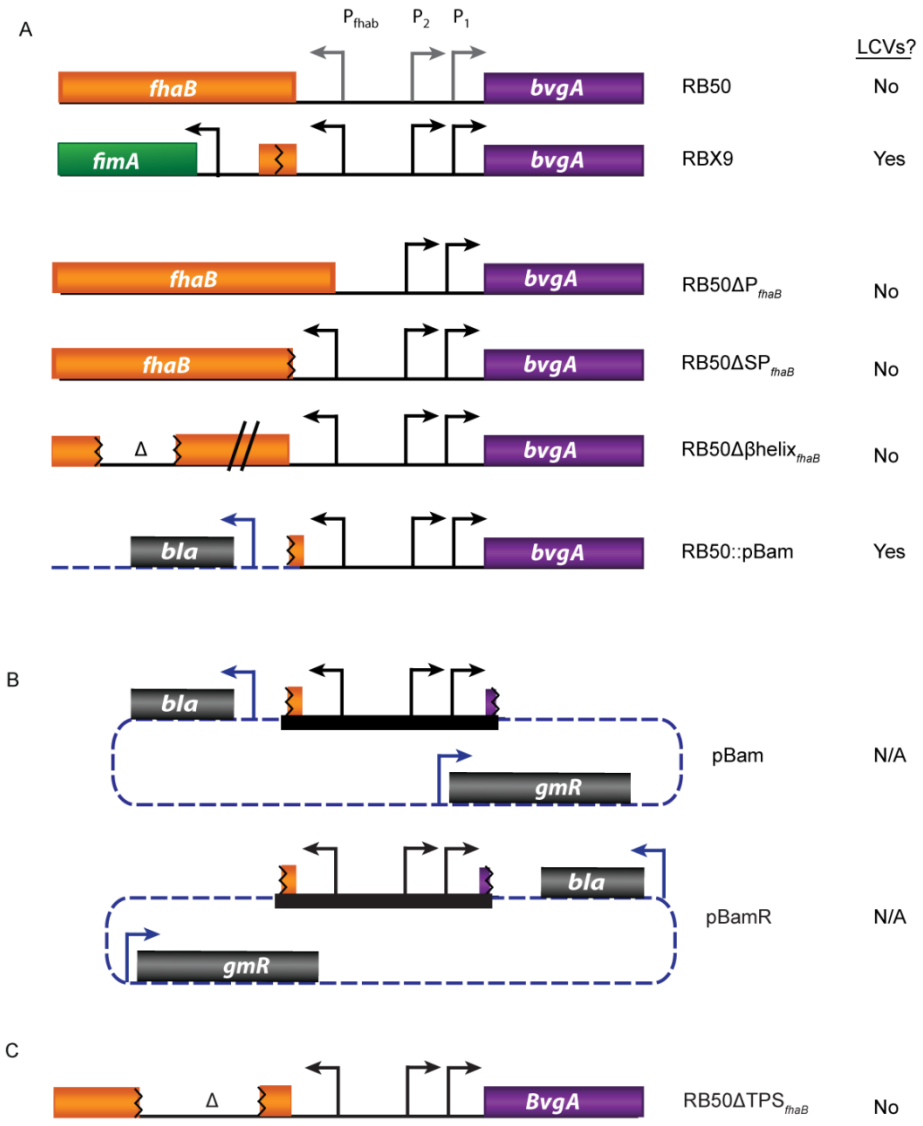

Figure S17. A, genetic architecture of strains that do and do not produce LCVs, including RB50ΔP*fhaB*, RB50ΔSP*fhaB*, RB50Δβhelix*fhaB*, and RB50::pBam with RB50 and RBX9 as a reference; B, schematic of pBam and pBamR plasmids and the orientation of their inserted sequences; blue dotted lines represent plasmid DNA; thick black lines represents *fhaB-bvgAS* intergenic region; C, Genetic architecture of strain RB50ΔTPS*fhaB*; not drawn to scale.

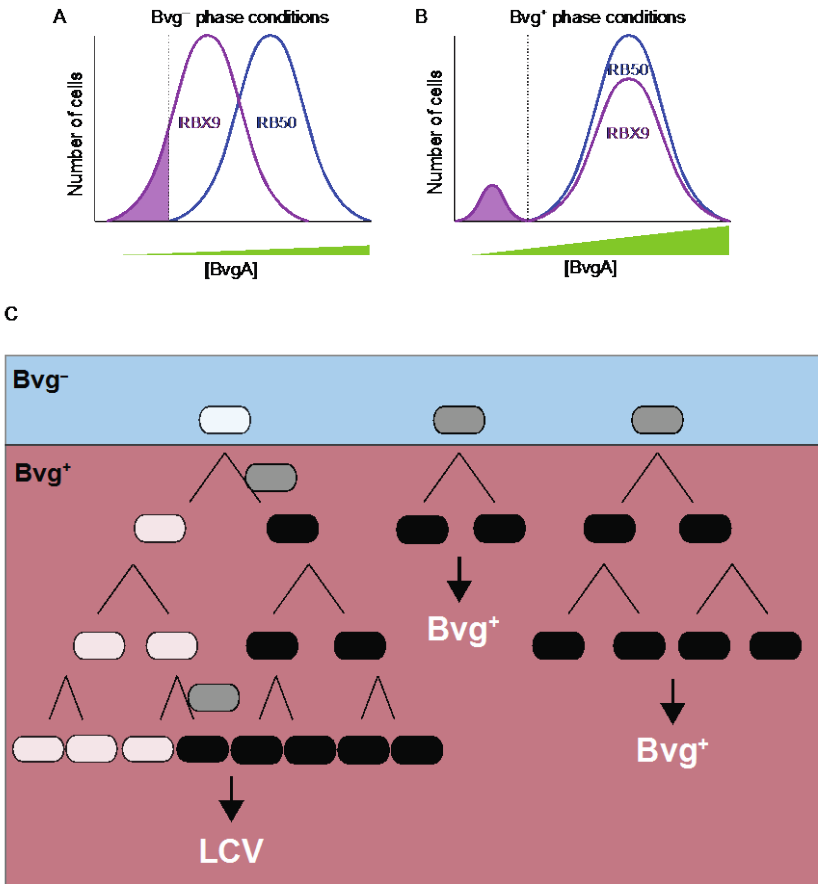

Figure S18. A and B, Proposed distribution of BvgA concentration within populations of RBX9 and RB50. A, In the Bvg$^-$ phase, a proportion of RBX9 cells (shaded region) are Bvg$^-$ phase-trapped (i.e., have a concentration of BvgA below the threshold [dotted line] necessary to stimulate positive autoregulation upon transition to Bvg$^+$ phase conditions). By contrast, all RB50 cells have a level of BvgA sufficient to initiate positive autoregulation upon transition to Bvg$^+$ phase conditions. B, In the Bvg$^+$ phase, the RBX9 cells that were below the threshold BvgA concentration in the Bvg$^-$ phase (shaded region as in A) maintain their low concentration of BvgA and are thus unable to switch to the Bvg$^+$ phase. These cells are able to initiate LCV formation as described in C. Consistent with our *in vitro* data, all RB50 cells are able to switch to the Bvg$^+$ phase. C, Model of LCV formation and propagation illustrated as a lineage diagram (see text for details). RBX9 bacteria exist as a heterogeneous population under Bvg$^-$ phase conditions, with some bacteria (white) being below the threshold of BvgA required to initiate positive autoregulation and others above this threshold (gray). When bacteria are switched to the Bvg$^+$ phase, the Bvg$^-$ phase trapped bacteria form LCVs, whereas the other bacteria transition into the Bvg$^+$ phase (black) and form Bvg$^+$ phase colonies. Occasionally, Bvg$^-$ phase-trapped bacteria "escape" and can transition into the Bvg$^+$ phase (indicated by gray cells between white and black cells), resulting in LCV formation after 48h.

Table S4 Strains and Plasmids used in this study

Strain or Plasmid	Description	Reference
Strains		
E. coli		
DH5α	Molecular cloning strain	(1)
RH03	Conjugation strain; Km^s, DAP auxotroph	(2)
Bordetella		
RB50	Wild-type *B. bronchiseptica* strain; Sm^r	(3)
RBX9	RB50 with an in-frame deletion mutation of *fhaB*	(4)
RB53	RB50 with the *bvgS*-C3 mutation (Bvg^+ phase-locked)	(3)
RB50i	RB50 with the *bvgS*-I1 mutation (Bvg^i phase-locked)	(5)
RBX9i	RBX9 with the *bvgS*-I1 mutation (Bvg^i phase-locked)	(5)
RBX9c	RBX9 with *bvgS*-CS3 mutation (Bvg^+ phase-locked)	This study
RB50::pBam	RB50 with pBam integrated between *bvgA* and *fhaB*; Gm^r	This study
RB50::pBamR	RB50 with pBamR integrated between *bvgA* and *fhaB*; Gm^r	This study
RB50Δ*fhaB*	RB50 with same Δ*fhaB* mutation as RBX9	This study
RBX9BatBN-HA*flaA-gfp*	RBX9 with N-terminal HA-encoding tag in *batB* (proceeding codon 55) and P_{flaA} *gfp* at *att*Tn7	This study
RB50ΔP_{fhaB}	RB50 with a deletion mutation of the *fhaB* promoter (nt -244 through -28 relative to the ATG)	This study
RB50ΔSP_{fhaB}	RB50 with a *fhaB* signal peptide deletion mutation (codons 2-70)	This study
RB50Δβhelix$_{fhaB}$	RB50 with an in-frame deletion mutation of codons 385 -1979 of *fhaB* (encoding the β-helix)	This study
RB50ΔTPS_{fhaB}	RB50 with a deletion mutation of bp 8 - 1256 (within codons 3 - 413) in *fhaB*	This study
RBX9*cyaA*FLP	RBX9 with *flp* driven by P_{cyaA} integrated at *att*Tn7	This study
RB50P_{short}*bvgAFLP*	RB50 with *flp* driven by $P_{bvgA\text{-}short}$ integrated at *att*Tn7	This study
RB50P_{long}*bvgAFLP*	RB50 with *flp* driven by $P_{bvgA\text{-}long}$ integrated at *att*Tn7	This study
RBX9F	RBX9 with a deletion mutation of the	This study

	fimA-fhaB intergenic region	
RBX9cF	RBX9ΔP$_{fimA}$ with the *bvgS*-CS3 mutation	This study
Plasmids		
pSS4245	pBR322-based allelic exchange plasmid; Ap^r, Km^r	(1)
pEG7S	*Bordetella* allelic exchange vector; Ap^r, Gm^r	(7)
pEG7	pBR322-based suicide plasmid; Ap^r, Gm^r	(5)
pEG3SO	Suicide plasmid encoding *bvgS*-CS3 mutation (R570H) with flanking sequence	(3)
pΔP$_{fhaB}$	pEG7S derivative with nt (-29) – (500) and (-750) – (-243) relative to *fhaB* ATG	This study
pΔSP$_{fhaB}$	pEG7S derivative with sequences comprising codons 30 of *bvgA* to codon 1 of *fhaB* and codons 71-238 of *fhaB*	This study
pΔβhelix$_{fhaB}$	pSS4245 derivative with codons 218-235 and 1979-2146 of *fhaB*	This study
pΔTPS$_{fhaB}$	pSS4245 derivative with sequences from codon 3 of *fhab* through codon 30 of *bvgA* and codons 413-567 of *fhaB*	This study
pX9ΔP$_{fimA}$	pSS4245 derivative with codons 1-183 of *fimA* and 16 bp 3' to the *fhaB* STOP codon through codon 30 of *bvgA* of RBX9	This study
pGFLIP	Tn7-based vector with PS12-*gfp* and nptII flanked by FRT sequences and *flp* 3' to the MCS; Ap^r, Km^r (conditional)	(8)
pGFLIP-P$_{cyaA}$	pGFLIP with *flp* driven by the RB50 *cyaA* promoter, Ap^r, Km^r (conditional)	(8)
pGFLIP-P$_{flaA}$	pGFLIP with *flp* driven by the RB50 *flaA* promoter, Ap^r, Km^r (conditional)	(8)
pGFLIP-P$_{bvgA\text{-}short}$	pGFLIP with *flp* driven by the *fhaB-bvgAS* intergenic region	This study
pGFLIP-P$_{bvgA\text{-}long}$	pGFLIP with *flp* driven by sequences 1200bp of *fhaB* to the *bvgAS* translational start site	This study
pTnS3	Tn7 transposase expression vector containing *tnsABCD*; Ap^r	(9)
pBam	pEG7 plasmid with *bvgAS-fhaB* intergenic region in the MCS	This study
pBamR	pEG7 plasmid with *bvgAS-fhaB* intergenic region (reverse orientation relative to pBam)	This study
pUC18Tn7-*flaA-gfp*	Tn7-based vector with P$_{flaA}$-*gfp;* Ap^r, Km^r	This study
pUC18T-mini-Tn7T-Km-*FRT*	Mobilizable transposition vector; Ap^r,	(9)

	Km^r	
pCW103	pSS4245 derivative with HA-encoding sequence flanked by *batB* sequences nt (-300 from ATG) to codon 55 and codons 56-216.	This study

Strain Construction. Allelic exchange was done using derivatives of pEG7S or pSS4245 according to (1, 10). All strains were confirmed by PCR and nucleotide sequence analysis.

RB50Δ*fhaB* was created by performing allelic exchange on RB50 using plasmid pΔ*fhaB*new.

RBX9BatBN-HA*flaA-gfp* was created by first performing allelic exchange on RBX9 using plasmid pCW103. To the resulting strain, the miniTn7-*flaAgfp* construct was delivered via tronsposase-mediated insertion.

RB50ΔP_{fhaB} was created by performing allelic exchange on RB50 using plasmid pΔP_{fhaB}.

RB50ΔSP_{fhaB} was created by performing allelic exchange on RB50 using plasmid pΔSP_{fhaB}.

RB50Δβhelix$_{fhaB}$ was created by performing allelic exchange on RB50 using plasmid pΔβhelix$_{fhaB}$.

RB50::pBam was created by introducing plasmid pBam into RB50 by conjugation and selecting co-integrants on BG Sm Gm agar as described by Akerley et al. 1995.

RB50::pBamR was created by introducing plasmid pBamR into RB50 by conjugation as described for RB50::pBam.

RBX9*cyaA*FLP was created by delivering pGFLIP-P_{cyaA} construct into the RBX9 chromosome via transposase-mediated insertion and selecting on BG Sm Km + 50mM $MgSO^4$.

RBX9*flaA*FLP was created by delivering pGFLIP-P_{flaA} construct into the RBX9 chromosome via transposase-mediated insertion and selecting on BG Sm Km.

RB50P_{short}*bvgAFLP* was created by delivering pGFLIP-P_{-short}*bvgA* construct into the RB50 chromosome via transposase-mediated insertion and selecting on BG Sm Km + 50mM $MgSO^4$.

RB50P_{long}*bvgAFLP* was created by delivering pGFLIP-P_{-long} *bvgA* construct into the RB50 chromosome via transposase-mediated insertion and selecting on BG Sm Km + 50mM $MgSO^4$.

RB50ΔTPS was created by performing allelic exchange on RB50 using plasmid pΔTPS_{fhaB}.

RBX9F was created by performing allelic exchange on RB50 using plasmid pΔP_{fimA}.

RBX9c was created by performing allelic exchange on RBX9 using plasmid pEG3S0 according to Cotter et al 1994.

RBX9cF was created by performing allelic exchange on RBX9F using plasmid pEG3SO.

JS20c was created by performing allelic exchange on JS29 using plasmid pEG3SO.

Plasmid Construction. All plasmids were confirmed by PCR and nucleotide sequence analysis.

pΔ*fhaB*new was created by PCR amplifying the 1kb region flanking the in-frame deletion of *fhaB* of RBX9 and ligating this insert into the MCS of pSS4245.

pΔP$_{fhaB}$ was created by PCR amplifying one fragment (corresponding to nt -574 through -244 relative to the *fhaB* ATG) ligated to another fragment (corresponding to nt -28 through 470) of RB50 and ligating this ~1kb insert into the MCS of pSS4245.

pΔSP$_{fhaB}$ was created by PCR amplifying one 500bp fragment (corresponding to codon 30 of *bvgA* to codon 1 of *fhaB*) ligated to another 500bp fragment (corresponding to codons 71-238 of *fhaB*) of RB50 and ligating this ~1kb insert into the MCS of pEG7S.

pΔβhelix$_{fhaB}$ was created by PCR amplifying one 501 bp fragment (corresponding to codons 218-385 of *fhaB*) ligated to another 501 bp fragment (corresponding to codons 1979-2146 of *fhaB*) of RB50 and ligating this ~1kb insert into the MCS of pSS4245.

pΔTPS$_{fhaB}$ was created by PCR amplifying one 460 bp fragment (corresponding to nt within codons 413-567 of *fhaB*) ligated to another 523 bp fragment (corresponding to nt within

codon 3 of *fhaB* to codon 30 of *bvgA*, including 426bp of intergenic region) from RB50 and ligating this ~1kb insert into the MCS of pSS4245.

pX9ΔP$_{fimA}$ was created by PCR amplifying one 550 bp fragment (corresponding to codons 1-183 of *fimA*) ligated to another 500 bp fragment (corresponding to 16 bp 3' to the *fhaB* STOP codon through codon 30 of *bvgA*) of RBX9 and ligating this ~1kb insert into the MCS of pSS4245.

pBam was created by PCR amplifying the *fhaB-bvgAS* intergenic region (corresponding to the 426 bp between each ATG) of RBX9 and ligating this fragment into the MCS of pEG7.

pBamR was created by digesting pBam with BamHI (where BamHI cut sites flanked the insert), ligating, and screening transformed clones for the reverse orientation relative to pBam.

pGFLIP-P$_{bvgA\text{-short}}$ was created by PCR amplifying the *fhaB-bvgAS* intergenic region (426bp) from RB50 and inserting this fragment into the MCS of pGFLIP with the *bvgAS* promoters driving *flp*.

pGFLIP-P$_{bvgA\text{-long}}$ was created by PCR amplifying a 1626 bp fragment including nt corresponding to codon 400 of *fhaB* through the ATG of *bvgA* in RB50 and inserting this fragment into the MCS of pGFLIP with the *bvgAS* promoters driving *flp.*

miniTn7-*flaAgfp* was created by PCR amplifying 500 nt 5' to the *flaA* ATG in RB50 and ligating this fragment into the MCS of pUC18T-miniTn7T-Km. To the resulting plasmid, we ligated sequences encoding promoterless *gfp* from miniTn7T-*kan-gfp* pUC such that the *flaA* promoter drives *gfp*.

pCW103 was created by PCR amplifying sequence encoding an HA-tag flanked by homology region from *batB* including -300 nt from ATG to codon 55 and codons 56-216 and ligating this insert into the MCS of pSS4245.

Supplemental References

1. **Inatsuka CS, Xu Q, Vujkovic-Cvijin I, Wong S, Stibitz S, Miller JF, Cotter P a**. 2010. Pertactin is required for Bordetella species to resist neutrophil-mediated clearance. Infection and immunity **78**:2901–9.

2. **López CM, Rholl DA, Trunck LA, Schweizer HP**. 2009. Versatile dual-technology system for markerless allele replacement in Burkholderia pseudomallei. Applied and environmental microbiology **75**:6496–503.

3. **Cotter PA, Miller JF**. 1994. BvgAS-mediated signal transduction: analysis of phase-locked regulatory mutants of Bordetella bronchiseptica in a rabbit model. Infection and immunity **62**: 3381-3390.

4. **Cotter PA, Yuk MH, Mattoo S, Akerley BJ, Boschwitz J, Relman DA, Miller JF**. 1998. Filamentous hemagglutinin of Bordetella bronchiseptica is required for efficient establishment of tracheal colonization. Infection and immunity **66**:5921-9.

5. **Cotter PA, Miller JF**. 1997. A mutation in the Bordetella bronchiseptica bvgS gene results in reduced virulence and increased resistance to starvation, and identifies a new class of Bvg-regulated antigens. Molecular microbiology **24**: 671–685.

6. **Noël CR, Mazar J, Melvin JA, Sexton JA, Cotter P A**. 2012. The prodomain of the Bordetella two-partner secretion pathway protein FhaB remains intracellular yet affects the conformation of the mature C-terminal domain. Molecular microbiology **86**:988–1006.

7. **Julio SM, Cotter PA**. 2005. Characterization of the filamentous hemagglutinin-like protein FhaS in Bordetella bronchiseptica. Infection and immunity **73**: 4960–4971.

8. **Byrd MS, Mason E, Henderson MW, Scheller E V, Cotter P A**. 2013. An improved RIVET-like reporter system reveals differential cyaA gene activation in Bordetella species. Infection and immunity **81**:1295–1305.

9. **Choi K-H, Mima T, Casart Y, Rholl D, Kumar A, Beacham IR, Schweizer HP**. 2008. Genetic tools for select-agent-compliant manipulation of Burkholderia pseudomallei. Applied and environmental microbiology **74**:1064–75.

10. **Tejada GM, Miller JF, Cotter PA**. 1996. Comparative analysis of the virulence control systems of Bordetella pertussis and Bordetella bronchiseptica. Molecular microbiology **22**:895–908.

CHAPTER 4: Conclusion

Pertussis remains one of the most common vaccine-preventable diseases. Although widespread vaccination and antibiotic usage have dramatically reduced the burden of *Bordetella* disease, these bacteria still proliferate in carrier and unvaccinated populations. The recent resurgence of pertussis is now a driving force to improve the current acellular vaccine, understand its shortcomings, and learn more about *Bordetella* pathogenesis. Despite almost a hundred years of research, our understanding of the factors that affect *Bordetella* disease progression, the development of host protective immunity, and the bacterial life cycle is incomplete.

Why is *Bordetella* virulence gene regulation interesting and how is it relevant to preventing and treating *Bordetella* disease? The *Bordetella* are unique pathogens with several phenotypic profiles that are controlled by a single, pervasive regulatory system, indispensable for virulence. BvgAS evolved to become the pinnacle of *Bordetella* sensory systems; dramatically changing the cell's physiology in response to a gradient of stimuli. Understanding BvgAS has simplified the identification and characterization genes required for pathogenesis. From an evolutionary perspective, we know that *B. pertussis* became more virulent and specifically adapted to its host through reductive evolution and alterations in gene regulation; not by gene acquisition. Therefore, understanding BvgAS, its natural signals, its evolution, and its complete regulon, is indispensable to understanding *Bordetella*

pathogenesis. The experiments presented in this dissertation have sought to explore *Bordetella* virulence by understanding the subtleties of BvgAS-mediated gene regulation.

One of the greatest mysteries of *Bordetella* and BvgAS is the role of modulation to the Bvg^{i} and Bvg^{-} phases. Especially for *B. pertussis,* the most fastidious of the *B. bronchiseptica* cluster, it is unclear why many of the *vrgs* remain intact. As an obligate human pathogen that cannot survive naturally outside of a host, transition out of the Bvg^{+} phase seems unnecessary, if not detrimental. In *B. bronchiseptica*, the Bvg^{-} phase permits survival under nutrient-limiting conditions, and, is likely the dominant phase while the bacteria occupy *ex vivo* niches. For *B. pertussis*, the Bvg^{-} phase has been proposed as an evolutionary remnant. However, the *vrgs* of each subspecies are diverse and thus appear to have evolved independently, suggesting distinct and important functions. For example, the *vrgs* encoding outer membrane proteins in *B. pertussis* are unique (by regulation), and therefore may perform alternate functions (or at least be required in a different context) distinct from the homologues in *B. bronchiseptica*. Additionally, the Bvg^{+} phase-locked phenotype can be accomplished through a single nucleotide mutation in *bvgS*. If the Bvg^{+} phase was necessary and sufficient for the entire lifecycle of *B. pertussis,* one would expect these mutations to appear frequently, although this is not observed. For *B. bronchiseptica* however, our experiments support previous data suggesting that modulation to the Bvg^{-} phase does not occur during lung infection.

Understanding *in vivo* gene expression has always been a prominent goal for studying pathogens; *Bordetella* is no exception. We designed a sensitive system, called pGFLIP, that can function as an *in vivo* reporter of gene activation in *Bordetella*. pGFLIP utilizes the site-specific recombinase gene *flp,* driven by a promoter of interest. Upon production of Flp (and

thus activation of the promoter), the *gfp* and *nptII* (kmR) genes are permanenty excised. Utilization of this system to detect *in vivo* gene expression is straightforward if promoter-inactive conditions are known: animals are infected with GFP^+ bacteria, which are later recovered and screened for loss of GFP. The main drawback of pGFLIP is that the readout is negative: detecting a loss of signal (fluorescence) is more difficult than detecting a gain of signal. To overcome this problem, we are enhancing pGFLIP with a constitutive *rfp* gene, which will permit the visualization of every cell, such that cells with activated promoters will fluoresce distinctly. This new system, pRGFLIP, will be informative in conjunction with flow cyotmetry- and microscopy-based assays.

pGFLIP was originally validated using *Bordetella*, and revealed unexpected differences in virulence gene regulation. In *B. bronchiseptica*, we showed that *cyaA*, characterized as a late Bvg^+ phase gene in *B. pertussis*, was expressed considerably earlier when bacteria were switched from the Bvg^- to the Bvg^+ phase. This difference was not accounted for by the species-specific *cyaA* promoters or the *bvgAS* loci. We also showed that *flaA* was not expressed to a detectable level within the murine lungs during infection, supporting the hypothesis that the Bvg^- phase does not play a role *in vivo*. These experiments demonstrate that pGFLIP is valuable as both an *in vitro* and *in vivo* reporter tool.

pGFLIP was also instrumental in the characterization of LCVs, affectionately known as “wonkies,” in *B. bronchiseptica*. The discovery of wonkies from RBX9 provided insight into BvgAS regulation as well as general bacterial transcription processes. Wonkies recovered from animals suggested that modulation to the Bvg^- phase occured *in vivo*, but as we later found out, had a negligible impact on infection. Interestingly, the mechanism by which wonkies are generated involves transcriptional interference of *bvgAS*. We term it

"passive" transcriptional interference because the distance between affected promoters is so great (≥800 bp) that physical blockage by RNAP is extremely unlikely. Wonkies are also interesting because they represent a bacterial population consisting of transiently Bvg^- phase-trapped bacteria and wild-type Bvg^+ phase bacteria. This phenomenon suggests that bistable phenotypes can emerge by subtle alterations of transcription in a positively autoregulated system.

We hope that these and other studies will someday contribute to the eventual eradication of *Bordetella* disease. Understanding BvgAS is fundamental to this goal.

APPENDIX A: Attempts to Create a Permanently Surface-Attached FHA Molecule in. *B bronchiseptica*

The purpose of these experiments was to create a *B. bronchiseptica* mutant that produced and secreted FHA in a wild-type manner but remained attached to the cell surface; i.e., an FHA that was not released. This strain would be used to investigate and distinguish the functions of the surface-associated and released forms of FHA. We took three approaches to accomplish this: 1, we created mutants that contained deletions of sequences encoding a large portion of the β-helical subdomain, hypothesized to provide the energy for secretion; 2, we created mutants containing several double cysteine mutations in an attempt to stall secretion though disulfide bond formation in the periplasm; and 3, we created a mutant containing a deletion of sequences encoding 22 residues in FHA predicted to be the secondary protease (SphB1-independent) cleavage site. None of the mutations were sufficient to inhibit FHA secretion into the supernatant under any of the conditions tested.

The energy source that drives all Type V Secretion exoproteins (including TPS and autotransporter systems) through the outer membrane remains unknown (1). Interestingly, almost all of these systems are predicted to contain β-helical structure (2–4). A popular hypothesis is that the sequential folding of a β-helical domain through the TpsB pore drives secretion of the rest of the TpsA molecule (3). To test this hypothesis and to determine if the β-helical domain was required for secretion, we deleted the majority of the sequences encoding the β-helical shaft domain of FHA, including approximately 1600 aa residues C-terminal to the conserved TPS domain but N-terminal to the MCD. Although the TPS domain (including the first ~250 residues of the N-terminus) also folds into β-helical

structure, it is indispensable for recognizing FhaC and initiating secretion (5–7), and was therefore kept intact in our studies.

We hypothesized that FHA lacking the majority of the β-helical shaft would become trapped within FhaC due to an absence of energy for the secretion of the globular MCD. Two strains were constructed: RBX20::pEM1, a Campbell-type integration that created an in-frame deletion mutation of sequences encoding residues 385-1979 with a stop codon following the MCD domain, and RBX11Δβ-helix, containing a clean in-frame deletion mutation of residues 285-1979 only. The primary difference between these strains is the presence of the prodomain, which affects the folding of FHA but is not required for release. We were unsure of the contribution of the prodomain to the secretion of these mutants.

To our surprise, neither of these strains produced FHA that was incapable of release, as visualized by western blot analysis of supernatants (Figure 19). In addition, when the same Δβ-helix mutations were introduced into a Δ*sphB1* background, the release of cleaved FHA was just as prominent (although the slightly larger 90 kD form is dominant in the RBX11Δβ-helixΔ*sphB1* sample.) Although unexpected, one possible explanation is that the folding of the β-helical structure in the TPS domain is sufficient for FHA secretion, regardless of the absence of additional β-helical length. Another possibility is that the β-helix structure does not provide energy for folding and thus is not required for secretion of the MCD. Whichever is the case, it is clear that none of these mutations are sufficient to prevent release of FHA into the supernatant.

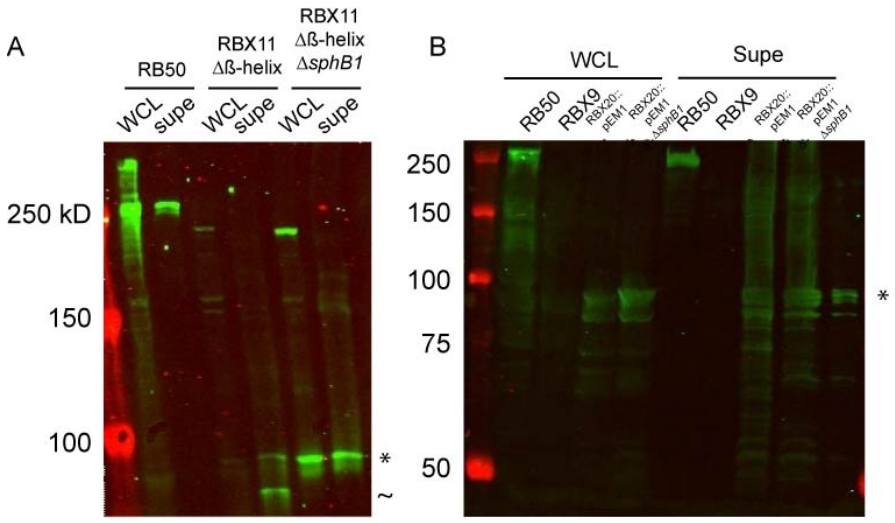

Figure 19. Western blots of strains containing deletion mutations of the β-helical shaft domain of FHA, compared to wild-type and Δ*sphB1* derivative strains. A, Blot showing whole cell lysates (WCL) and supernatants (supe) of RB50, RBX11Δβ-helix, and RBX11Δβ-helixΔ*sphB1* probed with α-MCD$_{FHA}$ (rabbit) primary antibody and α-rabbit 800λ secondary; The processed FHA fragment is approximately 90 kD (indicated by * on right of each blot), with another ~80kD (indicated by ~) form in the *sphB1*$^{+}$ background. B, Blot showing WCL and supes of RB50, RBX9Δ*fhaB*, RBX20::pEM1, and RBX20::pEM1Δ*sphB1*; mature FHA fragments are approximately 90 kD; antibodies are same as in A; molecular weight marker (red) is shown on left in kD.

Our second approach was inspired by other TPS systems that have evolved specific mechanisms for the surface retention of the TpsA exoprotein; namely, HMW1-type proteins. These proteins have two conserved cysteine residues near the C-terminus which form a disulfide bond in the periplasm, resulting in a stable plug that prevents release from the cell surface (8, 9). We hypothesized that by adding cysteine residues to FhaB, we could stall secretion through the same mechanism, as was done previously with pertactin (10), an autotransporter in *Bordetella*. Because FhaB has no natural cysteines, creating the mutations was straightforward. Several cysteine pair mutations were constructed within the TPS, β-helical, and MCD domains that were separated by intervals ranging from ten to several thousand residues. We hypothesized that if any of the mutant pairs stalled secretion, it would suggest that the two regions were in the periplasm and in close proximity at some point

during the secretion process. Therefore, in addition to creating a strain that could not be released, we could also learn about the localization of each region of FhaB during secretion.

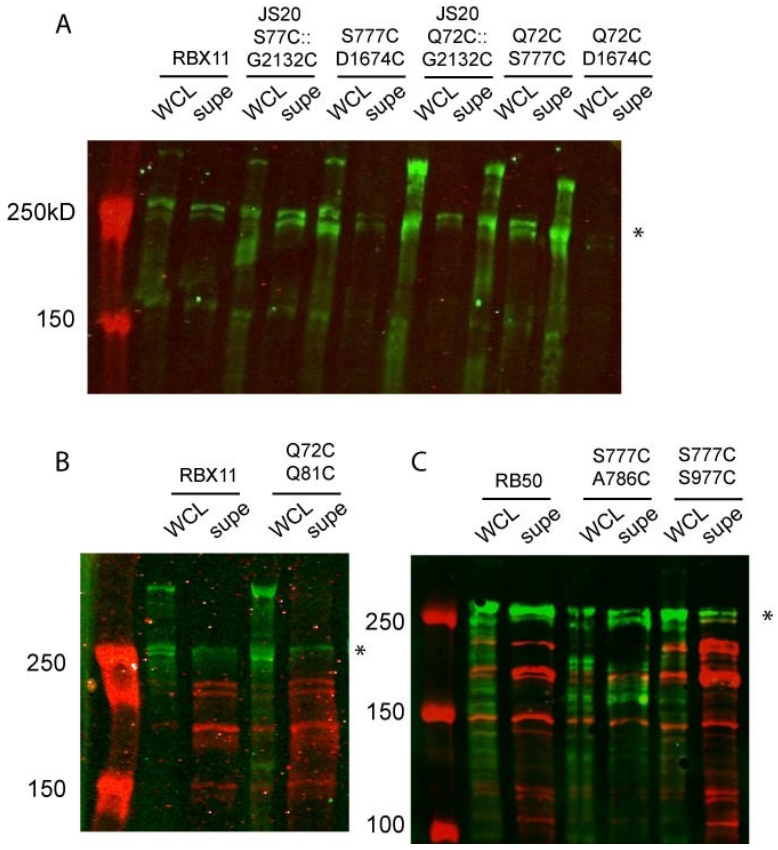

Figure 20. Western blots of strains containing cysteine pair mutations in *fhaB*, compared to wild-type strains, probed with α-MCD$_{FHA}$ (green) and α-cyaA (red). A, B, and C, Blots showing whole cell lysates and supernatants of strains indicated; RBX11 (Δ*fhaS*) and RB50 are wild-type controls; molecular weight indicator is on the left of each blot in kD; FhaB is approximately 350 kD whereas FHA is approximately 250 kD (indicated by * on right of each blot).

Figure 20 shows western blots of a wide panel of double cysteine mutation strains. Strains in the JS20 background were created via Campbell-type integration, whereas the others were created by using allelic exchange in the RBX11 (Δ*fhaS*) background. All of the strains produced FHA that was secreted into the supernatant (although RBX11 D1674C Q72C appears to have significantly reduced secretion (Figure 20A), this result was

inconsistent in subsequent blots, where typical amounts of FHA were detected). The ability of all of the strains to secrete FHA was unexpected, but indicates that none of the cysteine pair mutations were sufficient to halt secretion through FhaC. It is particularly surprising that some strains, such as RBX11 Q72C Q81C and RBX11 S777C S786C, which contain cysteines only ten residues apart (and equivalent to the cysteine spacing found in HMW1), did not form a disulfide bond that inhibited secretion through FhaC. Two possibilities could account for these results: 1, none of the cysteine pairs formed disulfide bonds or 2, disulfide bonds formed but were insufficient to stall secretion in this specific context. In HMW1, it is known that the TpsA protein remains closely associated with the TpsB pore, which forms a dimer on the cell surface (9). It is possible that specific sequences within HMW1B (the TpsB protein) are required for this anchoring.

Our third approach to creating a surface-attached FHA molecule was to target the SphB1-independent protease cleavage site. On the cell surface, SphB1 targets the PFLETRIK aa sequence in FhaB, and separates the MCD from the prodomain (11, 12). Previous attempts to prevent cleavage by deleting the sequences encoding the SphB1 cleavage site in *fhaB* were unsuccessful, indicating SphB1's level of sequence promiscuity. Additionally, deletion of *sphB1* itself does not prevent cleavage of FhaB, because another unidentified protease cleaves FhaB 5′ to the SphB1-recognition site (11, 13). Because we did not know the identity of the SphB1-independent protease, we predicted the location of its cleavage site based on experiments by Mazar and Cotter (11), and attempted to remove it.

We hypothesized that deletion of the SphB1-independent cleavage site would prevent cleavage (and possibly release) of FhaB in a Δ*sphB1* background. We created the strain RBX11Δ22, containing an in-frame deletion mutation of the sequences encoding residues

2526-2547 in *fhaB*, predicted to be the SphB1-independent cleavage site. We also created strain RBX11Δβ-helixΔ*sphB1*Δ22, since we know that in RBX11Δβ-helixΔ*sphB1* the processed FHA is released as a much smaller (~90kD) form (Figure 19). Neither of these mutations prevented the SphB1-independent cleavage event nor the release of FHA into the supernatant (Figure 21). It is likely that the residues 2526-2547 were predicted incorrectly as the SphB1-independent cleavage site. Alternatively, this protease may also be promiscuous. The future identification of the SphB1-independent protease will likely be more successful in engineering an unprocessed FHA molecule.

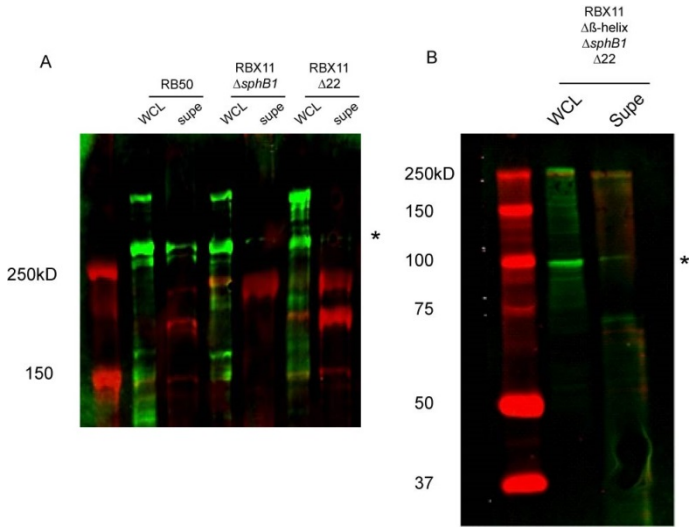

Figure 21. Western blots of Δ22 strains probed with α-MCD$_{FHA}$ (green) and in A, α-cyaA (red). A and B, whole cell and supernatant preps of strains indicated; matured FHA is ~250kD (A) and ~90kD (B), indicated by * on the right of each blot

Table 5. Strains and plasmids used in this study

Strain or Plasmid	Description
Strains	
RBX11Δ22	RBX11 with a deletion of the sequences for codons 2526-2547 in *fhaB*
RBX11Δβhelix	RBX11 with a deletion of the sequences for codons 385-1979 in *fhaB*
RBX21::pEM1	RBX20 with pEM1 cointegrated within the *fhaB* locus
RBX11ΔβhelixΔ21proΔSphB1	RBX11 containing deletion mutations of 2526-2547 and 385-1979 in *fhaB* as well as Δ*sphB1*
RBX11 D1674C S777C	RBX11 with mutations that encode cysteines at residues 1674 and 777 of *fhaB*. 65/29
RBX11 S777C Q72C	RBX11 with mutations that encode cysteines at residues 777 and 72 of *fhaB* 65/35
RBX11 Q72C Q81C	RBX11 with mutations that encode cysteines at residues 72 and 81 of *fhaB* 65/44
RBX11 S777C S977C	RBX11 with mutations that encode cysteines at residues 777 and 977 of *fhaB* 65/53
RBX11 S777C A786C	RBX11 with mutations that encode cysteines at residues 7774 and 786 of *fhaB* 5/57
JS20 Q72C::G2132C	JS20 with mutations that encode a cysteine at residue 72 as well as a plasmid cointegrated containing mutations that encode a cysteine at residue 2132 of *fhaB.*
Plasmids	
pEM1	pEG7 derivative containing flanking sequences of codons 385-1979 in *fhaB* followed by a STOP codon at residue
pTPS-MCD	pSS4245 derivative containing flanking sequences of codons Δ385-1979 in *fhaB*
pΔ22	pSS4245 derivative containing flanking sequences of codons Δ2526-2547 in *fhaB*

References

1. **Thanassi DG, Stathopoulos C, Karkal A, Li H**. 2005. Protein secretion in the absence of ATP: the autotransporter, two-partner secretion and chaperone/usher pathways of gram-negative bacteria (review). Molecular Membrane Biology **22**:63–72.

2. **Kajava A V, Cheng N, Cleaver R, Kessel M, Simon MN, Willery E, Jacob-Dubuisson F, Locht C, Steven AC**. 2001. Beta-helix model for the filamentous haemagglutinin adhesin of Bordetella pertussis and related bacterial secretory proteins. Molecular microbiology **42**:279–92.

3. **Junker M, Schuster CC, McDonnell A V, Sorg KA, Finn MC, Berger B, Clark PL**. 2006. Pertactin beta-helix folding mechanism suggests common themes for the secretion and folding of autotransporter proteins. Proceedings of the National Academy of Sciences of the United States of America **103**:4918–4923.

4. **Kajava A V, Steven AC**. 2006. Beta-rolls, beta-helices, and other beta-solenoid proteins. Advances in Protein Chemistry **73**:55–96.

5. **Clantin B, Hodak H, Willery E, Locht C, Jacob-Dubuisson F, Villeret V**. 2004. The crystal structure of filamentous hemagglutinin secretion domain and its implications for the two-partner secretion pathway. Proceedings of the National Academy of Sciences of the United States of America **101**:6194–6199.

6. **Delattre A-S, Saint N, Clantin B, Willery E, Lippens G, Locht C, Villeret V, Jacob-Dubuisson F**. 2011. Substrate recognition by the POTRA domains of TpsB transporter FhaC. Molecular microbiology **81**:99–112.

7. **Hodak H, Clantin B, Willery E, Villeret V, Locht C, Jacob-Dubuisson F**. 2006. Secretion signal of the filamentous haemagglutinin, a model two-partner secretion substrate. Molecular microbiology **61**:368–82.

8. **St Geme JW, Yeo H-J**. 2009. A prototype two-partner secretion pathway: the Haemophilus influenzae HMW1 and HMW2 adhesin systems. Trends in microbiology **17**:355–60.

9. **Buscher AZ, Grass S, Heuser J, Roth R, St Geme JW**. 2006. Surface anchoring of a bacterial adhesin secreted by the two-partner secretion pathway. Molecular microbiology **61**:470–83.

10. **Junker M, Besingi RN, Clark PL**. 2009. Vectorial transport and folding of an autotransporter virulence protein during outer membrane secretion. Molecular Microbiology **71**:1323–1332.

11. **Mazar J, Cotter PA**. 2006. Topology and maturation of filamentous haemagglutinin suggest a new model for two-partner secretion. Molecular microbiology **62**: 641–654.

12. **Coutte L, Antoine R, Drobecq H, Locht C, Jacob-Dubuisson F**. 2001. Subtilisin-like autotransporter serves as maturation protease in a bacterial secretion pathway. The EMBO journal **20**:5040–8.

13. **Noël CR, Mazar J, Melvin JA, Sexton JA, Cotter P a**. 2012. The prodomain of the Bordetella two-partner secretion pathway protein FhaB remains intracellular yet affects the conformation of the mature C-terminal domain. Molecular microbiology **86**:988–1006.

APPENDIX B: Characterization of the folding properties of the β-helix subdomain in *B. bronchiseptica* FHA

These experiments were done in collaboration with Dr. Omar Saleh at the University of California, Santa Barbara, and their data are reprinted here with permission. The purpose of these experiments was to assess the physical properties of the β-helix subdomain in FHA and to characterize the energetics of folding of this common but poorly understood structure (1). With this goal in mind, we overexpressed and purified several 50 kD FHA fragments corresponding to different β-helical domains (repeat and non-repeat regions) (2). These fragments were engineered to contain unique N and C-terminal tags (Cysteine and 6xHis, respectively) for tethering. Dr. Saleh and colleagues characterized the properties of the FHA fragments using magnetic tweezers, whereby single molecules can be manipulated and observed (3). In this assay, each molecule is tethered to a surface by a magnetic bead. Tension is created by applying a stable and constant force to the fragment, while the length of the fragment is measured. Folding and unfolding dynamics of molecules can therefore be observed through changes of the molecule length (3).

Five expression plasmids (using the pET21a vector, which contains a 6xHis tag) were constructed for the over-expression of different structural domains in FHA: four containing sequences encoding β-helix structure and one containing sequences within the MCD (Figure 22). These constructs contain approximately 1500 nt corresponding to different sub-domains and repeat domains within the β-helix (excluding the MCD construct) that were identified by Kajava et al (4). The first fragment to be purified and analyzed was R1/CR3; later, the R1, R2, CR3, and MCD constructs were engineered. For unknown reasons, the R1 and R2

constructs could not be induced and therefore were not analyzed. So far, only data for the R1/CR3 fragment has been collected (Figure 24).

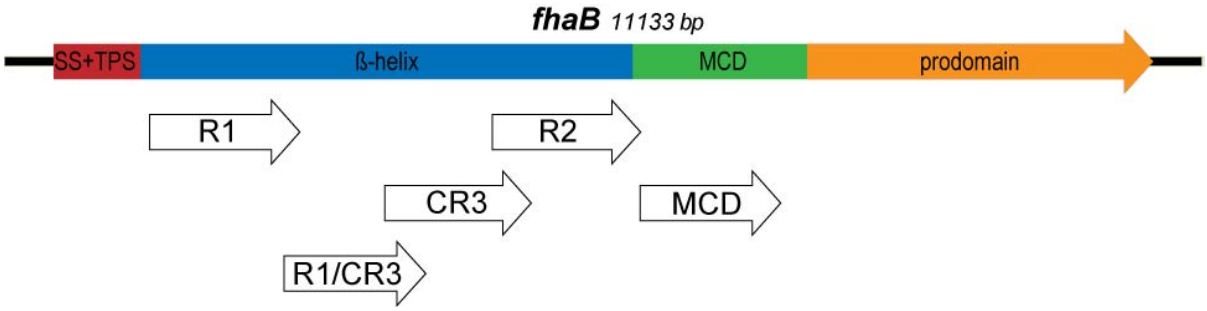

Figure 22. Schematic of the *fhaB* gene including the domains Signal Sequence (SS) and Two-Partner Secretion domain (TPS) (red), β-helical shaft (blue), Mature C-Terminal Domain (MCD) (green), and prodomain (orange); Schematic of each *fhaB* sequence fragment constructed for overexpression in this study (arrows).

A summary of the standard process of purification using nickel-affinity chromatography is as follows: constructs were induced in *E. coli* BL21* cultures by IPTG, cells were lysed, and lysates were bound to a column of nickel resin (via 6xHis), washed, and eluted (using ProBond resin, Invitrogen). Several steps of this process are visualized in the Coomassie-stained SDS-PAGE gel in Figure 23. The most concentrated elution fractions were then dialyzed, and sent to Dr. Saleh for analysis.

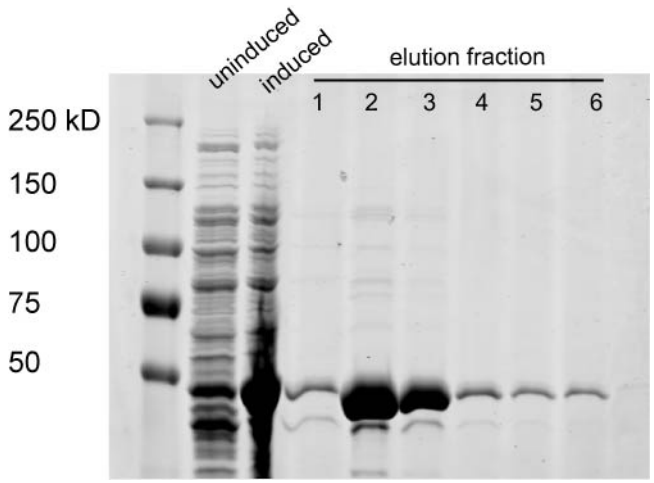

Figure 23. SDS-PAGE gel stained with Coomassie Blue showing various fractions in the process of purification of the R1/CR3 FHA fragment (approximately 48kD) using BL21:pET21aR1/CR3. From left to right: molecular weight ladder, shown in kD, uninduced culture, IPTG-induced culture, and elution fractions 1-6. Fractions 2 and 3 were subsequently dialyzed for further purification.

Saleh and colleagues observed equilibrium unfolding and refolding of the primary fragment, R1/CR3, in multiple discrete steps, supporting the hypothesis that the β-helix domain folds in a processive and vectorial manner (Figure 24). Surprisingly, the folding could not be modeled by a Brownian Ratchet system (5), which was hypothesized to account for unidirectional folding across the outer membrane (Dittmer and Saleh, unpublished results). Additionally, folding was observed as being distributed rather than cooperative, meaning that folding could nucleate at multiple locations and that numerous intermediate states existed. Additional work will be required to fully understand the β-helix structure contribution to the dynamics of FHA folding and secretion. One obvious caveat to this system is that natural folding of FHA may require the context of the complete FhaB protein (the prodomain may function as a chaperone (6)) as well as the interaction with FhaC and its specific pore environment. Therefore, we must use caution when interpreting these preliminary results.

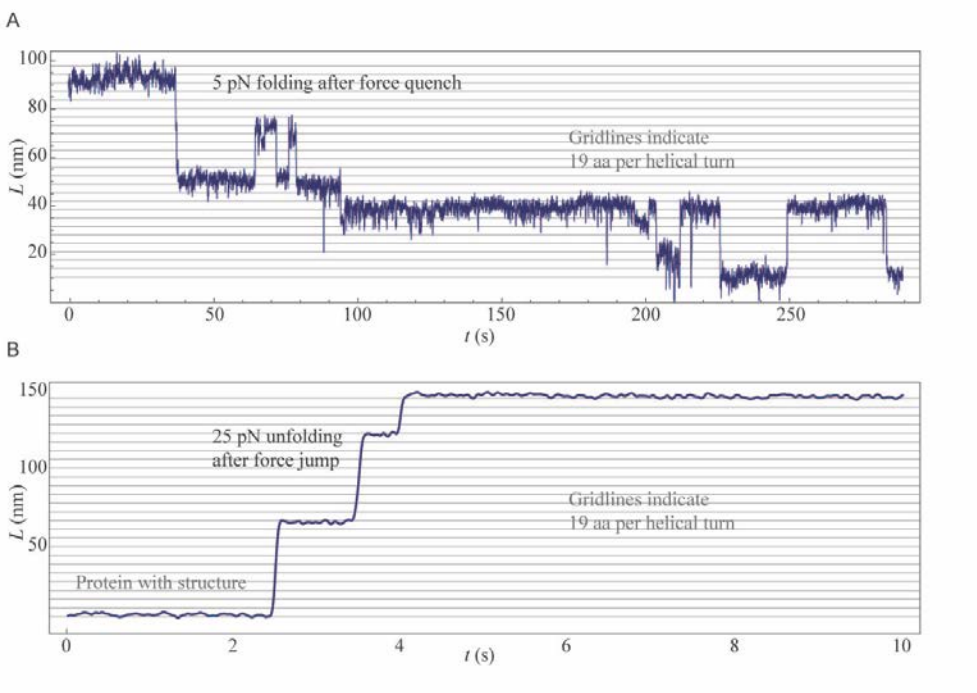

Figure 24. Force traces of the FHA R1/CR3 fragment using magnetic tweezers showing length of molecule (nm) versus time (s); A, rapid reduction of force (force quench) from 25pN to 5pN reveals the complete folding of the protein fragment and several intermediate forms; B, rapid increase of force (force jump) from 5pN to 25N reveals the unfolding process, in which the fragment unfolded in steps of 11, 10, and 4 helical turns.

Table 6. Strains and plasmids used in this study

Strain or Plasmid	Description
Strains	
BL21* pET21aβhelix (R1/CR3)	BL21* transformed with pET21aβhelix (R1/CR3)
BL21* pET21aMCD	BL21* transformed with pET21aMCD
BL21* pET21aR1	BL21* transformed with pET21aR1
BL21* pET21aCR3	BL21* transformed with pET21aCR3
BL21* pET21aR2	BL21* transformed with pET21aR2
pET21aβhelix (R1/CR3)	Sequences encoding codons 777-1256 of *fhaB* cloned into pET21a and includes sequences for a Cys residue at the N-terminus
pET21aMCD	Sequences encoding codons 1479-1954 of *fhaB* cloned into pET21a and includes sequences for a Cys residue at the N-terminus
pET21aR1	Sequences encoding codons 323-830 of *fhaB* cloned into pET21a and includes sequences for a Cys residue at the N-terminus
pET21aCR3	Sequences encoding codons 1117-1612 of *fhaB* cloned into pET21a and includes sequences for a Cys residue at the N-terminus
pET21aR2	Sequences encoding codons 1480-1980 of *fhaB* cloned into pET21a and includes sequences for a Cys residue at the N-terminus

References

1. **Kajava A V, Steven AC**. 2006. Beta-rolls, beta-helices, and other beta-solenoid proteins. Advances in Protein Chemistry **73**:55–96.

2. **Kajava A V, Steven AC**. 2006. The turn of the screw: variations of the abundant beta-solenoid motif in passenger domains of Type V secretory proteins. Journal of structural biology **155**:306–15.

3. **Kim K, Saleh OA**. 2009. A high-resolution magnetic tweezer for single-molecule measurements. Nucleic Acids Research **37**:e136.

4. **Kajava A V, Cheng N, Cleaver R, Kessel M, Simon MN, Willery E, Jacob-Dubuisson F, Locht C, Steven AC**. 2001. Beta-helix model for the filamentous haemagglutinin adhesin of Bordetella pertussis and related bacterial secretory proteins. Molecular microbiology **42**:279–92.

5. **González-Candela E, Romero-Rochín V, Del Río F**. 2011. Robustness of multidimensional Brownian ratchets as directed transport mechanisms. The Journal of Chemical Physics **135**:055107.

6. **Noël CR, Mazar J, Melvin JA, Sexton JA, Cotter P a**. 2012. The prodomain of the Bordetella two-partner secretion pathway protein FhaB remains intracellular yet affects the conformation of the mature C-terminal domain. Molecular microbiology **86**:988–1006.